LU TP 00-11
hep-ph/0003258
March 2000

$K_{\ell 4}$ Form-Factors and π-π Scattering

G. Amorós[a,b], J. Bijnens[b] and P. Talavera[b]

[a] Dept. of Physics, Univ. Helsinki, P.O. Box 9, FIN–00014 Helsinki
[b] Dept. of Theor. Phys., Univ. Lund, Sölvegatan 14A, S–22362 Lund

Pacs: 12.39.Fe, 12.40.Yx, 12.15.Ff, 14.40.-n
Keywords: Chiral Symmetry, Chiral Perturbation Theory, Kaon Decay

Abstract

The F and G form-factors of $K_{\ell 4}$ and the quark condensates are calculated to $\mathcal{O}(p^6)$ in Chiral Perturbation Theory (CHPT). Full formulas are presented as much as possible. A full refit of most of the $\mathcal{O}(p^4)$ CHPT parameters is done with a discussion of all inputs and underlying assumptions. We discuss the consequences for the vacuum expectation values, decay constants, pseudoscalar masses and π-π scattering.

Contents

1 Introduction

The low-energy realization of QCD is still disconnected from the high-energy structure where perturbative QCD applications have made it clear beyond doubt that QCD is the theory of the strong interaction. At low energies it is possible to obtain a family of theories within a low-energy expansion using only symmetry principles from QCD. This family of low-energy theories is known as Chiral Perturbation Theory (CHPT) [1]. The perturbation expansion is in terms of the energy, momenta and meson masses, collectively denoted as p. Since this is a perturbative framework, in order to compare with experiment it is very important to have calculations performed to as high an order as possible. CHPT in the three flavour sector was firmly worked out in [2] where all parameters were determined to $\mathcal{O}(p^4)$.

The K_{e4} decay[1], is one of the several processes that can be calculated in the framework of CHPT. It has been calculated to tree level, to one-loop [4] and to improved one-loop [5]. More precise K_{e4} experiments in progress will go beyond the precision of these calculation. In addition K_{e4} is the main input in determining three of the CHPT parameters. A lot of work has gone into improving the calculation of π-π scattering in CHPT, [6, 7, 8]. The precision of the prediction on the latter process is now such that these CHPT parameters are the main uncertainty thus requiring an extension of the calculation for K_{e4} as well.

This is the purpose of the present work: one further step in the perturbative CHPT series of K_{e4} or, in other words, to obtain a two-loop result. Using previous two-loop results [9] a complete three-flavour and, as far as possible, a model independent result is obtained. We discuss several model dependent assumptions, mainly standard, to increase confidence in the generality of the numerical results. In addition we also present the calculation of the vacuum expectation values to two-loops.

There are several papers where a complete two-loop calculation is done. Most of them with the two-flavour chiral Lagrangian as the effective theory, with the other light flavour and the excited states contributing only through the local constants in the CHPT Lagrangian. This two-flavour framework seems to be the best one to extract the low-energy parameters of the pion-pion scattering, with other states starting to modify the behaviour at higher energies. Also, it is the two-flavour sector where chiral symmetry predictions are expected to work best because of the clean feature of pseudo-Goldstone bosons for the pions, since the relevant quark mass is so small. On the other hand, the two-flavour effective Lagrangian can be applied in a small region of physical phenomena. A more interesting Lagrangian has to include the third flavour, but in this case the convergence is not so obvious and we can ask the question: is the Kaon mass small enough to allow a perturbative theory? To answer this we need a large spectrum of calculations to two-loop accuracy.

At present, besides results to tree and one-loop level, there is some work to try to estimate the K_{e4} two-loop contribution [5] and there exist several complete two-loop results [10, 11] for other processes. We presented a short summary of the main results with a slightly different input in [12]. Here we extend the discussion, present full results and discuss more implications.

In Sect. 2.1 we present the kinematics with the description of the process and the variables. Sect. 2.2 introduces the standard notation for the form-factors followed by a short overview of CHPT, Sect. 2.3, and a discussion of the available data in Sect. 2.4. Previous theoretical results are described in Sect. 3. Next we discuss the calculation, method and checks, Sect. 4 and in Sect. 5 some of the $\mathcal{O}(p^6)$ constants in CHPT are estimated using resonance saturation. Details about the $\mathcal{O}(p^4)$ constants (LEC), fits and errors are in Sect. 6.1. We also discuss all the inputs and underlying assumptions there and compare with previous results and a few models, Sect. 6.1.2. The resulting theoretical form-factors and partial waves are shown in Sect. 6.2. The comparison with a proposed experimental parametrization is done in Sect. 6.2.1. Sect. 6.3 updates the π-π scattering threshold parameters with our fit for the LEC as well as comparisons with available low-energy data. Using the LEC fit, we discuss the behaviour of the vacuum expectation values, masses and decay constants with the ratio of the quark masses in Sects. 6.4 and 6.5. Finally we shortly summarize the results. The appendices provide explicit formulas for the form-factors, vacuum expectation values and the one-loop integrals.

2 Definitions and the Data

2.1 Kinematics

We shortly review the variables that parametrize the processes

$$\begin{aligned} K^+(p) &\rightarrow \pi^+(p_+)\pi^-(p_-)\ell^+(p_\ell)\nu_\ell(p_\nu)\,, \\ K^+(p) &\rightarrow \pi^0(p_+)\pi^0(p_-)\ell^+(p_\ell)\nu_\ell(p_\nu)\,, \end{aligned}$$

---

[1] The early history of this decay is reviewed in [3].

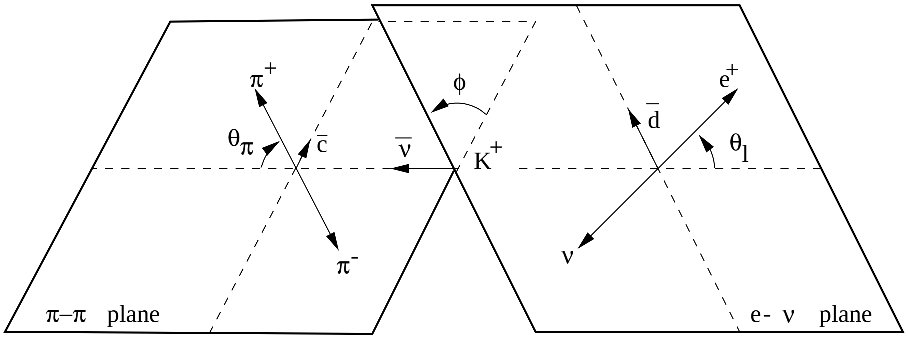

Figure 1: Kinematical variables in $K_{\ell 4}$ decays.

$$K^0(p) \quad \to \quad \pi^-(p_+)\pi^0(p_-)\ell^+(p_\ell)\nu_\ell(p_\nu)\,. \tag{2.1}$$

In brackets we have labelled the corresponding momentum. For the last two processes we keep the momentum notation of the first. The amplitudes for the three processes we denote by T^{+-}, T^{00} and T^{-0} respectively. Following the original work [13] we consider three reference frames, the Kaon rest frame, the dipion center-of-mass system ($\pi - \pi$ plane) and the dilepton center-of-mass system ($e - \nu$ plane). The $K_{\ell 4}$ decays can be parametrized in terms of five kinematical variables (see Fig. 1):

i) s_π, the squared effective mass of the dipion system.
ii) s_ℓ, the squared effective mass of the dilepton system.
iii) θ_π, the angle between the π^+ and the dipion line of flight with respect to the Kaon rest frame.
iv) θ_ℓ, the angle between the ℓ^+ and the dilepton line of flight with respect to the Kaon rest frame.
v) ϕ, the angle between the $\pi - \pi$ and $e - \nu$ planes with respect to the Kaon rest frame.

These variables can vary inside the range

$$\begin{aligned}4m_\pi^2 \le s_\pi = (p_+ + p_-)^2 \le (m_K - m_\ell)^2\,,\\ m_\ell^2 \le s_\ell = (p_\ell + p_\nu)^2 \le (m_K - \sqrt{s_\pi})^2\,,\\ 0 \le \theta_\pi, \theta_\ell \le \pi, \quad 0 \le \phi \le 2\pi\,.\end{aligned} \tag{2.2}$$

Instead of using the previous variables, and besides s_π, $\cos\theta_\pi$ and ϕ, we also use

$$t_\pi = (p_+ - p)^2 \quad \text{and} \quad u_\pi = (p_- - p)^2\,, \tag{2.3}$$

related through

$$\begin{aligned}&s_\pi + t_\pi + u_\pi = m_K^2 + 2\,m_\pi^2 + s_\ell\,,\\ &t_\pi - u_\pi = -2\sigma_\pi X \cos\theta_\pi\,,\end{aligned} \tag{2.4}$$

with

$$\begin{aligned}X &= \frac{1}{2}\lambda^{1/2}(m_K^2, s_\pi, s_\ell)\,,\\ \sigma_\pi &= \sqrt{1 - 4m_\pi^2/s_\pi}\,,\\ \lambda(m_1, m_2, m_3) &= m_1^2 + m_2^2 + m_3^2 - 2\,(m_1 m_2 + m_1 m_3 + m_2 m_3)\,.\end{aligned} \tag{2.5}$$

2.2 Form-Factors

With the previous notation the amplitude for the decay $K^+ \to \pi^+\pi^-\ell^+\nu_\ell$ is

$$T^{+-} = \frac{G_F}{\sqrt{2}} V_{us}^* \overline{u}(p_\nu)\gamma_\mu(1-\gamma_5)v(p_\ell)(V^\mu - A^\mu)\,, \tag{2.6}$$

with

$$
\begin{aligned}
V_\mu &= -\frac{H}{m_K^3}\epsilon_{\mu\nu\rho\sigma}(p_\ell+p_\nu)^\nu(p_+ + p_-)^\rho(p_+ - p_-)^\sigma \;, && (2.7)\\
A_\mu &= -\frac{i}{m_K}[(p_+ + p_-)_\mu\, F + (p_+ - p_-)_\mu\, G + (p_\ell + p_\nu)_\mu\, R]\;. && (2.8)
\end{aligned}
$$

V_{us} is the relevant CKM matrix-element. The other two amplitudes, T^{-0} and T^{00}, are defined similarly.

Here we are interested in the F and G form-factors. The H form-factor is already known to $\mathcal{O}(p^6)$ [14] and the R form-factor always appears with the m_ℓ^2 factor and is negligible for the electron case. R is known to $\mathcal{O}(p^4)$ [5]. The form-factors are functions of s_π, s_ℓ and $\cos\theta_\pi$ only, or alternatively of s_π, t_π and u_π.

The relations between the form-factors and the intensities, easier to obtain from the experiment, can be found in [15] or in [5].

The amplitudes for the three processes of Eq. (2.1) are related using isospin by

$$
T^{+-} = \frac{T^{-0}}{\sqrt{2}} + T^{00} \tag{2.9}
$$

with T^{ij} the matrix element defined in Eq. (2.6). T^{-0} is anti-symmetric under the interchange of the pion momenta while T^{00} is symmetric. This also implies relations between the form-factors themselves. Observe the different phase convention in the isospin states compared to [5] where M^{00} appears with a minus sign because of the Condon–Shortley phase convention.

2.3 Chiral Perturbation Theory

CHPT is an expansion in the energy, with the light mesons being pseudo-Goldstone bosons. The main feature is the spontaneously broken chiral symmetry. The pseudoscalar fields are the lowest mass excitations of the vacuum expectation values. Several realizations are possible, the non-linear realization is more useful with the power counting present explicitly. Explicit chiral symmetry breaking terms are included as perturbations of the symmetry. For an extensive discussion about CHPT we refer the reader to [1] and references therein. In the following we include the basic notation and terms we are working on.

The pseudoscalar fields are included in

$$
U(\phi) = u(\phi)^2 = \exp(i\sqrt{2}\Phi/F_0)\,, \tag{2.10}
$$

where

$$
\Phi(x) \equiv \frac{\vec{\lambda}}{\sqrt{2}}\,\vec{\phi} = \begin{pmatrix} \dfrac{\pi^0}{\sqrt{2}} + \dfrac{\eta_8}{\sqrt{6}} & \pi^+ & K^+ \\ \pi^- & -\dfrac{\pi^0}{\sqrt{2}} + \dfrac{\eta_8}{\sqrt{6}} & K^0 \\ K^- & \bar{K}^0 & -\dfrac{2\,\eta_8}{\sqrt{6}} \end{pmatrix}. \tag{2.11}
$$

With the chiral symmetry constraints and the transformation properties under this symmetry as well as Lorentz invariance and charge conjugation invariance, the Lagrangian starts as

$$
\mathcal{L}^{\text{effective}} = \mathcal{L}_2 + \mathcal{L}_4 + \mathcal{L}_6 + \cdots = \mathcal{L}_2 + \sum_{i=1}^{10} L_i\, O_4^i + \sum_{i=1}^{2} H_i\, \tilde{O}_4^i + \sum_{i=1}^{90} C_i\, O_6^i + \sum_{i=91}^{94} C_i\, \tilde{O}_6^i + \cdots \tag{2.12}
$$

where the subscripts stand for the power of the low momenta, energies or masses, collectively denoted as p.

The expressions for the first two terms are (F_0 is the pion decay constant in the chiral limit)

$$\mathcal{L}_2 = \frac{F_0^2}{4}\{\langle D_\mu U^\dagger D^\mu U\rangle + \langle \chi^\dagger U + \chi U^\dagger\rangle\}\,, \tag{2.13}$$

and

$$\begin{aligned}
\mathcal{L}_4 &= L_1\langle D_\mu U^\dagger D^\mu U\rangle^2 + L_2\langle D_\mu U^\dagger D_\nu U\rangle\langle D^\mu U^\dagger D^\nu U\rangle \\
&+L_3\langle D^\mu U^\dagger D_\mu U D^\nu U^\dagger D_\nu U\rangle + L_4\langle D^\mu U^\dagger D_\mu U\rangle\langle\chi^\dagger U + \chi U^\dagger\rangle \\
&+L_5\langle D^\mu U^\dagger D_\mu U(\chi^\dagger U + U^\dagger\chi)\rangle + L_6\langle\chi^\dagger U + \chi U^\dagger\rangle^2 \\
&+L_7\langle\chi^\dagger U - \chi U^\dagger\rangle^2 + L_8\langle\chi^\dagger U\chi^\dagger U + \chi U^\dagger\chi U^\dagger\rangle \\
&-iL_9\langle F^R_{\mu\nu}D^\mu U D^\nu U^\dagger + F^L_{\mu\nu}D^\mu U^\dagger D^\nu U\rangle \\
&+L_{10}\langle U^\dagger F^R_{\mu\nu} U F^{L\mu\nu}\rangle + H_1\langle F^R_{\mu\nu}F^{R\mu\nu} + F^L_{\mu\nu}F^{L\mu\nu}\rangle + H_2\langle\chi^\dagger\chi\rangle\,.
\end{aligned} \tag{2.14}$$

The next-to-next-to-leading order $\mathcal{L}_6$ is a rather long expression and can be found in [16]. It contains 90+4 terms compared to the 10+2 of $\mathcal{L}_4$.

The notation for the covariant derivative is

$$D_\mu U = \partial_\mu U - i r_\mu U + i U l_\mu\,, \tag{2.15}$$

with l_μ and r_μ the left and right external currents related with the vector and axial-vector external currents

$$r_\mu = v_\mu + a_\mu, \quad l_\mu = v_\mu - a_\mu. \tag{2.16}$$

Their field strength tensors are

$$F_L^{\mu\nu} = \partial^\mu l^\nu - \partial^\nu l^\mu - i[l^\mu, l^\nu], \quad F_R^{\mu\nu} = \partial^\mu r^\nu - \partial^\nu r^\mu - i[r^\mu, r^\nu]\,. \tag{2.17}$$

Scalar (s) and pseudoscalar (p) external fields are introduced with

$$\chi = 2B_0(s + ip) \tag{2.18}$$

where the explicit masses are included through the scalar current s

$$s = \mathcal{M} + \cdots\,. \tag{2.19}$$

$\mathcal{M}$ stands for the diagonal quark mass matrix, $\mathcal{M} = \mathrm{diag}\,(m_u, m_d, m_s)$. For later use we define the following quantities

$$\begin{aligned}
v^{\mu\nu} &= (F_R^{\mu\nu} + F_L^{\mu\nu})/2\,, \\
a^{\mu\nu} &= (F_R^{\mu\nu} - F_L^{\mu\nu})/2\,, \\
u_\mu &= i\{u^\dagger(\partial_\mu - i r_\mu)u - u(\partial_\mu - i l_\mu)u^\dagger\}\,, \\
\Gamma_\mu &= \frac{1}{2}\{u^\dagger(\partial_\mu - i r_\mu)u + u(\partial_\mu - i l_\mu)u^\dagger\}\,, \\
\chi_\pm &= u^\dagger\chi u^\dagger \pm u\chi^\dagger u\,, \\
\nabla_\mu X &= \partial_\mu X + \Gamma_\mu X - X\Gamma_\mu\,.
\end{aligned} \tag{2.20}$$

2.4 Available $K_{\ell 4}$ Experimental Results

Let us briefly comment on the status of the present data. There are two experiments [17, 18] on which our analysis is based. These two dominate in statistics and precision over previous ones. Earlier experiments are within errors compatible using isospin relations with these two and are discussed in [4]. In fact our main results rely entirely on [17] and [18] is used to give an idea on the experimental uncertainties involved. In the experiment [17] the data are analyzed with the partial wave expansion

$$\begin{aligned} F &= f_s e^{i\delta_s} + f_p e^{i\delta_p} cos\theta_\pi + d\text{-wave}\,, \\ G &= g e^{i\delta_p} + d\text{-wave}\,, \end{aligned} \tag{2.21}$$

where f_s, f_p and g are assumed to be real. Within the experimental sensitivity no dependence of the form-factors on s_ℓ nor on d-waves was observed. We confirm this using our calculation as shown in Figs. 9 and 10 in Sect. 6.2. The expected errors in the planned experiments will allow to see the s_ℓ dependence. The form-factor f_p was found to be compatible with zero and consequently neglected when the final value of g was derived. As we show below, Fig. 12, this is a borderline assumption even for the present sensitivity. Neither was there dependence on s_π found for the reduced form-factor

$$\overline{g} = \frac{g}{f_s}\,, \tag{2.22}$$

thus the latter is assumed to be constant.

Furthermore $f_s(s_\pi)$ was parametrized as

$$f_s(s_\pi) = f_s(0)(1+\lambda_f q^2)\,, \quad q^2 = (s_\pi - 4m_\pi^2)/4m_\pi^2\,. \tag{2.23}$$

Notice that f_s is assumed to have only a linear dependence in s_π. As shown in Fig. 9 future experiments might detect curvature. The linear dependence can *only* be ensured for $s_\pi < 0.11$ GeV^2. The assumption of constant $\overline{g}$ constrains the g form-factor parametrization to be

$$g(s_\pi) = g(0)(1+\lambda_g q^2)\,, \tag{2.24}$$

with the same slope as the f_s form-factor, i.e $\lambda = \lambda_f = \lambda_g$. As is clear, from Fig. 9 the theoretical slopes are different but the effect still remain within present errors. Using $V_{us} = 0.220$ the values of [17] yield for the form-factors and slope at threshold

$$f_s(0) = 5.59 \pm 0.14, \quad g(0) = 4.77 \pm 0.27, \quad \lambda = 0.08 \pm 0.02\,. \tag{2.25}$$

From [18] the same assumptions and using isospin give

$$g(0) = 5.50 \pm 0.50\,, \tag{2.26}$$

thus both experiments are marginally compatible. Using the PDG averaging methods [19] on both results we obtain

$$g(0) = 4.93 \pm 0.31\,, \tag{2.27}$$

that we use in fit 9.

3 Form-Factors at Next-to-Leading Order

For completeness we start with the calculation up to one-loop precision. At tree level –see diagram (a) in Fig. 2– both the F and G form-factors are equal and given by a single insertion of $\mathcal{L}_2$ [20]

$$F = G = \frac{m_K}{\sqrt{2}F_\pi}\,, \tag{3.1}$$

where m_K is the physical Kaon mass. At one-loop [4] F and G come through the topologies shown in Fig. 2, containing two vertices of $\mathcal{L}_2$ in (b-c) or a single vertex of $\mathcal{L}_4$ in (a). The result can be cast in the general form

$$\begin{aligned} F(s_\pi, t_\pi, u_\pi) &= \frac{m_K}{\sqrt{2}F_\pi}\Big\{1 + \frac{F_{1-loop}}{F_\pi^2}\Big\} + \mathcal{O}(p^6)\,, \\ G(s_\pi, t_\pi, u_\pi) &= \frac{m_K}{\sqrt{2}F_\pi}\Big\{1 + \frac{G_{1-loop}}{F_\pi^2}\Big\} + \mathcal{O}(p^6)\,. \end{aligned} \tag{3.2}$$

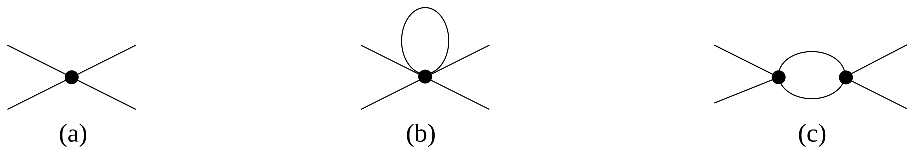
(a) (b) (c)

Figure 2: (a) One-particle irreducible tree level diagram. (b) One-particle irreducible one-loop diagrams. Dots refer to strong vertices or current insertions from $\mathcal{L}_2$, $\mathcal{L}_4$ or $\mathcal{L}_6$. External legs stand for pseudoscalar or weak current. Internal lines are pseudoscalars only.

F_{1-loop} (G_{1-loop}) contain three possible contributions:
i) a unitary correction generated by the loop graphs –see diagram (c) in Fig. 2– given by the functions $\overline{B}_i$ –see App. D– some of which develop an imaginary part responsible for the $I=0$ s-wave, $I=1$ p-wave π-π phase-shift.
ii) A purely logarithmic piece coming from the tad-pole, (b) diagram in Fig. 2.
iii) A polynomial part which split in two pieces. The first one cures the scale dependence of the one-loop functions, making the full process scale-independent while the remaining finite piece is tuned to match some experimental observables.

A straightforward calculation [4] leads to

$$\begin{aligned}
F_{1-loop} = {} & 4m_\pi^2(-16L_1^r+4L_2^r-3L_3^r+8L_4^r+L_5^r-L_9^r)+2m_K^2(8L_2^r+2L_3^r-L_9^r) \\
& +2s_\pi(16L_1^r+4L_3^r+L_9^r)-2t_\pi(4L_2^r+2L_3^r-L_9^r)+2u_\pi(-4L_2^r+L_9^r) \\
& +7/24\Big(\overline{A}(m_\pi^2)+6\overline{A}(m_K^2)+3\overline{A}(m_\eta^2)\Big)+(-3/2m_\pi^2+s_\pi)\,\overline{B}(m_\pi^2,m_\pi^2,s_\pi) \\
& +(m_\pi^2+m_K^2-t_\pi)/4\,\overline{B}(m_\pi^2,m_K^2,t_\pi)+(2m_\pi^2+m_K^2-u_\pi)/3\,\overline{B}(m_\pi^2,m_K^2,u_\pi) \\
& +s_\pi/2\Big(\overline{B}(m_K^2,m_K^2,s_\pi)+\overline{B}(m_\eta^2,m_\eta^2,s_\pi)\Big)+(2m_\pi^2+s_\pi/3)\,\overline{B}_1(m_\pi^2,m_\pi^2,s_\pi) \\
& +(m_\pi^2+m_K^2/2-2t_\pi)/3\,\overline{B}_1(m_\pi^2,m_K^2,t_\pi)-u_\pi/3\,\overline{B}_1(m_\pi^2,m_K^2,u_\pi)+s_\pi/2\,\overline{B}_1(m_K^2,m_K^2,s_\pi) \\
& +(-m_\pi^2/3+7m_K^2/3-t_\pi)/4\overline{B_1}(m_K^2,m_\eta^2,t_\pi)-2/3s_\pi\,\overline{B}_{21}(m_\pi^2,m_\pi^2,s_\pi) \\
& +(3m_\pi^2-3m_K^2-5/3t_\pi)/4\,\overline{B}_{21}(m_\pi^2,m_K^2,t_\pi)+(3m_\pi^2-3m_K^2-t_\pi)/4\,\overline{B}_{21}(m_K^2,m_\eta^2,t_\pi) \\
& -2/3\,\overline{B}_{22}(m_\pi^2,m_\pi^2,s_\pi)-8/3\,\overline{B}_{22}(m_\pi^2,m_K^2,t_\pi)-5/2\,\overline{B}_{22}(m_K^2,m_\eta^2,t_\pi)\,, \qquad (3.3)
\end{aligned}$$

and for the G form-factor to

$$\begin{aligned}
G_{1-loop} = {} & m_\pi^2 4(-L_3^r+L_5^r-L_9^r)-2m_K^2(2L_3^r+L_9^r)+2s_\pi L_9^r+2t_\pi(4L_2^r+2L_3^r+L_9^r) \\
& +2u_\pi(-4L_2^r+L_9^r)+1/24\Big(35\overline{A}(m_\pi^2)+14\overline{A}(m_K^2)-3\overline{A}(m_\eta^2)\Big) \\
& +(-m_\pi^2-m_K^2+t_\pi)/4\,\overline{B}(m_\pi^2,m_K^2,t_\pi)+(2m_\pi^2+m_K^2-u_\pi)/3\,\overline{B}(m_\pi^2,m_K^2,u_\pi) \\
& +(-m_\pi^2-m_K^2/2+2t_\pi)/3\,\overline{B}_1(m_\pi^2,m_K^2,t_\pi)-u_\pi/3\,\overline{B}_1(m_\pi^2,m_K^2,u_\pi) \\
& +(m_\pi^2/3-7/3m_K^2+t_\pi)/4\,\overline{B}_1(m_K^2,m_\eta^2,t_\pi)+3/4(-m_\pi^2+m_K^2+5/9t_\pi)\,\overline{B}_{21}(m_\pi^2,m_K^2,t_\pi) \\
& +(-3m_\pi^2+3m_K^2+t_\pi)/4\,\overline{B}_{21}(m_K^2,m_\eta^2,t_\pi)-2\,\overline{B}_{22}(m_\pi^2,m_\pi^2,s_\pi)-\overline{B}_{22}(m_\pi^2,m_K^2,t_\pi)/3 \\
& -\overline{B}_{22}(m_K^2,m_K^2,s_\pi)-\overline{B}_{22}(m_K^2,m_\eta^2,t_\pi)/2\,. \qquad (3.4)
\end{aligned}$$

It is worthwhile to point out at this level some relevant features in Eqs. (3.3), (3.4). For instance they depend on the $\mathcal{L}_4$ constants $L_1^r, L_2^r, L_3^r, L_4^r, L_5^r$ and L_9^r. Provided we make some assumptions (large N_c and neglecting d-waves) we can use the low-energy data together with Eqs. (3.3), (3.4) to obtain values for L_1^r, L_2^r and L_3^r. Eqs. (3.3), (3.4) have also acquired a different energy dependence that brings the one-loop result nearer to the experimental values [17]. In fact these one-loop corrections are rather large making the low-energy constants evaluation sensitive to variations of the treatment of F_π and pseudoscalar masses.

A possible improvement in the L_1^r, L_2^r and L_3^r evaluation is to consider an Omnès-representation for both form-factors. In other words, to calculate the dispersive contribution from the next chiral order considering that no intermediate new channels are opened [5]. Even more, renormalization group analysis allows to fully calculate the double logarithm contribution [21]. Both showed that in this particular case the next order is expected to be quite sizeable.

This together with the discrepancy between the $SU(2)$ CHPT constants $\bar{l}_1$ and $\bar{l}_2$ obtained from the $K_{\ell 4}$ fit [5] and Roy equation analysis at $\mathcal{O}(p^4)$ [22] and $\mathcal{O}(p^6)$ [23] motivated us to calculate the two-loop contribution to $K_{\ell 4}$.

4 Form-Factors at Next-to-Next-to-Leading Order

4.1 General Technique

The calculation is done with dimensional regularization (DR) with the extended dimension $d = 4 - 2\epsilon$. In this scheme the chiral symmetry is preserved and because of the mass independent regularization the divergences do not mix different orders in the chiral expansion.

Once we have all the mathematical tools to calculate all the integrals, the process to obtain the form-factors is quite general. We summarize here the main steps and checks.

One-loop: We reproduce the one-loop result obtained some time ago [4]. For reasons explained later, in the expansion with the DR parameter ϵ we keep the $\mathcal{O}(\epsilon^1)$ term.

Masses and decay constants: A two-loop calculation is a step beyond and with some differences with the one-loop calculation. One has to be much more careful in precisely defining quantities. E.g. in a one-loop calculation we can safely write all the masses as physical because the difference is in the next order. This is the reason why we have to keep in mind which are the masses to consider in the two-loop result. The masses can be written as:

$$m^2 = m_0^2 + m^{2(4)} + m^{2(6)} + \ldots \tag{4.1}$$

with m_0 the lowest-order mass and where the superscripts (4) and (6) stand for $\mathcal{O}(p^4)$ and $\mathcal{O}(p^6)$. For any $\mathcal{O}(p^6)$ contribution the masses m_0^2 can be used since the difference is $\mathcal{O}(p^8)$. However for $\mathcal{O}(p^4)$ contribution the masses with the first two terms of Eq. (4.1) should be taken. For the tree level the three terms are needed. In CHPT lowest-order and renormalized masses are finite and then the result can be in principle be obtained with lowest-order masses appearing inside the loops and in the chiral symmetry breaking terms, but we have to use the full Eq. (4.1) for the squared momenta. We choose to write all the masses in terms of the physical ones. The same discussion can be done for the decay constants; we choose also to write the physical decay constant F_π instead of the lowest-order one F_0.

Wave-function-renormalization (WFR): We have to include the WFR for each external leg. That means the matrix element is multiplied by $Z_K^{1/2} Z_{\pi_1}^{1/2} Z_{\pi_2}^{1/2}$, with $Z_{K,\pi}$ the renormalization constant for the fields including $\mathcal{O}(p^6)$. This is equivalent to include the one-particle-reducible diagrams.

Cancellation of divergences: There are two kind of divergences to cancel. The first one is pure polynomial; they cancel with the renormalization of the C_i constants (see Eq. (2.12)). These divergences were already found in [24].

Another kind of divergences are non-local, i.e., can not be expressed as contributions from terms in the effective Lagrangian. They appear in the separate contributions and cancel in any quantum field theory. But this is a global cancellation, so it taking place, as is the case for our calculation, is a strong check of the result.

A new feature of the two-loop calculations is that the expansion in the DR parameter until $\mathcal{O}(\epsilon^1)$ needs to be kept. The reason for that is the existence of terms as $L_i A(m^2)$ (or as $L_i L_j$, $L_i B_j$, $\cdots$; in general products of one-loop contributions: one-loop× one-loop) where $A(m^2)$ is a one-loop integral. Once the L_i constant is renormalized

$$L_i = L_i^r + \Gamma_i \lambda \tag{4.2}$$

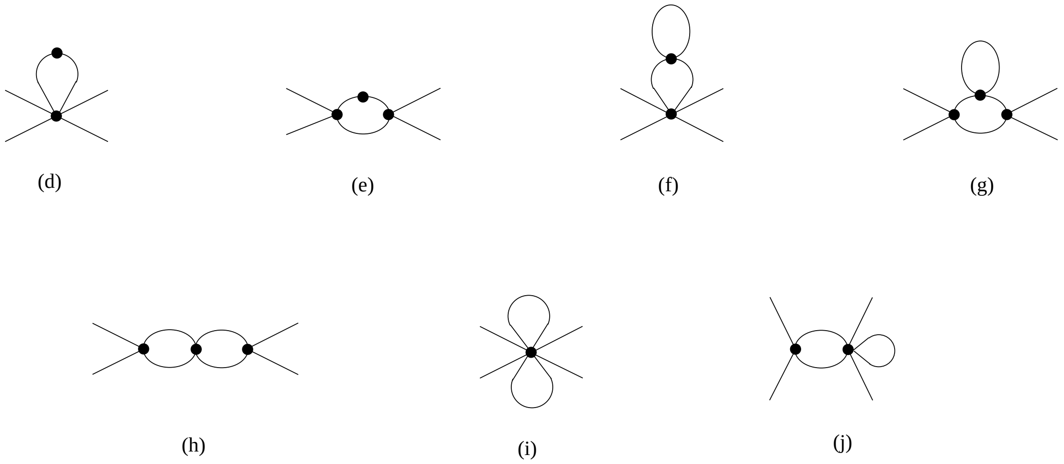

Figure 3: One-particle irreducible $\mathcal{O}(p^6)$ diagrams with only one-loop integrals. The dots are $\mathcal{O}(p^2)$ vertices except the top dot in (d) and (e) which is an $\mathcal{O}(p^4)$ vertex. In addition there are the diagrams (b) and (c) of Fig. 2 with one of the dots replaced by a $\mathcal{O}(p^4)$ vertex.

Figure 4: One-particle irreducible $\mathcal{O}(p^6)$ diagrams with irreducible two-loop integrals. The dots are $\mathcal{O}(p^2)$ vertices

where $\lambda = \frac{1}{2\epsilon} + C$ and with Γ and C real and finite numbers, there appears a new finite term.

Double logarithms: Because the nonlocal divergences have to cancel, the double poles in ϵ can be obtained from a one-loop calculation. These can be calculated in general [21] or from the $L_i \times$one-loop graphs for a particular process. We obtain the same result as [21] for the double logarithms and the products $L_i \times L_j$ and $L_i \times \log$.

Three-point one-loop integrals: The contribution from the first four diagrams in the Fig. 3, (d–g), could be obtained through the renormalization of the meson line in diagrams (b) and (c) of Fig. 2. Therefore the result should be a product of at most two-point one-loop integrals and the naive three-point one-loop integrals from diagrams (e) and (g) must cancel when (c) is rewritten in terms of physical masses.

Irreducible two-loop integrals: The diagrams in Fig. 4 generate sunset-integrals and vertex-integrals already known in the literature. In a previous work [9] on the masses and decay constants of the pseudoscalar mesons to two-loops, the sunset-integrals are calculated using the results obtained in [25, 26]. For the vertex-integrals we use another technique explained in [27] and also useful to recalculate the sunset-integrals. This provided another check on our integral calculations. Additionally, in the vertex-integrals we obtain the same imaginary part from the two-particle discontinuities as using the Cutkosky rules. This check is done below the three-particle thresholds. We refer to [27] for a longer discussion.

Isospin relations: Isospin symmetry relates the decays as discussed in Sect. 2.2. Satisfying these relations is another check of our result.

Gell-Mann-Okubo (GMO) relation: The last comment in this subsection is related to effects from $\mathcal{O}(p^8)$. As explained in the previous paragraph about masses, the correction to the $\mathcal{O}(p^6)$ using the physical masses instead of the bare masses is $\mathcal{O}(p^8)$. Then, to two-loop order it is safe to use the GMO relation $3m_\eta^2 = 4m_K^2 - m_\pi^2$. We can calculate with and without this relation. The result is a variation roughly of 10% of the tail of the $\mathcal{O}(p^6)$ part of the form-factors in Fig. 5. The plot in the kinematic regime accessible for the experiment ($s_\pi < 0.16$ GeV^2) is not modified. This particular effect is mainly due to terms containing $(3m_\eta^2 - 4m_K^2 + m_\pi^2)/(u_\pi, t_\pi, s_\pi)$ which appear when reducing the integrals to a more minimal basis. Another example of this type of effects is discussed in Sects. 6.4 and 6.5.

4.2 Results

Up to $\mathcal{O}(p^6)$ we split the contributions as follows

$$\begin{aligned}
F(s_\pi, t_\pi, u_\pi) &= \frac{m_K}{\sqrt{2}F_\pi}\Big\{1 + \frac{F_{1-loop}}{F_\pi^2} + \frac{1}{F_\pi^4}(F_{LL} + F_V + F_{ct})\Big\} + \mathcal{O}(p^8)\,, \\
G(s_\pi, t_\pi, u_\pi) &= \frac{m_K}{\sqrt{2}F_\pi}\Big\{1 + \frac{G_{1-loop}}{F_\pi^2} + \frac{1}{F_\pi^4}(G_{LL} + G_V + G_{ct})\Big\} + \mathcal{O}(p^8)\,. \qquad (4.3)
\end{aligned}$$

The two first terms have been explained in Sect. 3. The $\mathcal{O}(p^6)$ part is split as follows:
$\mathbf{F(G)_V}$: the part from diagrams with vertices from only the lowest-order Lagrangian, it contains the pure two-loop unitarity contribution. F_V depends only on the physical masses of the pseudoscalars.
$\mathbf{F(G)_{ct}}$: is the part of the polynomial contribution depending on the couplings of $\mathcal{L}_6$.
$\mathbf{F(G)_{LL}}$: is the remaining part, in particular all dependence at $\mathcal{O}(p^6)$ on the L_i^r is collected here.

The diagrams in the Fig. 3 can be written as product of one-loop integrals and evaluated with the standard methods. For the diagrams in the Fig. 4 we profit from previous work with the sunset [9] and the vertex-integrals [27]. The method to manage the sunset-integrals is extensively explained in [9] and we refer to this work. For the vertex diagram we refer to [27] since we do not explicitly present any formulas containing them. We observe a fairly strong numerical cancellation between the contributions from irreducible vertex-integrals and the rest of the terms in F_V and G_V.

We present the results for $F(G)_{LL}$ and $F(G)_{ct}$ in App. A.1 and App. A.2 respectively. For $F(G)_V$ a significantly longer expression is found. Since it only depends on the physical masses, which are not likely to change significantly, a simple parametrization is sufficient. We present it for three sets of masses for the three possible decays. Using m_{K^+} and m_{π^+} for $K^+ \to \pi^+\pi^-\ell^+\nu_\ell$; m_{K^+} and m_{π^0} for $K^+ \to \pi^0\pi^0\ell^+\nu_\ell$ and m_{K^0} and $m_{\pi\text{av}} = (m_{\pi^+} + m_{\pi^0})/2$ for $K^0 \to \pi^-\pi^0\ell^+\nu_\ell$.

Notice that in all cases we quote F and G as for $K^+ \to \pi^+\pi^-\ell^+\nu_\ell$. Taking the even or odd part in $\cos\theta_\pi$ then gives the form-factors for the other decays.

The parametrization is given by

$$\begin{aligned}
F(G) &= (a_1 + \cos\theta_\pi a_2)(1 + s_\ell a_{11}) + s_\pi(a_3 + \cos\theta_\pi a_4) + s_\pi^2(a_5 + \cos\theta_\pi a_6) \\
&\quad + s_\pi^3(a_7 + \cos\theta_\pi a_8) + \sigma_\pi X(a_9 + \cos\theta_\pi a_{10})\,. \qquad (4.4)
\end{aligned}$$

where $X = 1/2\sqrt{(m_K^2 - s_\pi - s_\ell)^2 - 4s_\pi s_\ell}$ and $\sigma_\pi = \sqrt{1 - 4m_\pi^2/s_\pi}$ depend on s_π and s_ℓ. The values of the parameters are given in Table 1. In Fig. 5 we show how well this parametrization fits the calculated expressions.

5 Estimates of Some $\mathcal{O}(p^6)$ Constants

In this section we estimate some of the $\mathcal{O}(p^6)$ constants that appear in the results. We assume saturation by the lightest vector, axial-vector and scalar mesons, extending the formalism used in [28] to the present case.

Table 1: The parameters in the fit to F_V and G_V for the three mass cases.

	F_V	G_V	F_V	G_V	F_V	G_V
masses	m_{K^+}, m_{π^+}		m_{K^+}, m_{π^0}		$m_{K^+}, m_{\pi\mathrm{av}}$	
$10^5 a_1$	1.14408	0.92331	1.4238	0.90367	1.456	0.91997
	$-i1.0993$	$+i0.00198$	$-i0.88056$	$+i0.000468$	$-i0.9431$	$-i0.000496$
$10^6 a_2$	0.1061	0.060766	0.09106	-0.06771	0.09514	-0.068565
$10^5 a_3$	-1.5445	3.0270	-1.7479	3.5074	-1.6368	3.5262
	$+i14.659$	$-i0.21235$	$+i11.457$	$-i0.17035$	$+i12.041$	$-i0.15502$
$10^7 a_4$	-9.3974	-5.5732	-7.8875	-23.294	-8.5278	22.837
$10^5 a_5$	-30.562	3.4592	-31.254	0.037925	-30.653	0.035941
	$-i0.7821$	$+i2.6824$	$+i17.946$	$+i2.5087$	$+i14.810$	$+i2.4139$
$10^7 a_6$	-0.59204	2.1912	-7.1682	-215.51	-5.5226	-206.17
$10^4 a_7$	-3.6231	-0.803725	-3.5113	-0.078793	-3.6377	-0.0812
	$+i7.6144$	$-i0.28955$	$+i4.1122$	$-i0.26763$	$+i4.4861$	$-i0.24452$
$10^6 a_8$	7.519	3.1053	8.3521	54.23	8.4695	50.816
$10^6 a_9$	-0.54512	0.69997	-0.78072	0.29854	-0.46175	0.27801
	$+i5.7286$	$-i0.02308$	$+i6.901$	$-i0.29305$	$+i6.9589$	$-i0.17864$
$10^5 a_{10}$	-7.6007	-9.7289	-7.5832	-9.7041	-7.6143	-9.7514
a_{11}	-2.7610	-3.0277	-2.8042	-3.1412	-2.7268	-3.0970

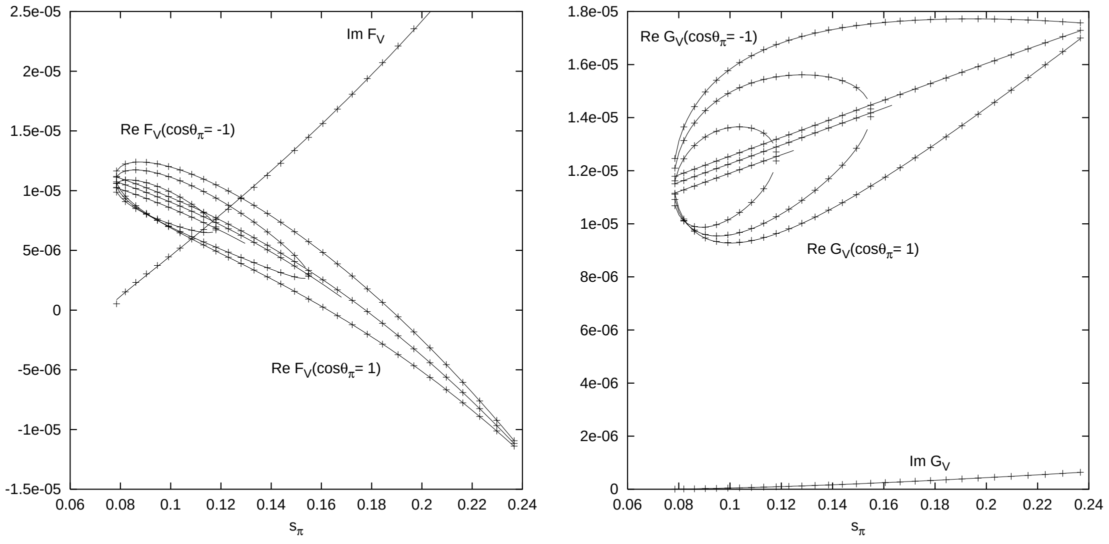

Figure 5: Fit to the F_V and G_V contribution. Plotted are the fit with lines and the full calculation with $+$. In all cases we plotted $\cos\theta_\pi = 0, \pm 1$ and $s_\ell = 0, 0.01, 0.0225$ GeV^2.

With higher orders in the chiral Lagrangian the number of constants to estimate increases. This is due to the fact that the chiral Lagrangian is constructed using only some general conditions and can describe all the possible theories compatible with these. For any specific theory, QCD in our case, there is a large correlation expected between these effective constants. Of course in principle they are calculable from the underlying theory but this is not possible at present. The data are also not sufficient to determine all of them so we need to estimate using some other method. Their main contribution is expected to come from the exchange of higher mass resonances. For these we use a Lagrangian with chiral symmetry incorporating extra, higher mass, fields. The precise input we use for this is described in this section.

For the spin-1 mesons we use the realization where the vector contribution to the chiral Lagrangian starts at $\mathcal{O}(p^6)$. We will only discuss terms relevant for $K_{\ell 4}$, masses and decay constants. Specifically we use for the vector matrix V_μ

$$\begin{aligned}\mathcal{L}_V &= -\frac{1}{4}\langle V_{\mu\nu}V^{\mu\nu}\rangle + \frac{1}{2}m_V^2\langle V_\mu V^\mu\rangle - \frac{f_V}{2\sqrt{2}}\langle V_{\mu\nu}f_+^{\mu\nu}\rangle \\ &\quad -\frac{ig_V}{2\sqrt{2}}\langle V_{\mu\nu}[u^\mu,u^\nu]\rangle + f_\chi\langle V_\mu[u^\mu,\chi_-]\rangle + i\alpha_V\langle V_\mu[u_\nu,f_-^{\mu\nu}]\rangle \qquad (5.1)\end{aligned}$$

and for the axial-vector A_μ

$$\mathcal{L}_A = -\frac{1}{4}\langle A_{\mu\nu}A^{\mu\nu}\rangle + \frac{1}{2}m_A^2\langle A_\mu A^\mu\rangle - \frac{f_A}{2\sqrt{2}}\langle A_{\mu\nu}f_-^{\mu\nu}\rangle + \gamma_A^{(1)}\langle A_\mu u_\nu u^\mu u^\nu\rangle + \gamma_A^{(2)}\langle A_\mu\{u^\mu,u_\nu u^\nu\}\rangle\,. \qquad (5.2)$$

with

$$V_{\mu\nu} = \nabla_\mu V_\nu - \nabla_\nu V_\mu\,,\qquad f_\pm^{\mu\nu} = u(v^{\mu\nu}-a^{\mu\nu})u^\dagger \pm u^\dagger(v^{\mu\nu}+a^{\mu\nu})u\,,$$

V_μ and A_μ are three-by-three matrices describing the full vector and axial-vector nonets. The rest of the notation is as in Sect. 1.

There are other terms with the same order in momenta as in the previous Lagrangian, however they are related to the anomalous sector, which we do not consider here.

The scalar mesons are considered through

$$\begin{aligned}\mathcal{L}_S &= \frac{1}{2}\langle\nabla^\mu S\nabla_\mu S - M_S^2S^2\rangle + c_d\langle Su^\mu u_\mu\rangle + c_m\langle S\chi_+\rangle + \frac{d_m}{2}\langle S^2\chi_+\rangle \\ &\quad +c_\gamma\langle Sf_{+\mu\nu}f_+^{\mu\nu}\rangle + c'_\gamma\langle Sf_{-\mu\nu}f_-^{\mu\nu}\rangle\,. \qquad (5.3)\end{aligned}$$

The last two terms are needed for the calculation of the vector and axial-vector two-point functions and not interesting for the present discussion. We remark that these are not all the allowed contributions from the scalar mesons. We can construct other terms similar to the terms in the $\mathcal{O}(p^4)$ Lagrangian. However that will increases the number of unknown constants to determine without improvement for the estimates. It is however one source of error to keep in mind.

There are two ways to calculate the contribution from these Lagrangians: using the equations of motion to integrate out directly the heavy fields; or diagrammatically, considering all the diagrams with explicit resonance fields and expanding the result to the $\mathcal{O}(p^6)$. In this case it seems faster to use the equations of motion. For the spin-1 mesons it is immediate to derive the Lagrangian; for the scalars also shifts in their vacuum expectation values have to be considered.

The result after the integration of resonances is for the vector fields

$$\begin{aligned}\mathcal{L}_V &= -\frac{if_\chi g_V}{\sqrt{2}M_V^2}\langle\nabla_\lambda([u^\lambda,u^\nu])[u^\nu,\chi_-]\rangle + \frac{g_V\alpha_V}{\sqrt{2}M_V^2}\langle[u_\lambda,f_-^{\nu\lambda}](\nabla^\mu[u_\mu,u_\nu])\rangle \\ &\quad -\frac{ig_Vf_V}{2M_V^2}\langle(\nabla_\lambda f_+^{\lambda\nu})(\nabla^\mu[u_\mu,u_\nu])\rangle - \frac{i\alpha_Vf_\chi}{M_V^2}\langle[u_\nu,\chi_-][u_\lambda,f_-^{\nu\lambda}]\rangle \\ &\quad -\frac{f_\chi f_V}{\sqrt{2}M_V^2}\langle(\nabla_\lambda f_+^{\lambda\mu})[u_\mu,\chi_-]\rangle\,, \qquad (5.4)\end{aligned}$$

for the axial-vector fields

$$\mathcal{L}_A \quad = \quad -\frac{f_A\gamma_A^{(1)}}{\sqrt{2}M_A^2}\langle(\nabla_\mu f_-^{\mu\nu})u^\lambda u_\nu u_\lambda\rangle - \frac{f_A\gamma_A^{(1)}}{\sqrt{2}M_A^2}\langle(\nabla_\mu f_-^{\mu\nu})\{u_\nu, u_\lambda u^\lambda\}\rangle\,, \tag{5.5}$$

and for the scalar mesons

$$\mathcal{L}_S \quad = \quad \frac{c_d^2}{2M_S^4}\langle\nabla_\nu(u_\mu u^\mu)\nabla^\nu(u_\lambda u^\lambda)\rangle + \frac{c_m^2}{2M_S^4}\langle(\nabla_\nu\chi_+)(\nabla^\nu\chi_+)\rangle + \frac{c_d c_m}{M_S^4}\langle\nabla_\nu(u_\mu u^\mu)(\nabla^\nu\chi_+)\rangle\,. \tag{5.6}$$

The three Lagrangians are $\mathcal{O}(p^6)$. However we remark that the spin-1 Lagrangians are directly of this order after the integration. For the scalar case the expansion of the scalar propagator produces $\mathcal{O}(p^4)$ as leading contribution but that part is already included via the values of the L_i^r constants. For the work here we take the next term in this expansion to estimate the unknown $\mathcal{O}(p^6)$ constants.

Besides these ways to estimate the constants it is in some cases possible to obtain the $\mathcal{O}(p^6)$ couplings from experiment. This has been done in previous calculations [29], where the use of finite sum rules could provide the values for the combination of the unknown constants appearing in the considered process. It was also done for the pion form-factors [11]. In all cases the obtained value is in reasonable agreement with the resonance estimate.

Some of the terms of Eqs. (5.4-5.6) are already directly listed in the full list of the $\mathcal{O}(p^6)$ Lagrangian terms of [16]. The others can be rewritten in terms of them but the resulting list is rather long. The combination of terms we are interested in, can be more easily calculated directly from Eqs. (5.4-5.6). The resulting resonance contribution is displayed in App. A.2.1. Together with these we take the couplings

$$\begin{aligned}
&f_V = 0.20, \quad f_\chi = -0.025, \quad g_V = 0.09,\\
&\alpha_V = -0.014, \quad f_A = 0.1, \quad \gamma_A^{(1)} = 0.1,\\
&\gamma_A^{(2)} = -0.01, \quad c_m = 42\text{ MeV}, \quad c_d = 32\text{ MeV},\\
&c_\gamma = 19\cdot 10^{-3}\text{ GeV}^{-1}, \quad c'_\gamma \sim c_\gamma,
\end{aligned} \tag{5.7}$$

and the masses are the experimental ones [19].

$$m_V = m_\rho = 0.77\text{ GeV}, \quad m_A = m_{a_1} = 1.23\text{ GeV}, \quad m_S = 0.98\text{ GeV}. \tag{5.8}$$

The values for f_V, g_V, f_χ, f_A and c_γ are taken from experiment [28, 7]. c_m and c_d are from comparison with the resonance saturation at $\mathcal{O}(p^4)$ [28]. For the remainder we use the ENJL model estimates of [30]. We test the influence of the scalar fields by also performing the fit with vector meson contributions only as discussed below (fit 6).

Before continuing with the next section, it is worth it to summarize some ideas. There are $90 + 4$ $\mathcal{O}(p^6)$ constants in the most general three-flavour chiral Lagrangian, that are supposed to be strongly correlated if they give the low-energy behaviour of QCD. Considering the Lagrangian for heavier states, with the same symmetries as the pseudoscalar one, some correlations among the constants are obtained. The behaviour of the resonances is different from that for the Goldstone bosons: no perturbative theory as for the pseudoscalar mesons exists. However the above procedure is arguably the correct picture in the large N_c limit.

5.1 The η' Field

Another possible contribution from heavier states is given through the η' meson that at low-energies does not play as essential a rôle as for instance the ρ, except for η properties. The η-η' mixing which affects considerably the η properties is known to be fully contained at $\mathcal{O}(p^4)$ in the low-energy constant L_7^r. In order to include explicitly the η' degrees of freedom we can enlarge the pseudoscalar multiplet including the singlet state, in such a way that the η and η' fields are a combination of the singlet and octet fields when $SU(3)$ symmetry is broken but $SU(2)$ is still respected. An alternative equivalent way is to introduce it as a separate pseudoscalar singlet field P_1 described by the Lagrangian [28]

$$\mathcal{L}_{\eta'} = \frac{1}{2}\partial_\mu P_1 \partial^\mu P_1 - \frac{1}{2}M_{\eta'}^2 P_1^2 + \frac{i\gamma F_0}{2\sqrt{6}} P_1 \langle \chi_- \rangle \,. \tag{5.9}$$

At $\mathcal{O}(p^4)$ the η' contribution is entirely encoded in L_7^r and dominates its value. The next order expansion in the P_1 propagator, $\mathcal{O}(p^6)$, gives

$$\mathcal{L}_{\eta'} = -\frac{\tilde{d}_m^2}{2M_{\eta'}^4}\partial_\mu \langle \chi_- \rangle \partial^\mu \langle \chi_- \rangle \text{ with } \tilde{d}_m = 20 \text{ MeV}. \tag{5.10}$$

Similar to the scalar case we can add terms to Eq. (5.9) that will contribute as well to $\mathcal{O}(p^6)$. The contribution is of relevance to our fit only via the η mass and the prediction for the η decay constant, affecting mainly the value for L_7^r with a small modification for L_8^r. Again, rewriting Eq. (5.10) into the terms of [16] leads to a long expression so we do not present it.

We remark that although the two-point functions, used to calculate the decay constants and the masses, are obtained with the external currents from the octet, the pole in the propagator of course corresponds to the real η and the decay constant is the coupling of the real η to the octet current.

A more complete list of terms including their integrating out shows only small modifications to the phenomenological implications [31].

6 Phenomenological Applications

There are two points to address with the two-loop result for $K_{\ell 4}$. The first one is to obtain a prediction for the form-factors to be compared with experiment and to use our prediction to check the validity of assumptions made in the data analysis. This is presented below in Sect. 6.2.1. The second one is to extract a fit for the low-energy constants L_i^r which values will be used to predict other quantities of interest. In particular, they are needed to obtain predictions for low-energy π-π scattering, one phase-shift combination can be obtained independently from the same decay data. The comparison with the scattering quantities obtained directly is a consistency check of CHPT. We remark that in this two-loop calculation the only way to obtain an imaginary part for $K_{\ell 4}$ is through the intermediate states of two pions. However the π-π amplitude appearing here is one-loop. It is then not possible to obtain indirectly a three-flavour two-loop result for the rescattering quantities. We therefore use below the known two-flavour two-loop result for the scattering [6, 7].

6.1 Values of the Low-Energy Constants

The previous values of L_i^r are obtained from one-loop or one-loop improved calculations [2, 5]. These values are obtained through partially independent fits, in particular L_1^r, L_2^r, L_3^r are obtained from $K_{\ell 4}$ taking fixed the other L_i^r. In the present work we avoid to fix them and perform the first global fit of most of the $\mathcal{O}(p^4)$ low-energy parameters simultaneously. The total number of parameters up to $\mathcal{O}(p^4)$ is 13. They are $B_0\hat{m}$, $B_0 m_s$, F_0 and L_1^r–L_{10}^r. L_{10}^r does not contribute to any of the quantities considered here and is thus fully independent. L_9^r is discussed below. In practice we thus need to fit 11 free parameters. The values are updated fitting the results obtained for the masses and decay constants to two-loops [9] and the result of the present work, see also [12].

The other free quantities in the full result are the C_i^r, that are estimated in the previous section, Sect. 5. The values of L_i^r can be reasonably well predicted from resonance exchange, so a similar rough estimate is expected to work for the C_i^r. We test the dependence by removing all the resonance contributions except for the vector ones, whose couplings are determined experimentally elsewhere, and the η', and see if the results change. Changing the values of the C_i^r by 50% changes the fitted values within the fit errors. We also present a reasonable variation of the other inputs.

Unfortunately, it is not possible to find at present 11 fully independent inputs from direct experimental quantities. Below we use as inputs m_π^2, m_K^2, m_η^2, F_π, F_K and three inputs from $K_{\ell 4}$, $f_s(0)$, $g_p(0)$ and λ_f, defined below. The three additional inputs are the quark-mass ratio $m_s/\hat{m}$, L_4^r and L_6^r. In the future we hope to be able to include additional experimental input to constrain these as well.

The fit is performed by minimizing the χ^2 function defined by

$$\chi^2 = \sum_{i=1,6} \chi_i^2 = \sum_{i=1,6} \left(\frac{x_i - x_{i\mathrm{input}}}{\Delta x_{i\mathrm{input}}} \right)^2 , \tag{6.1}$$

with as weight $\Delta x_{\mathrm{input}}$ the error in the input values $x_{i\mathrm{input}}$.

This allows us to fit everything since in all higher orders we have replaced quark masses and F_0 by the relevant physical quantities. Then we can use the mass and decay constant expressions up to $\mathcal{O}(p^6)$ to determine $B_0\hat{m}$ and F_0 from the physical input afterwards. Let us now discuss the various inputs and χ_i^2.

Physical masses and decay constants: For these quantities we use the pion masses $m_{\pi^+} = 139.56995\,\mathrm{MeV}$, $m_{\pi^0} = 0.1349764\,\mathrm{MeV}$, the Kaon masses $m_{K^+} = 493.677\,\mathrm{MeV}$, $m_{K^+} = 497.672\,\mathrm{MeV}$ and η mass $m_\eta = 547.30\,\mathrm{MeV}$, the pion decay constant $F_\pi = 92.4\,\mathrm{MeV}$ and the Kaon decay constant $F_K/F_\pi = 1.22 \pm 0.01$ [19].

$\mathbf{L_4^r, L_6^r}$: The first main feature that we use is the behaviour under the large N_c limit. The consequences for the L_i^r are discussed in [2] and for the C_i^r in [16]. This limit tells us that some of the constants are expected to vanish at some unknown scale. This is the case for L_4^r and L_6^r that are both set zero for the main fit (at m_ρ scale). Fit 5 in Table 2 assumes them to be zero at a scale of m_η^2 instead. For other fits relaxing this assumption we refer to Section 6.5.1.

$\mathbf{L_9^r}$: Another point is the value for L_9^r. This constant is related to the charge radius of the pion. The value is completely saturated by the ρ resonance, and for this reason the contribution from the logarithms is negligible. Moreover L_9^r appears with the factor s_ℓ in $K_{\ell 4}$, such that it is not necessary for the main fit where we use $s_\ell = 0$. For the other fits we can safely use the value $L_9^r = 6.9\ 10^{-3}$.

Other $\mathbf{L_i^r}$: The remaining constants will be taken as free parameters, at the end six LEC's to fit.

The quark-mass ratio $m_s/\hat{m}$: To $\mathcal{O}(p^2)$ it is possible to relate the ratio of the strange quark mass m_s over the isospin doublet quark mass $\hat{m} = (m_u + m_d)/2$, with a combination of the meson masses. If we assume that $\mathcal{O}(p^4)$ and $\mathcal{O}(p^6)$ do not appreciably modify this ratio we can use this as input or alternatively the values from QCD sum rules and/or the lattice. As standard input we use $m_s/\hat{m} = 24$ and we check that $m_s/\hat{m} = 26$ does not lead to significantly different results (fit 2 in Table 2). We remark that there are two possible ways to calculate this ratio from the lowest-order meson masses, using or not the η mass

$$\left.\frac{m_s}{\hat{m}}\right|_1 = \frac{2\,m_{0K}^2 - m_{0\pi}^2}{m_{0\pi}^2}\,; \quad \left.\frac{m_s}{\hat{m}}\right|_2 = \frac{3\,m_{0\eta}^2 - m_{0\pi}^2}{2\,m_{0\pi}^2}\,, \tag{6.2}$$

where m_0 stands for the lowest-order mass that we calculate in terms of the physical masses, F_π and the L_i^r. We included both relations in the fit. The expression of the bare masses in terms of the physical masses to two-loop is taken from [9]. For the pion mass we use the neutral pion mass. For the Kaon mass we subtract the electromagnetic contribution through the formula

$$m_{K\mathrm{av}}^2 = \frac{1}{2}(m_{K^+}^2 + m_{K^0}^2 - 1.8(m_{\pi^+}^2 - m_{\pi^0}^2)) = (494.53\,\mathrm{MeV})^2\,, \tag{6.3}$$

where the factor 1.8 is a modification due to the corrections to Dashen's theorem [32]. Whenever we fit or calculate masses we use $m^2_{K\mathrm{av}}$ and $m^2_{\pi^0}$. The contribution to χ^2 is

$$\chi_1^2 + \chi_2^2 = \sum_{i=1,2} \left(\frac{\frac{m_s}{\hat{m}}\big|_i - \frac{m_s}{\hat{m}}\big|_{\mathrm{input}}}{0.1\ \frac{m_s}{\hat{m}}\big|_{\mathrm{input}}} \right)^2 . \tag{6.4}$$

$\mathbf{F_K/F_\pi}$: This quantity is calculated using the formulas of [9][2], and enters in the fit as

$$\chi_3^2 = \left(\frac{(F_K/F_\pi) - 1.22}{0.01} \right)^2 . \tag{6.5}$$

$\mathbf{K_{\ell 4}}$ decay: The expression for the form-factors F and G obtained in the theoretical part is compared with the experimental analysis from [17]. The results we are interested in are the extraction of the s-wave contribution from the F form-factor and the p-wave from the G form-factor. The others contributing waves are not appreciable [17]. This is also confirmed in the expressions as discussed below. In [17] the s-wave f_s and p-wave g_p are fitted with the expressions

$$\begin{aligned} f_s(q^2) &= f_s(0)\,(1+\lambda_f\, q^2)\,, \\ g_p(q^2) &= g_p(0)\,(1+\lambda_g\, q^2)\,, \end{aligned} \tag{6.6}$$

where $f_s(0)$ and $g_p(0)$ are the form-factors at threshold of the dipion system. The slopes are taken to be the same $\lambda_f = \lambda_g$.

In order to keep the computer time needed in reasonable limits, we use the following approximation

$$f_s(0) = F(s_\pi, s_\ell = 0, \cos\theta_\pi = 0). \tag{6.7}$$

We use $s_\pi = (2m_\pi + 1\,\mathrm{MeV})^2$ to avoid numerical problems at threshold. The s_ℓ dependence is very mild, we checked this by performing an alternative fit with $\sqrt{s_\ell} = 100$ MeV (fit 3 in Table 2). Only using $\cos\theta_\pi = 0$ corresponds to assume d and higher waves to be negligible. Similarly

$$g_p(0) = G(s_\pi, s_\ell = 0, \cos\theta_\pi = 0). \tag{6.8}$$

We do not make use of the derivative at threshold as the slope. This has both numerical problems and does not correspond to the experimental situation. Instead we shift a bit from the threshold. The slope is then given by

$$\lambda_f = \Big(\frac{|F(s'_\pi, s_\ell, \cos\theta_\pi = 0)|}{|F(s_\pi, s_\ell, \cos\theta_\pi = 0)|} - 1 \Big) \frac{4m_\pi^2}{s'_\pi - s_\pi} \tag{6.9}$$

with the value $s_\pi = (2\,m_\pi + 1\,\mathrm{MeV}\,)^2$ and $s'_\pi = (336\,\mathrm{MeV}\,)^2$. As an alternative we also present a fit with $s'_\pi = 293$ MeV (fit 4 in Table 2).

These quantities enter in the fit via

$$\chi_4^2 = \left(\frac{f_s(0) - 5.59}{0.14} \right)^2 , \quad \chi_5^2 = \left(\frac{g_p(0) - 4.77}{0.27} \right)^2 , \quad \chi_6^2 = \left(\frac{\lambda_f - 0.08}{0.02} \right)^2 . \tag{6.10}$$

We also present an alternative fit, fit 9, where we include additionally the $g_p(0)$ measurement in $K_L^0 \to \pi^0\pi^- e^+\nu$ of Ref. [18]. Combining errors using the PDG procedure [19], Eq. (6.10) is modified with

$$\chi_5^2 = \left(\frac{g_p(0) - 4.93}{0.31} \right)^2 . \tag{6.11}$$

---

[2] The published version has in App. A.2 the formulas in terms of lowest-order masses and decay constant, contrary to what is stated in the text there. Here we use the formulas in terms of physical masses.

Table 2: Results for $L_i^r(\mu)$ for the various fits described in the main text. Notice that L_4^r, L_6^r and L_9^r are input, $L_4^r = 0, L_6^r = 0$ and $L_9^r = 6.90\ 10^{-3}$. Errors are fitting errors described in the text. All $L_i^r(\mu)$ values quoted have been brought to the scale $\mu = 0.77$ GeV. The standard values are $m_s/\hat{m} = 24$, $\sqrt{s'_\pi} = 0.336$ GeV and $s_\ell = 0$.

	Main Fit	[2, 5]	$\mathcal{O}(p^4)$	fit 2	fit 3	fit 4	fit 5	fit 6	fit 7	fit 8	fit 9
$10^3\ L_1^r$	0.52±0.23	0.37±0.23	0.46	0.53	0.50	0.49	0.52	0.45	0.44	0.63	0.65
$10^3\ L_2^r$	0.72±0.24	1.35±0.23	1.49	0.73	0.67	0.74	0.80	0.51	1.04	0.73	0.85
$10^3\ L_3^r$	−2.70±0.99	−3.5 ±0.85	−3.18	−2.71	−2.58	−2.73	−2.75	−2.16	−2.95	−2.67	−3.27
$10^3\ L_5^r$	0.65±0.12	1.4 ±0.5	1.46	0.62	0.65	0.64	0.82	0.67	1.00	0.51	0.60
$10^3\ L_7^r$	−0.26±0.15	−0.4 ±0.2	−0.49	−0.20	−0.26	−0.26	−0.30	−0.26	−0.23	−0.25	−0.26
$10^3\ L_8^r$	0.47±0.18	0.9 ±0.3	1.08	0.35	0.47	0.47	0.58	0.46	0.52	0.44	0.48
changed			$\mathcal{O}(p^4)$	$m_s/\hat{m}$	$\sqrt{s_\ell}$	$\sqrt{s'_\pi}$	$L_4^r; L_6^r$	V_μ, η'	μ	μ	$g(0)$
quantity				26	0.1	0.293	$-0.3; -0.2$	only	0.5	1.0	4.93
Unit					GeV	GeV	10^{-3}		GeV	GeV	

With the previous fit procedure we find for the values of the low-energy constants

$$
\begin{aligned}
&10^3 L_1^r = 0.52 \pm 0.23\,, \quad 10^3 L_2^r = 0.72 \pm 0.24\,, \quad 10^3 L_3^r = -2.70 \pm 0.99\,, \\
&10^3 L_5^r = 0.65 \pm 0.12\,, \quad 10^3 L_7^r = -0.26 \pm 0.15\,, \quad 10^3 L_8^r = 0.47 \pm 0.18\,. \qquad (6.12)
\end{aligned}
$$

In Table 2 we present the alternative fits discussed above. The difference with the results of [12] is due to the η' inclusion everywhere, this mainly affects the values of L_7^r.

We also included two fits (fit 7 and 8) with a different choice for the scale, $\mu = 0.5$ and $\mu = 1$ GeV. The rescaling of the L_i^r is considered such that in the table we quote the shifted value at $\mu = 0.77$ GeV. These choices imply different scales for the resonance saturation on the C_i^r. As can be noticed the changes due to the scale are quite considerable, but almost covered by the fitting errors. This suggest that the errors quoted in the main fit are unlikely to be reduced if there is more control over the $\mathcal{O}(p^6)$ constants.

The errors are those quoted by MINUIT and are those that give $\Delta\chi^2 = 1$ assuming the quadratic approximation near the minimum.

In addition we have performed a fit where V_{us} was changed to 0.226 which showed no significant deviations from our main fit. This value is from using unitarity in the CKM matrix and $V_{ud} = 0.9740$ [19, 33].

6.1.1 Errors and Correlations

The problem in determining errors on derived quantities is that the L_i^r values given above are very strongly correlated and that with 6 free parameters the chance that all of them are within their one sigma error, is negligibly small. We have thus generated a distribution of sets of L_i^r that have a correlated Gaussian distribution according to the χ^2 function defined above. We then keep the sets that have a χ^2 less than the value corresponding to 68% confidence level. Projecting this distribution on the relevant variable leads to larger ranges than the errors quoted above. Those are the errors quoted in the remainder since they are more relevant than those calculated from propagating the errors of Table 2.

As examples of the correlations we show the plot of L_1^r, L_2^r and L_3^r together with their projections on the two-variable planes and the plot of L_7^r and L_8^r in Figure 6. Each point correspond to one set of L_i^r of the distribution described above. Similar plots can be made for all other combinations. Notice that this only shows the *experimental* type of error. Not included are the errors due to the restriction to $\mathcal{O}(p^6)$ and other theory uncertainties.

6.1.2 Comparison with Previous Results and Models

In this section we want to give some insight about the sizeable corrections of the LEC, Eq. (6.12), with respect to the unitary calculation, second column in Table 2, and to show the differences with

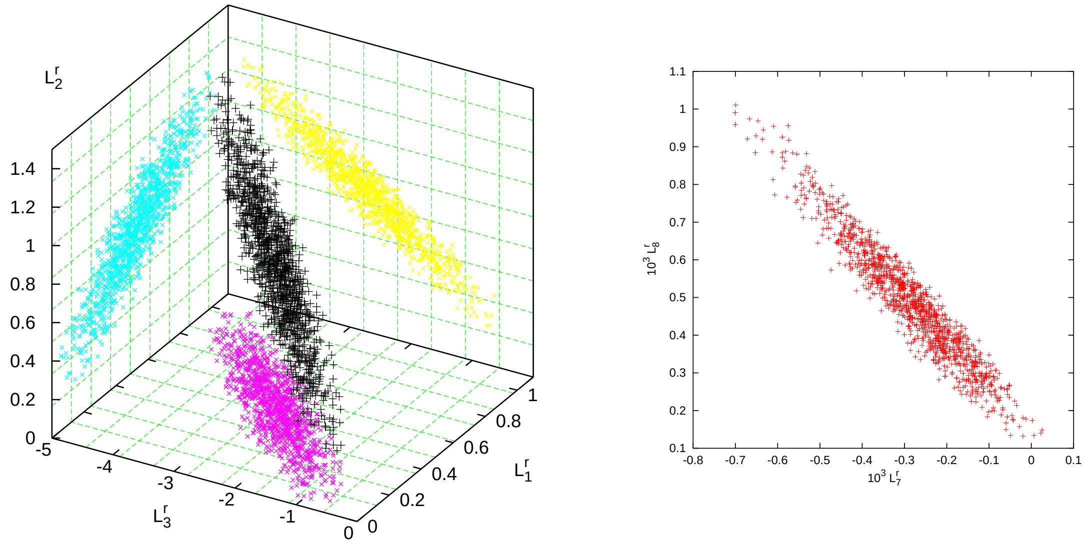

Figure 6: The sets of L_i^r within a 68% confidence level range of χ^2. In the first plot we show $+$ the values of the first three L_i^r and $\times$ the projections on the coordinate planes. The second plot shows the L_7^r–L_8^r correlations.

some existing models based on large N_c [34, 35]. Due to the high correlation between the various variables this is not a trivial affair. To make the analysis more transparent we remove first of all the constraints on the masses and decay constants, i.e we deal *almost* with the same assumptions as in previous calculations [2, 5]. Therefore we fix L_5^r, L_7^r and L_8^r to their $\mathcal{O}(p^4)$ value. All in all this amounts to determine L_1^r, L_2^r and L_3^r from the slope (λ), the s–wave (f_s) and the p–wave (g_p) –see Eq. 6.6. The results obtained after that are displayed in fit A of Table 3. A close look, shows that the results are *quite* similar to those quoted in Eq. (6.12), thus the constraints imposed by the masses and decay constants do not drive at all the differences. To disentangle the pieces from the full calculation and compare with [5] is extremely delicate. For instance, using the dispersive method only some pieces of diagrams (h), (j) in Fig. 3 and of those depicted in Fig. 4 are kept. The rest has no new imaginary part and is therefore modeled by a pure multiplicative constant only. Furthermore, the dispersive approach misses the full two-loop renormalization, only the one-loop renormalization of F_π, masses and WFR is introduced. Besides these obvious remarks a less straightforward point needs clarification: in [5] the full relativistic resonance propagator is kept, thus resumming all chiral orders. This has some influence on G. The main point to stress is that already at threshold there is a significant shift of the form-factors with respect to the dispersive calculation. In Fig. 7 we show this fact, comparing $\mathcal{O}(p^4)$, the Omnès improvement and the $\mathcal{O}(p^6)$ for the F form-factor using the results of [5] as input as well as $F_\pi = 93.2 MeV$. Pieces that can account for the difference at threshold are the $L_i \times L_j, L_i \times \log, \log \times \log$ and the resonance saturation piece. All of them, except the last one, are $\mathcal{O}(p^6)$ contributions not considered in the dispersive approach [5]. The Omnès improved calculation for F had the right sign but the wrong magnitude. In Fig. 7 we have compared the Omnès improved calculation with the full $\mathcal{O}(p^6)$. Notice the considerable shift already at threshold. To take into account this difference the values of the LEC, L_1^r, L_2^r and L_3^r, have to change substantially. In the figure we have used the values of the low-energy constants obtained in [5], and as a consequence the Omnès calculation matches the experimental result, shadow area. With those parameters the $\mathcal{O}(p^6)$ result is outside the experimental errors.

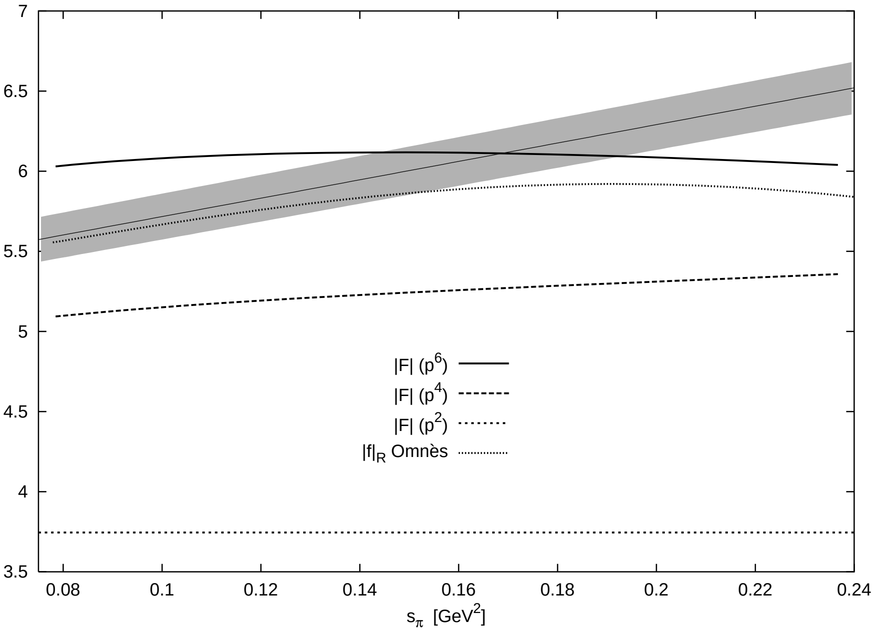

Figure 7: Comparison of the Omnès improved estimate with the full $\mathcal{O}(p^6)$ calculation using the same *old* set of values of L_i^r as input together with $F_\pi = 93.2$ MeV. The shaded band is the experimental result.

Table 3: Values of L_i^r for comparison with Eq. (6.12). The first column is the fit without the constraints from the masses and decay constants. Second is the result from the Resonance Saturation model. Third and fourth columns are values from other large N_c based models as described in the text.

	fit A	Ref. [28]	Ref. [34]	Ref. [35, 38]
$10^3 L_1^r$	0.53 ± 0.24	0.6	0.79	0.81
$10^3 L_2^r$	0.67 ± 0.25	1.2	1.58	1.62
$10^3 L_3^r$	-2.74 ± 1.09	-3.0	-3.17	-4.24
$10^3 L_5^r$	fixed	$1.4^{(a)}$	0.43	1.21
$10^3 L_8^r$	fixed	$0.9^{(a)}$	0.46	0.60

$^{(a)}$ Input

In our calculation we have assumed a resonance saturation for the $\mathcal{O}(p^6)$ coefficients. To some extent this assumption was successful at $\mathcal{O}(p^4)$ [28]. In the second column of Table 3 we quote the values for this model-approach to some of the LECs. One can see that L_1^r and L_3^r in Eq. (6.12) are in good agreement with the resonance saturation hypothesis. L_2^r is off from this hypothesis, and violates the relation $2L_1^r = L_2^r$ by 20%, which is of the expected size of deviations from the large N_c limit. As is discussed in [36] there is some indication that the resonance saturation assumption fails in the scalar sector. For this matter, one should compare between different models. It is clear that our result is within the range as exemplified by the two examples discussed below.

We also compare in Table 3 with two model-predictions of CHPT parameters, including also the values of L_5^r and L_8^r. In Ref. [34] the large N_c and chiral limits lead including the leading gluonic contribution to[3]

$$\begin{aligned} 4L_1 = 2L_2 &= \frac{N_c}{96\pi^2}\left[1 + \mathcal{O}(1/M_Q^6)\right], \\ L_3 &= -\frac{N_c}{96\pi^2}\left[1 + \frac{\pi^2}{5N_c}\frac{\langle \frac{\alpha_S}{\pi} GG\rangle}{M_Q^4} + \mathcal{O}(1/M_Q^6)\right], \end{aligned} \tag{6.13}$$

where M_Q can be interpreted as a constituent quark mass. Comparing the second column in Table 3 with Eq. (6.12) one can see an improvement in the central value of L_1^r, L_5^r and L_8^r with respect to the one-loop result, while the values for L_2^r and L_3^r, which essentially agrees with the $\mathcal{O}(p^4)$ LEC's, went off suggesting the relevance of higher gluonic or large N_c corrections.

The model of [34] was extended to the full ENJL model with gluonic corrections in [37]. The resulting relations led to the proposal of a new model, LMD [35]. It mimics QCD by taking into account the first resonance plus the continuum obtaining the relations

$$6L_1 = 3L_2 = -\frac{8}{7}L_3 = 4L_5 = 8L_8 = \frac{3}{8}\frac{F_\pi^2}{m_\rho^2} = \frac{15}{8\sqrt{6}}\frac{1}{16\pi^2}\,, \tag{6.14}$$

where the last equality is obtained using higher orders in QCD sum rules [38]. Its values are given in the third column of Table 3 and the same comments as in the previous model apply for L_1^r, L_2^r, L_3^r and L_8^r, while the central value of L_5^r turns out to be worse.

6.2 $K_{\ell 4}$ Form-Factors and Partial Wave Expansions

We now plot the form-factors F and G at $\cos\theta_\pi = 0$ for the main fit, Eq. (6.12), and the various separate contributions. We show the full result for F in Fig. 8a and for G in Fig. 8b. Notice that the convergence of the series is reasonable for both form-factors and that for F the contribution from the $\mathcal{O}(p^6)$ Lagrangian is fairly small. For G this is dominated by vector exchange with experimentally determined parameters so the uncertainty from this source is quite small.

Let us now look at the dependence on s_ℓ. In Fig. 9 we show the absolute value of F and G for $\sqrt{s_\ell} = 0$, 100 MeV and 150 MeV, together with the experimental error band. The lines for the higher s_ℓ-values stop at the kinematical limits. Notice the change in scale with respect to Figures 8a and 8b. Given the accuracy of the present data we can safely neglect the s_ℓ dependence completely.

The form-factors F and G can be decomposed in partial waves[4] as [13, 15]

$$\begin{aligned} F(s_\pi, t_\pi, u_\pi, s_\ell) &= \sum_{l=0}^{\infty} P_l(\cos\theta_\pi) f_l(s_\pi, s_l) - \frac{\sigma_\pi P L}{X}\cos\theta_\pi G(s_\pi, t_\pi, u_\pi, s_\ell) \\ G(s_\pi, t_\pi, u_\pi, s_\ell) &= \sum_{l=1}^{\infty} P_l'(\cos\theta_\pi) g_l(s_\pi, s_\ell)\,, \end{aligned} \tag{6.15}$$

---

[3] The predictions for L_5^r and L_8^r of Ref. [34] are sensitive to the precise regularization scheme chosen in the chiral quark model.

[4] The partial wave expansion is not simply for F and G since the components with a well defined $L_z = 0, \pm 1$ need to be expanded [13, 15].

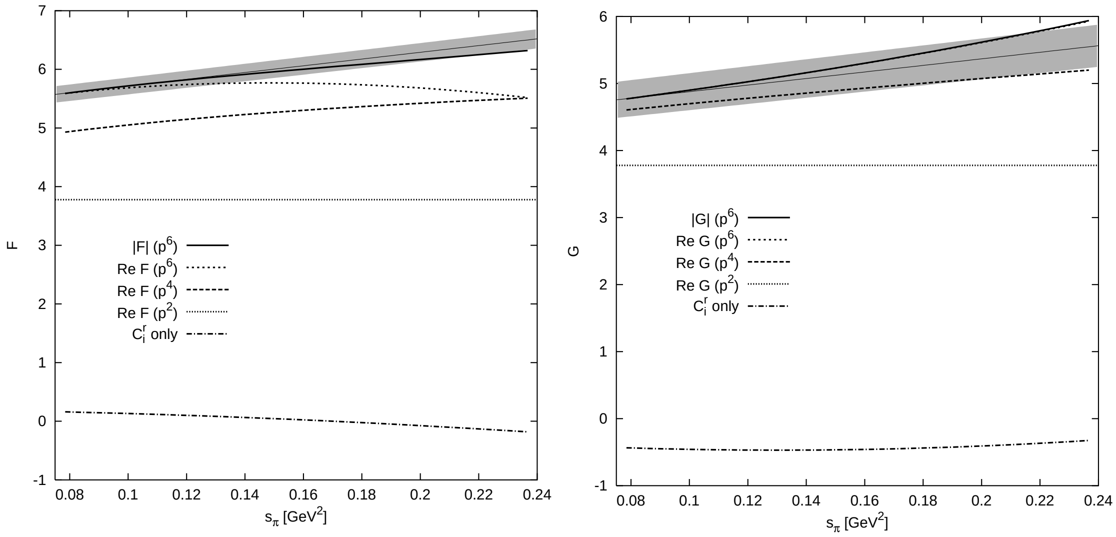

(a) (b)

Figure 8: The F (a) and G (b) form-factor at $s_\ell = 0$ and $\cos\theta_\pi = 0$. The shaded band is the result of [17]. Shown are the full result for the absolute value, and the real part to lowest-order, $\mathcal{O}(p^4)$ and $\mathcal{O}(p^6)$. We also show the contribution from the $\mathcal{O}(p^6)$ Lagrangian; this is dominated by the vector contribution.

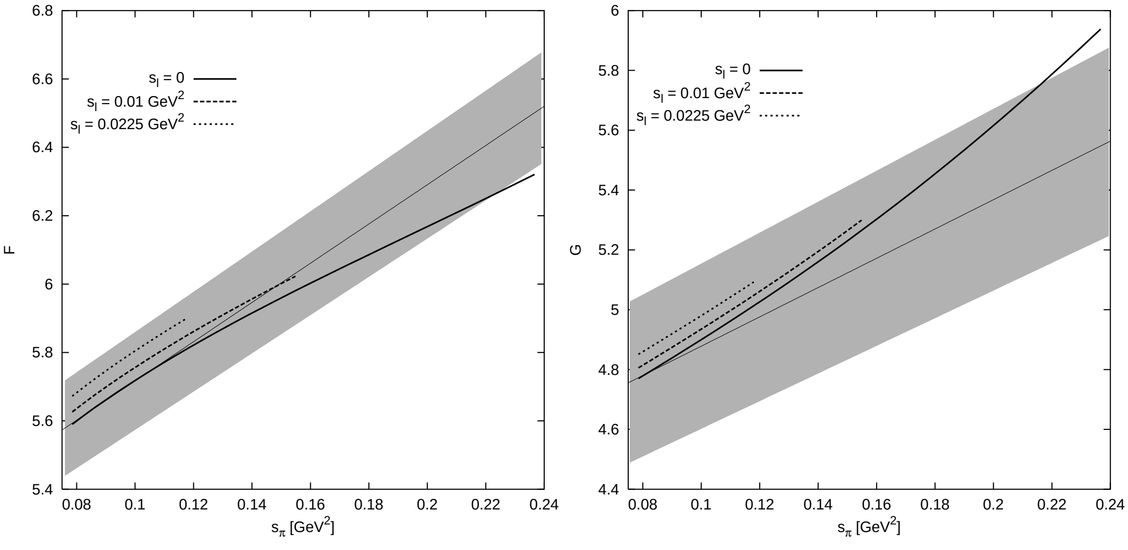

Figure 9: The absolute value of the F and G form-factor at $\sqrt{s_\ell} = 0$, 100 MeV and 150 MeV. All cases with $\cos\theta_\pi = 0$. The shaded band is the result of [17].

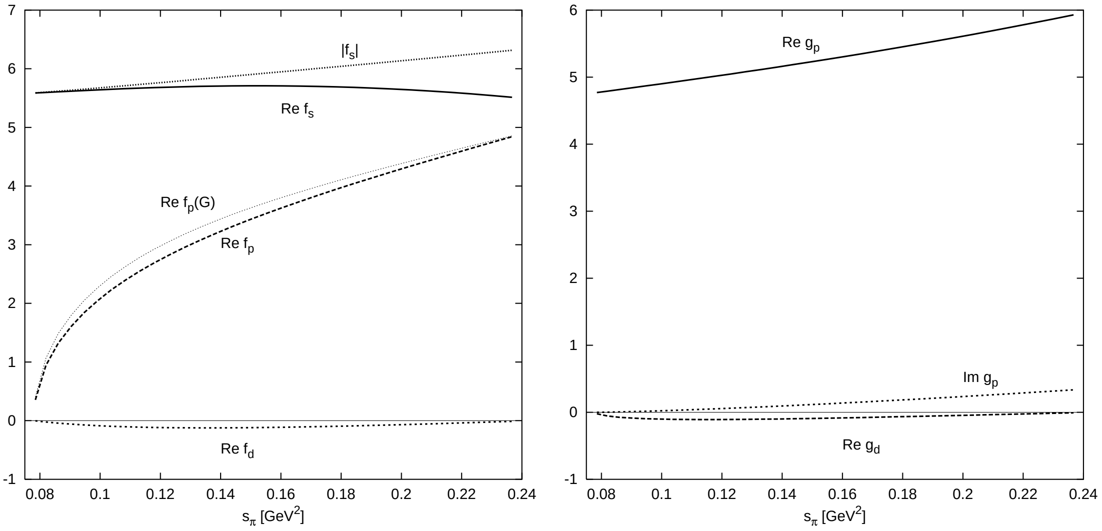

(a) (b)

Figure 10: (a) The partial wave expansion of the combination $\bar{F} = F + \sigma_\pi PL\cos\theta_\pi G/X$. Plotted are the absolute value of f_s and the real part of f_s, f_p and f_d. We also show the f_p contribution from the second term in $\bar{F}$. (b) The partial wave expansion of G. Plotted are the real part of g_p and g_d and the imaginary part of g_p.

where

$$P_l'(z) = \frac{d}{dz} P_l(z)\,. \tag{6.16}$$

$P_l(x)$ are the Legendre polynomials and the functions $f_l(s_\pi, s_\ell)$, $g_l(s_\pi, s_\ell)$ have as phase the phase-shifts $\delta_l^I(s_\pi)$ from π-π scattering with isospin $I = 0$ for even angular-momentum l, and $I = 1$ for odd l. We perform this expansion numerically for the full F and G expressions. The results are plotted in Figs. 10a and 10b.

The d-waves are very small and the f-waves are not visible on this scale. The contribution to f_p coming from the term with G, $f_p(G)$ is dominant. The difference between f_p and $f_p(G)$ is negligible with the present data as was also found by [17]. f_s has an appreciable imaginary part. The imaginary part of f_p is also dominated by the part from G. The imaginary part for the other waves is negligible. Similarly we see that for G the d-waves are very small. The g_f and higher waves are not visible on this scale and only g_p has a visible imaginary part.

We can discuss one possible isospin breaking effect. As described for the parametrization in Sect. 4.2 we use slightly different masses for the three K_{e4} decays. The effect this has on F and G is plotted in Fig. 11. It is obvious that with the present experimental accuracy this source of isospin breaking is fully negligible.

6.2.1 A Parametrization for $K^+ \to \pi^+\pi^- e^+\nu$

In [39] two of us proposed a parametrization to be used to extract form-factors and phase-shifts from $K_{\ell 4}$ data. Here we check how well the approximations inherent in the parametrization are satisfied by our full two-loop calculation.

The proposed parametrization was

$$\begin{aligned} F &= (\tilde{f}_s + \tilde{f}_s' s_\pi + \tilde{f}_s'' + \tilde{f}_1 s_\ell) e^{i\delta_0^0(s_\pi)} + \tilde{f}_p \sigma_\pi X \cos\theta_\pi e^{i\delta_1^1(s_\pi)}\,, \\ G &= (\tilde{g}_p + \tilde{g}_p' s_\pi + \tilde{g}_1 s_\ell) e^{i\delta_1^1(s_\pi)} + \tilde{g}_d \sigma_\pi X \cos\theta_\pi e^{i\delta_2^0(s_\pi)}\,. \end{aligned} \tag{6.17}$$

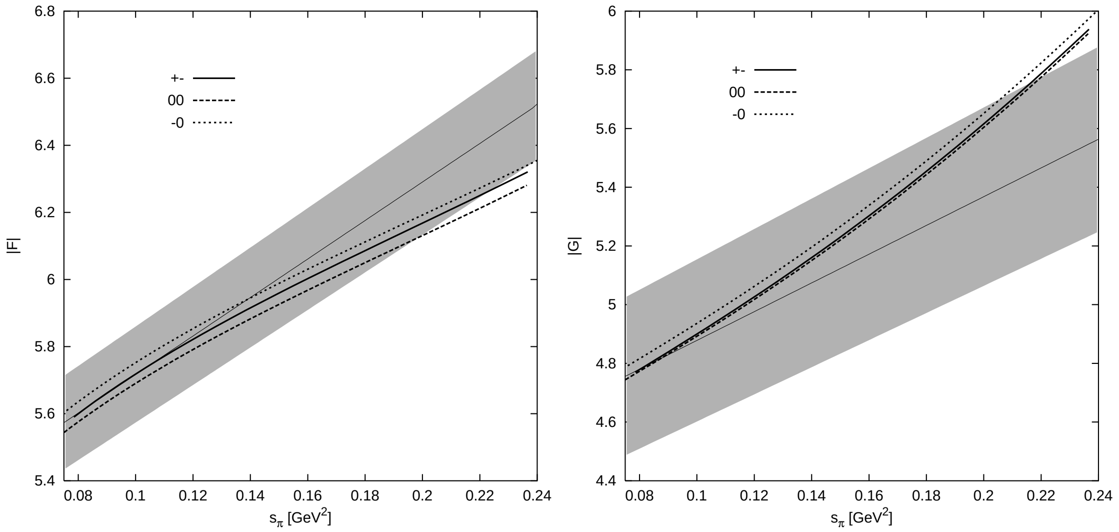

(a) (b)

Figure 11: The absolute value form-factors calculated with the different masses used for the three possible K_{e4} decays. The labels indicate the charges of the pion. The curves shown are with $\cos\theta_\pi = s_\ell = 0$. (a) $|F|$ (b) $|G|$. The experimental results are indicated with the grey bands.

We can now fit these parametrizations to the partial waves obtained in the previous section. The tilde notation is because these quantities are related to the partial-wave expansion but not identical.

As foreseen in [39] the parametrization works extremely well. We have plotted in Fig. 12 how well the absolute value of the s and p-waves of F, $\overline{f}_s$ and $\overline{f}_p$, and the absolute value of the p and d-waves of G are parametrized by Eq. (6.17). The higher partial waves are completely negligible within the experimental precision expected in the near future. The fits are performed for $s_\pi < 0.16$ GeV^2 only, since that is the region where most events of the data will be.

6.3 Partial Wave Expansion and Threshold Parameters for π-π Scattering Amplitudes

With the main fit result for the $\mathcal{O}(p^4)$ low-energy constants, we can discuss how the threshold parameters and phase-shifts in π-π scattering are affected with respect to the analysis performed in [7] and [23]. For this purpose one expands the π-π amplitude as combinations of definite isospin amplitudes in the s-channel

$$\begin{aligned}
T^0(s,t) &= 3A(s,t,u) + A(t,u,s) + A(u,s,t)\,,\\
T^1(s,t) &= A(t,u,s) - A(u,s,t)\,,\\
T^2(s,t) &= A(t,u,s) + A(u,s,t)\,. \qquad (6.18)
\end{aligned}$$

These isospin amplitudes are expanded into partial waves

$$T^I(s,t) = 32\pi \sum_{I=0}^{\infty} (2l+1) P_l(\cos\theta) t_l^I(s)\,, \qquad (6.19)$$

with s, t and u the usual Mandelstam kinematical variables, and θ is the scattering angle in the center of mass frame. Unitary implies that

$$t_l^I(s) = \left(\frac{s}{s-4m_\pi^2}\right)^{1/2} \frac{1}{2i}\{e^{2i\delta_l^I} - 1\} \qquad (6.20)$$

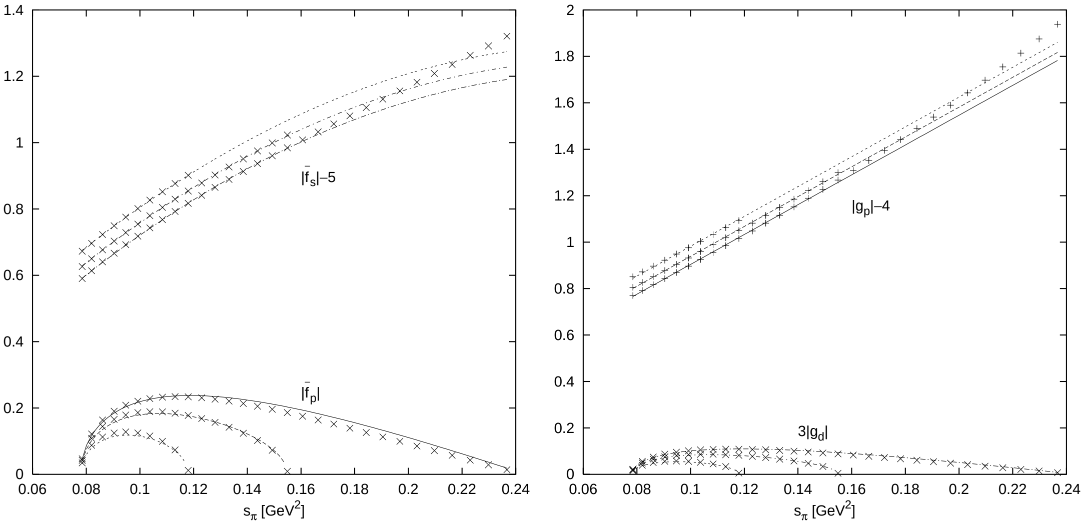

Figure 12: The agreement of the parametrization with our full two-loop result. The points are the full result. The lines are the parametrization. We have shown $s_\ell = 0, 0.01, 0.0225$ GeV^2. Notice that for comparison purposes, the main parts have been strongly shifted downwards. The fits are performed for $s_\pi < 0.16$ GeV^2 only.

holds in the elastic region $4m_\pi^2 \le s \le 16 m_\pi^2$ with real phase-shifts $\delta_l^I(s)$. $s = 4(m_\pi^2 + q^2)$ and q is the center-of-mass three-momentum of the pions. An expansion near threshold in Eq. (6.20) gives

$$\mathcal{R}e[t_l^I(s)] = q^{2l}\{a_l^I + q^2 b_l^I + \mathcal{O}(q^4)\}\,. \tag{6.21}$$

This last expansion defines the threshold parameters, the scattering lengths a_l^I and the slopes b_l^I.

The π-π scattering amplitude is known up to $\mathcal{O}(p^6)$ [7] –see also [8] for a dispersive calculation– in two-flavour CHPT. Expanding this amplitude into partial waves and in q^2, allows to obtain the threshold parameters in terms of the low-energy two-flavour $\mathcal{O}(p^4)$ constants, l_i^r. We can study the variations of these parameters with the L_i^r of this work, Eq. (6.12). However the two-loop relations between two- and three-flavour constants is unknown. A full matching would need the knowledge of processes involving the relevant constants in both CHPT versions and to the same order, this is at present not the case. We use as a first estimate the relations obtained from a $\mathcal{O}(p^4)$ matching [2]

$$\begin{aligned}
l_1^r &= 4L_1^r + 2L_3^r - \frac{1}{24}\nu_K + \mathcal{O}(p^6)\,,\\
l_2^r &= 4L_2^r - \frac{1}{12}\nu_K + \mathcal{O}(p^6)\,,\\
l_3^r &= -8L_4^r - 4L_5^r + 16L_6^r + 8L_8^r - \frac{1}{16}\nu_\eta + \mathcal{O}(p^6)\,,\\
l_4^r &= 8L_4^r + 4L_5^r - \frac{1}{2}\nu_K + \mathcal{O}(p^6)\,,
\end{aligned} \tag{6.22}$$

with

$$l_i^r = \frac{\gamma_i}{32\pi^2}\left\{\bar{l}_i + \ln(\frac{m_\pi^2}{\mu^2})\right\} \quad\text{and}\quad \nu_P = \frac{1}{32\pi^2}\left\{\ln(\frac{m_P^2}{\mu^2}) + 1\right\}\,. \tag{6.23}$$

We want to emphasize that the relations in Eq. (6.22) are affected by higher –$\mathcal{O}(p^6)$– chiral corrections which might be quite sizeable. Bearing this last issue in mind, in Table 4 we compare previous results and the experimental data [40] with the scattering lengths and slopes obtained with the values

$$\bar{l}_1 = 0.40 \pm 2.40\,,\quad \bar{l}_2 = 4.90 \pm 1.0\,,\quad \bar{l}_3 = 2.61^{+1.9}_{-2.4}\,,\quad \bar{l}_4 = 4.05 \pm 0.18\,. \tag{6.24}$$

Table 4: Threshold parameters in units of m_{π^+}. Set I is $\bar{l}_1 = -1.7$ and $\bar{l}_2 = 6.1$ while Set II is $\bar{l}_1 = -1.5$ and $\bar{l}_2 = 4.5$. Both sets have $\bar{l}_3 = 2.9$ and $\bar{l}_4 = 4.3$. Experimental values are taken from [40]. Errors are from the 68% confidence level ranges only.

	Eq. (6.12)	$\mathcal{O}(p^2)$	$\mathcal{O}(p^4)$	$\mathcal{O}(p^6)$ Set I	$\mathcal{O}(p^6)$ Set II	experiment
a_0^0	0.219 ± 0.005	0.159	0.203	0.222	0.212	0.26 ± 0.05
b_0^0	0.279 ± 0.011	0.182	0.254	0.282	0.256	0.25 ± 0.03
$-10a_0^2$	0.420 ± 0.010	0.454	0.423	0.420	0.450	0.28 ± 0.12
$-10b_0^2$	0.756 ± 0.021	0.908	0.755	0.729	0.81	0.82 ± 0.08
$10a_1^1$	0.378 ± 0.021	0.303	0.356	0.404	0.38	0.38 ± 0.02
$10^2 b_1^1$	0.59 ± 0.12	0	0.31	0.83	0.56	–
$10^2 a_2^0$	0.22 ± 0.04	0	0.16	0.28	input	0.17 ± 0.03
$-10^3 b_2^0$	0.32 ± 0.10	0	0.40	0.24	0.27	–
$10^3 a_2^2$	0.29 ± 0.10	0	0.32	0.24	input	0.13 ± 0.30
$-10^3 b_2^2$	0.36 ± 0.9	0	0.23	0.33	0.22	–
$10^4 a_3^1$	0.62 ± 0.11	0	0.20	0.65	0.48	–
$-10^4 b_3^1$	0.36 ± 0.02	0	0.15	0.38	0.37	–

Table 5: The b_i quantities as defined in [6]. Set I and Set II are defined in the caption of Table 4. Errors are the projections of the 68% confidence level domain only.

	Eq. (6.12)	$\mathcal{O}(p^6)$ Set I	$\mathcal{O}(p^6)$ Set II
$10^2 b_1$	-6.56 ± 2.10	-9.14	-8.65
$10^2 b_2$	6.50 ± 2.00	8.88	8.03
$10^3 b_3$	-1.27 ± 3.20	-4.33	-2.64
$10^3 b_4$	5.44 ± 1.25	7.08	4.83
$10^4 b_5$	2.32 ± 1.20	2.32	-0.37
$10^4 b_6$	1.16 ± 0.23	1.49	0.83

using the L_i^r of Eq. (6.12) and Eq. (6.22). The errors are given by projections on the relevant variable of the 68% confidence level domain.

In Figure 13 we plot the predictions of a_0^0 and a_0^2 for the the set of L_i^r distributed according to the χ^2 function as discussed earlier. The projection of the filled ellipse on the axis produces the errors in Table 4.

The interesting result that comes out from Table 4 is that with the large difference in the input parameters, $\bar{l}_i$, the changes obtained with Eq. (6.12) barely shift the results of set I [7]–with exception of b_1^1, a_2^0 and b_2^0. As was shown in [7], that is due to the fact that the contribution from the double logarithms almost saturates the result to $\mathcal{O}(p^6)$. However the new experiments are expected to have enough accuracy to distinguish small changes in the scattering lengths and slopes. The results of set I and II differ from [7] because of the different value of F_π and we have kept some $\mathcal{O}(p^8)$ parts which were dropped in the numerics there. Similar remarks apply to Figures 14 and 15.

The threshold parameters which were not listed in [7] were calculated by doing the relevant expansions in the formulas there to higher order, see App. B.

For completeness we also display in Table 5 the value of the variables b_i defined in [6] as a finite combination of the two-flavour low-energy constants and which determines the polynomial piece in the π-π scattering at $\mathcal{O}(p^6)$.

In Fig. 14 we show the difference of phase-shifts $\delta_0^0 - \delta_1^1$ as a function of the center of mass energy. This is the combination measured in $K_{\ell 4}$ decays. As can be appreciated the agreement

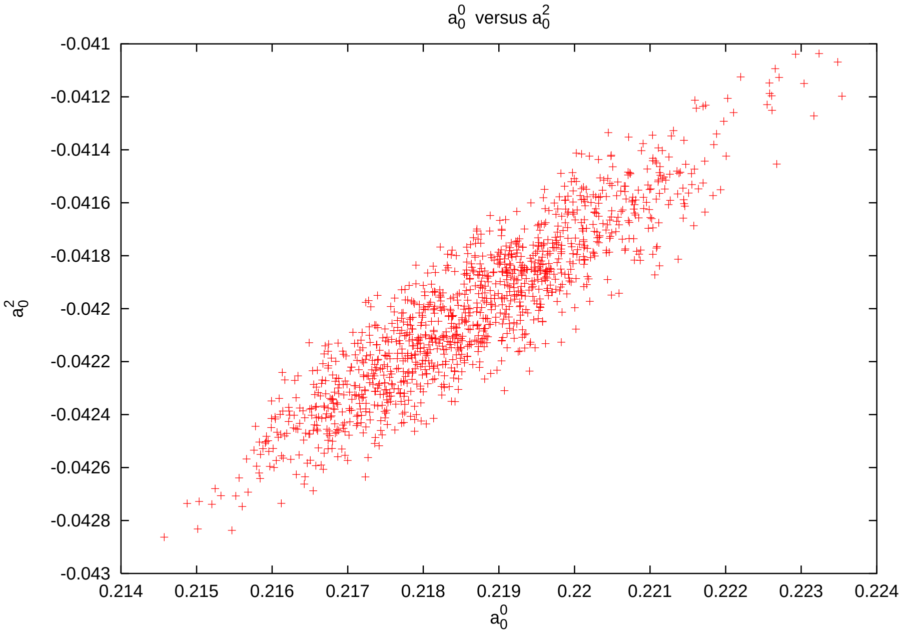

Figure 13: The prediction for the a_0^0 and a_0^2 scattering lengths for the set of L_i^r distributed according to the correlations of our main fit. Only points within the 68% confidence level domain are plotted.

between Eq. (6.24) and set I is excellent and also with the available data.

In Fig. 15 we plot the $I = 2$ s-wave phase-shift δ_0^2 as function of the center of mass energy together with available experimental data. The phase-shift corresponding to Eq. (6.24) just interpolates between both sets, I and II.

All in all, the conclusions that can be drawn from the π-π scattering analysis is that good agreement is obtained for all the threshold parameters and with $\delta_0^0 - \delta_1^1$ and a substantial improvement with the data in the δ_0^2 phase-shift case.

6.4 Vacuum Expectation Values

The lowest-order effective Lagrangian of QCD is not determined by the pion decay constant alone, but involves a second low-energy constant, B_0, which is intimately related with the vacuum expectation values of the scalar densities in the chiral limit

$$\langle 0|\overline{q}^i q^j|0\rangle = -F_0^2 B_0 \delta^{ij} \,. \tag{6.25}$$

In the absence of external scalar and pseudoscalar fields it is only observable in combination with the quark masses. It is, however, a quantity of theoretical interest and thus deserves study at the two-loop level as well. The value of B_0 depends on the way the scalar quark bilinear is defined in QCD. In particular it depends on the QCD renormalization scale μ_{QCD}.

The calculation of the one-point scalar Green function without any external pseudoscalar field is rather simple as it only involves one-loop×one-loop diagrams at $\mathcal{O}(p^6)$. The results are displayed in App. C in terms of the renormalized quantities, masses and decay constants. The procedure is the same as described in Sect. 4.1. In fact, the contributing diagrams form only a small subset of those entering in the decay constant evaluation [9]. This amounts to consider diagrams with one vertex involving the external field s part of the matrix χ defined in Sect. 2.3.

We write the full $\mathcal{O}(p^6)$ result as

$$\langle 0|\bar{q}q|0\rangle = -F_0^2 B_0 \Big\{ 1 + \langle 0|\bar{q}q|0\rangle^{(4)} + \langle 0|\bar{q}q|0\rangle^{(6)} + \dots , \Big\} . \tag{6.26}$$

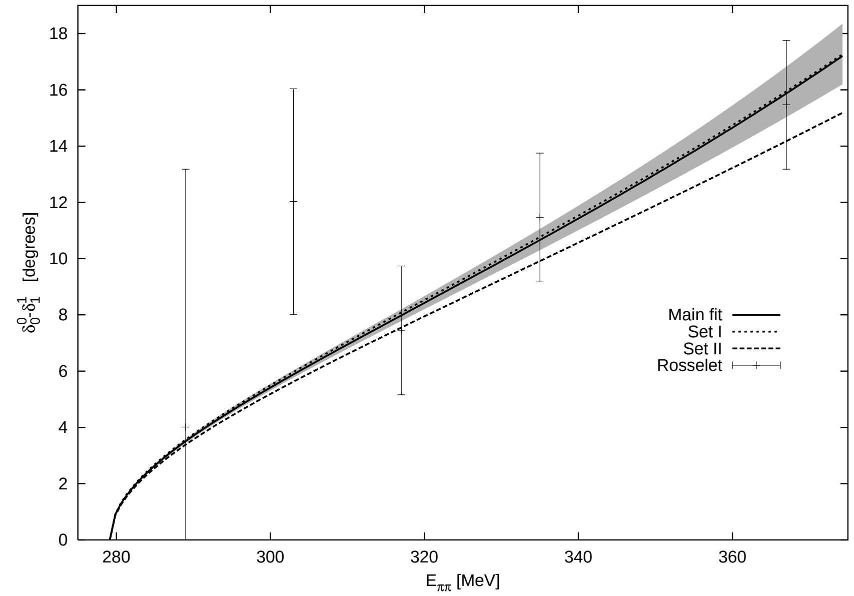

Figure 14: Difference of phase-shifts $\delta_0^0 - \delta_1^1$ plotted as a function of the center of mass energy $E_{\pi\pi}$. Data points are taken from [17]. The shaded band is the 68% confidence level range.

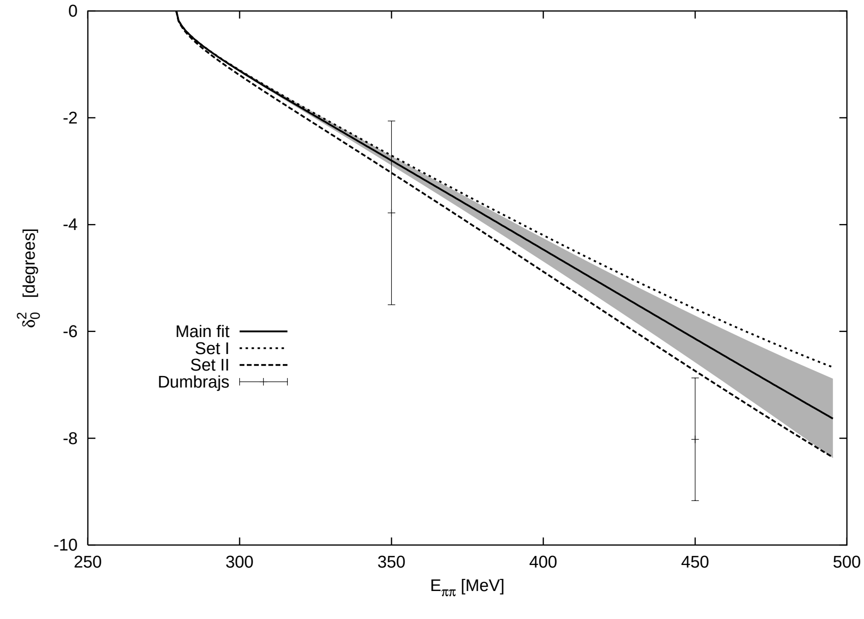

Figure 15: Phase-shift δ_0^2 as function of the center of mass energy $E_{\pi\pi}$. Data points are taken from [41]. The shaded band indicates the 68% confidence level range.

Note that $\langle 0|\bar{q}q|0\rangle^{(4)}$ and $\langle 0|\bar{q}q|0\rangle^{(6)}$ are scale independent. The soft $SU(3)$ breaking, due to the quark masses, introduces an additional dependence on the high-energy constant H_2^r, whose value also depends on the precise definition of the quark bilinear in QCD. This ambiguity is forced by the need of a subtraction in the scalar two-point function at zero separation. I.e. at the first order in perturbation theory

$$\langle 0|\bar{q}q|0\rangle = \langle 0|\bar{q}q|0\rangle\Big|_{\text{chiral limit}} - i\int d^4x \langle 0| : (\bar{q}\mathcal{M}q)(x)(\bar{q}q)(0) : |0\rangle + \mathcal{O}(\mathcal{M}^2)\,, \tag{6.27}$$

which blows up as $x \to 0$. In contrast [42] the non-analytic contribution is unambiguous. As a last point we mention that as QCD predicts [43] the vacuum condensate increases once the quark masses are switched on.

In order to quote results we need to make certain assumptions on the value of H_2^r. We use the scalar dominance assumption that leads to

$$H_2^r = 2L_8^r\,, \tag{6.28}$$

with the value of L_8^r that follows from Eq. (6.12). The numerical results are

$$\begin{aligned} \langle 0|\overline{u}u|0\rangle &= -B_0F_0^2\,[1 + 0.277 + 0.103]\,, \\ \langle 0|\overline{s}s|0\rangle &= -B_0F_0^2\,[1 + 0.832 + 0.247]\,, \end{aligned} \tag{6.29}$$

where the numbers correspond to lowest-order, $\mathcal{O}(p^4)$ and $\mathcal{O}(p^6)$ respectively.

We can also see how the vacuum expectation value changes as a function of the quark masses. For this we can use for $B_0\hat{m}$, B_0m_s and F_0 the values derived using the main fit and the higher order formulas expressed in terms of real pseudoscalar masses and F_π. We then insert these values into the expressions for the vacuum expectation values in terms of the unrenormalized masses and decay constants and vary $B_0\hat{m}$ and B_0m_s. In Fig. 16 we plotted the vacuum expectation values as a function of $m_s/(m_s)_{\text{phys}}$. The difference with the values in Eq. (6.29) comes from higher orders.

6.5 Masses and Decay Constants

In this section the pseudoscalar masses are studied using the new values for the LEC, Eq. (6.12).

All masses are written as in Eq. (4.1) with the higher orders expressed in terms of F_π and the physical masses, [9]. The separate contributions for them are

$$\begin{aligned} m_\pi^2/(m_\pi^2)_{\text{phys}} &= 0.746 + 0.007 + 0.247\,, \\ m_K^2/(m_K^2)_{\text{phys}} &= 0.695 + 0.019 + 0.286\,, \\ m_\eta^2/(m_\eta^2)_{\text{phys}} &= 0.742 - 0.040 + 0.298\,. \end{aligned} \tag{6.30}$$

where the numbers are the lowest-order, $\mathcal{O}(p^4)$ and $\mathcal{O}(p^6)$ contribution respectively.

We can now also check how the pseudoscalar masses vary with the quark masses. For this purpose we rewrite the pseudoscalar masses as

$$m^2_{phys} = m_0^2 + (m^2)^{(4)} + (m^2)^{(6)} \tag{6.31}$$

where $(m^2)^{(i)}$ is a function of $B_0\hat{m}$, B_0m_s and F_0 is defined through

$$F_\pi = F_0\left(1 + F^{(4)} + F^{(6)}\right)\,. \tag{6.32}$$

Plugging in the values following from the lowest-order contribution in Eq. (6.30) we can now vary them at a fixed ratio $m_s/\hat{m} = 24$. The result is shown in Fig. 17a. The difference with the results in Eq. (6.30) is due to higher orders. We believe that the results using the physical decay constant

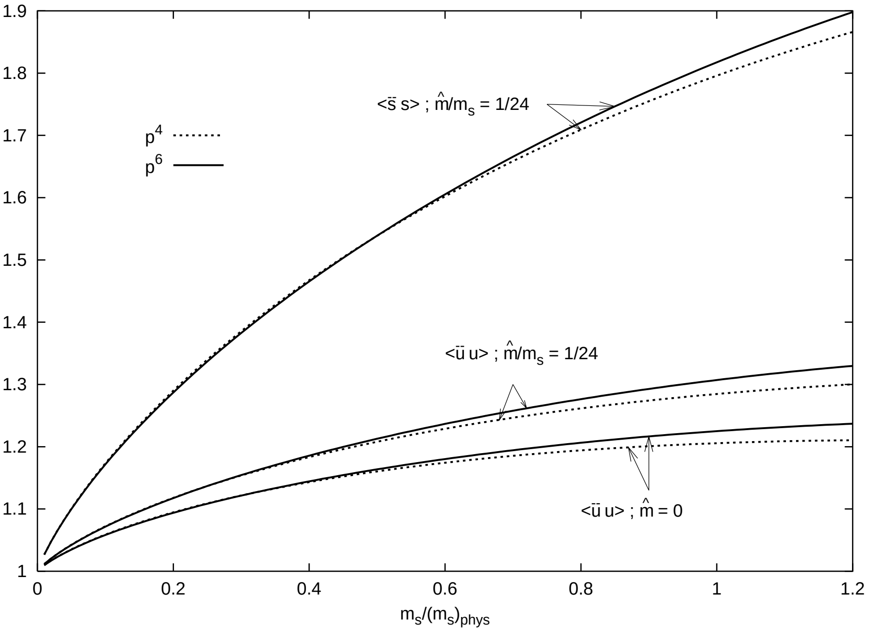

Figure 16: The vacuum expectation values (VEV) as a function of $m_s/(m_s)_{\text{phys}}$. Plotted are the strange and light quark VEV for the ratio $m_s/\hat{m} = 24$ and the light quark VEV for $\hat{m} = 0$. The curves are normalized to the chiral limit.

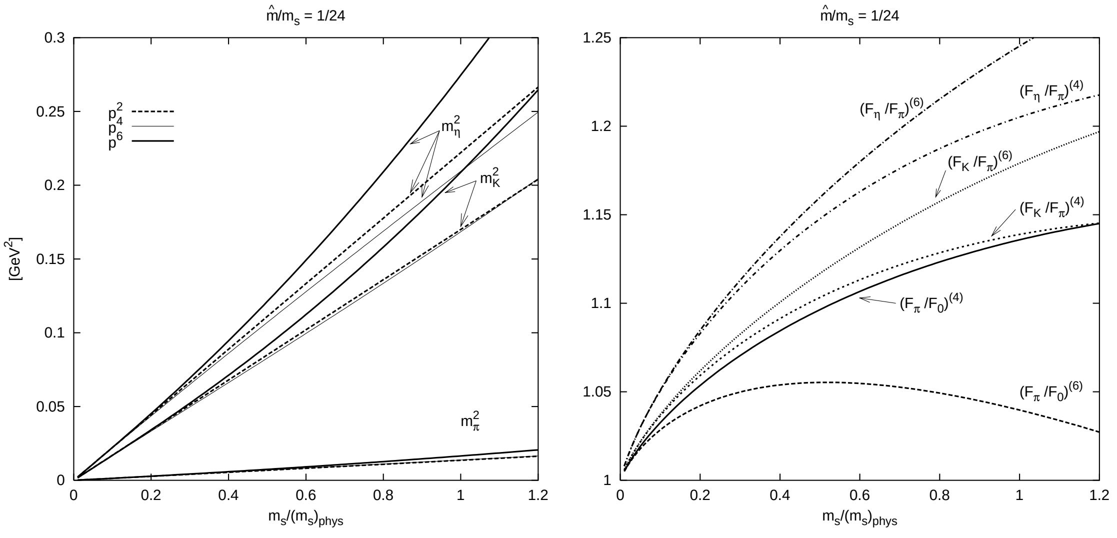

(a) (b)

Figure 17: (a) The pseudoscalar masses as a function of the quark mass at fixed ratio $\hat{m}/m_s$. The results up to $\mathcal{O}(p^2)$, $\mathcal{O}(p^4)$ and $\mathcal{O}(p^6)$ are shown for the three pseudoscalar masses. (b) The pseudoscalar decay constants as a function of the quark mass at fixed ratio $\hat{m}/m_s$. The results up to $\mathcal{O}(p^4)$ and $\mathcal{O}(p^6)$ are shown for the three pseudoscalar decay constants. For the η it is the coupling to the octet axial current.

and the physical masses in the higher orders are numerically more reliable since they incorporate part of the higher order corrections that we know will appear.

As has been previously noticed [9, 12], Eq. (6.30) the light meson masses at $\mathcal{O}(p^6)$ have a large contribution which seems in conflict with the convergence of the chiral series. The $\mathcal{O}(p^4)$ contribution is much smaller than the $\mathcal{O}(p^6)$ one. This is due to two adding effects. First, there are cancellations that happen inside the $\mathcal{O}(p^4)$ contribution. E.g. for the Kaon mass the contribution is given by 0.066(L_i^r)$-$0.047(loops)=0.019(total p^4). And second and mainly, the partial contributions at $\mathcal{O}(p^6)$, $\log\times\log$, $L_i\times\log$, $L_i\times L_j$ and pure two-loop, all go in the same direction. In other observables we typically had cancellations between these various contributions. The corrections to physically measurable quantities are in fact not so large. Eq. (6.30) can be expressed as

$$\begin{aligned} \frac{m_K^2}{m_\pi^2} &= 12.5(p^2);\;\; 12.7(p^4);\;\; 13.4(p^6)\,, \\ \frac{m_\eta^2}{m_\pi^2} &= 16.3(p^2);\;\; 15.3(p^4);\;\; 16.4(p^6)\,, \end{aligned} \tag{6.33}$$

which shows that the corrections to the ratios are much smaller.

We have checked that relaxing some of the constraints used in the fits can improve the above mentioned behaviour, one of these possibilities is discussed in Sect. 6.5.1. This does not qualitatively change any of the predictions for decay constants and $K_{\ell 4}$ form-factors made here. Other options are ad hoc choosing the values of some of the C_i^r to diminish the large $\mathcal{O}(p^6)$ corrections. Some arguments for this can be found in [36] where it is argued that resonance saturation seems to fail in the 0^{++} sector. Without new input we feel we cannot discuss further this question.

For the pseudoscalar decay constants we use the formulas of [9] and obtain using our main fit

$$\begin{aligned} F_\pi/F_0 &= 1+0.136-0.076\,, \\ F_K/F_\pi &= 1+0.134+0.086\,, \\ F_\eta/F_\pi &= 1+0.202+0.069\,. \end{aligned} \tag{6.34}$$

The η-decay constant here is the coupling of the physical η to the octet axial current. The numerical result allows to obtain

$$F_0 = 87 \text{ MeV}\,. \tag{6.35}$$

Using this value of F_0 and the lowest-order masses obtained above we can now plot the dependence of the decay constants on the quark masses. We therefore rewrite the full formulas in terms of F_0 and the quark masses. The results is shown in Fig. 17b. Again, the difference with Eq. (6.34) is higher order.

6.5.1 Large N_c, Zweig Rule

In this subsection we relax some of our assumptions to see whether the unusual relative size of the $\mathcal{O}(p^6)$ versus the $\mathcal{O}(p^4)$ contribution in Eq. (6.30) can be avoided.

We have performed fits with $m_s/\hat{m}=20$ and $m_s/\hat{m}=30$ but otherwise the same input as the main fit. Neither of these changes the relative size of the contributions to the masses qualitatively.

Another possibility is to relax the accepted common wisdom about the large N_c [44] behaviour of the low-energy constants. In particular we will focus on L_4^r and L_6^r, recapitulating some of the reasoning of [2].

In principle the main question is whether the corrections of the relative order m_s and m_s^2 to the ground state are small in comparison with the scale of the theory. If the answer is no, clearly one can not trust large N_c arguments in CHPT. Large corrections would also cast doubt on CHPT beyond one-loop calculations in the three-flavour sector.

At $\mathcal{O}(p^4)$ the effects of m_s on $\langle 0|\bar{u}u|0\rangle$, F_π and m_π^2 are small if both L_4^r and $L_6^r\sim 0$. The main question is now if higher chiral orders in those quantities are still protected against a strong m_s dependence. As it is shown, there is a range in L_4^r and L_6^r values that allows large N_c and CHPT at $\mathcal{O}(p^6)$ to coexist without conflict. Thus there is no reason to argue for large deviations from the Zweig rule.

Setting $U = \mathbf{1}$ in Eq. (2.14) the large N_c counting comes automatically, after using some trace identities [2]

$$\begin{array}{cl} \mathcal{O}(N_c) & L_1, L_2, L_3, L_5, L_8, L_9, L_{10}, H_1 \text{ and } H_2\,, \\ \mathcal{O}(1) & 2L_1 - L_2, L_4, \text{ and } L_6\,. \end{array}$$

The behaviour of the constant L_7 depends on the treatment of the singlet η_1 [2, 45]. In the constants of $\mathcal{O}(1)$ there are two different behaviours: i) the combination $2L_1^r - L_2^r$ is scale independent, but ii) L_4^r and L_6^r are scale dependent. This last dependence should cancel via the meson loops that explicitly violate large N_c. In order to estimate possible sizes we can just vary the scale inside a reasonable range. Using

$$|\Delta L_i^r| = |L_i^r(\mu_2) - L_i^r(\mu_1)| = \left|\frac{\Gamma_i}{16\pi^2}\ln\left(\frac{\mu_1}{\mu_2}\right)\right| \qquad (6.36)$$

with the choice $\mu_1 : \mu_2 = 2$, leads to

$$L_4^r = (0 \pm 0.5)\cdot 10^{-3} \text{ and } L_6^r = (0 \pm 0.3)\cdot 10^{-3}\,. \qquad (6.37)$$

The central value correspond to the main fit presented in Table 2, i.e. considering that large N_c is reached at the ρ scale. Fit 5 corresponds to use large N_c at the η scale. Neither Eq. (6.12), as shown in Eq. (6.30), nor fit 5 have the expected ordering of $\mathcal{O}(p^4)$ and $\mathcal{O}(p^6)$ contribution to the pseudoscalar masses.

Other constraints on L_4^r and L_6^r are from a recent analysis [36] based on the positivity of the fermionic measure giving a lower bound $10^3 L_6^r(M_\rho) \geq 0.13$ and on QCD sum-rules [46] which allow a band $0.2 \lesssim 10^3 L_6^r(M_\rho) \lesssim 0.6$. The latter reference also quotes $10^3 L_4^r(M_\rho) \simeq 0.4$ with unknown errors. The values and bounds from [36, 46] use $\mathcal{O}(p^4)$ expressions so these ranges might well change when those calculations are performed to $\mathcal{O}(p^6)$.

Let us now check for which ranges of L_4^r and L_6^r we find results where *all* the quantities considered up to now have an expansion of the form

$$X = X_2 + X_4 + X_6 \quad \text{with} \quad |X_2| > |X_4| > |X_6|\,, \qquad (6.38)$$

where the subscript refers to the chiral order. This is for reasonable variations always the case for $f_s(0)$, $g_p(0)$, λ_f, $\langle 0|\bar{s}s|0\rangle$ and F_η/F_π. The ratios of the pseudoscalar masses always have small corrections even if they do not always obey Eq. (6.38). We will refer to Eq. (6.38) above as a convergent series. For $\langle 0|\bar{u}u|0\rangle$ H_2^r has only a small influence but it is very large for $\langle 0|\bar{s}s|0\rangle$. For this quantity we thus allow $|X_2| \lesssim |X_4|$ since this can easily be changed by varying H_2^r.

The problematic quantities are F_π/F_0, F_K/F_π, the pseudoscalar masses separately and the vacuum expectation value $\langle 0|\bar{u}u|0\rangle$.

In Fig. 18 we show the allowed region in the plane $L_4^r - L_6^r$ consistent with Eq. (6.38) for all quantities[5]. The allowed bottom right region extends further to the right but with $(F_K/F_\pi)_4 < (F_K/F_\pi)_6$ even though both are small. As can be seen there is a region where Eq. (6.38), large N_c constraints and the other bounds are reasonably satisfied, taking into account possible higher order corrections to the bounds. Notice that a large deviation from the Zweig rule is not needed thus the bounds, Eq. (6.37), still hold.

Let us mention some general features in the behaviour of these quantities as a function of L_4^r and L_6^r. For instance, the decay constant has the broadest range (in both parameters) of convergence, while the mass seems to be the most restrictive. A low, negative value for both L_4^r and L_6^r is penalized for the mass and the vacuum expectation value. If we increase L_4^r fixing the value of L_6^r the vacuum expectation value recover once more the convergent pattern. The mass behaviour is quite unexpected: large, absolute values of L_6^r reorder the series making $\mathcal{O}(p^4) > \mathcal{O}(p^6)$, but then $\mathcal{O}(p^4)$ starts to compete with $\mathcal{O}(p^2)$ contribution.

---

[5] Quantities are only calculated on the points of the grid.

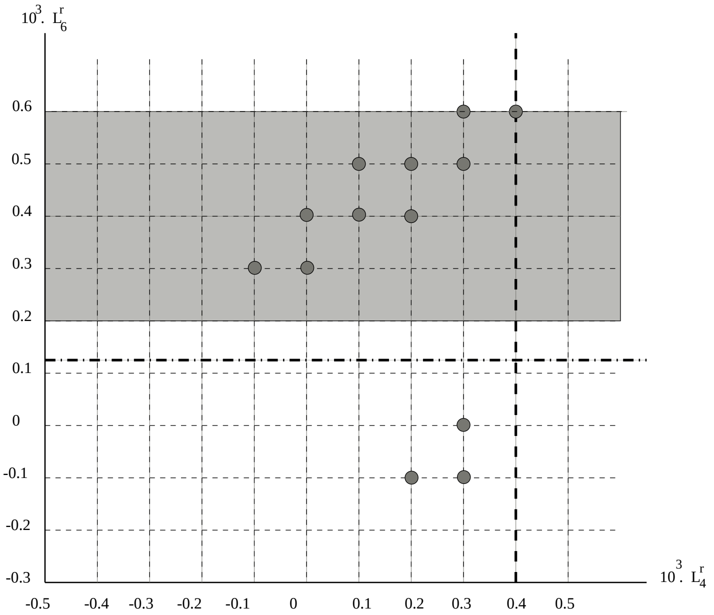

Figure 18: The L_4^r–L_6^r plane. The grey circles are the points where Eq. (6.38) is satisfied for all quantities considered in this manuscript. The grey band shows the bounds on L_6^r from QCD sum-rules. The dash-dotted line is the lower bound that follows from positivity constraints [36] and the thick dashed line the value of L_4^r of Ref. [46]. Fits were only performed for points on the grid.

7 Summary

Let us summarize our results. We have described the calculation to $\mathcal{O}(p^6)$ in CHPT of $K_{\ell 4}$ decays and of the vacuum expectation values, giving some general lines on the methods that we used and all the various checks on the final results. The explicit formulas have been presented as much as possible. The long expressions involving the vertex- and sunset-type integrals we simply parametrized, Eq. (4.4). The rest of the expressions, involving the low-energy constants, are fully listed in App. A.

We have assumed resonance saturation to estimate the new $\mathcal{O}(p^6)$ parameters that appear. With all this at hand, and large N_c assumptions on L_4^r and L_6^r we updated most of the values of the $\mathcal{O}(p^4)$ parameters, L_i^r, Eq. (6.12), testing the validity of the large N_c relation $(L_2^r - 2L_1^r)/L_3^r \sim 0$. To this end we made use of the existing $K_{\ell 4}$ data, pseudoscalar masses and decay constants. We varied the inputs over a fairly wide regime and discussed in detail the underlying assumptions and their consequences once some of them are relaxed, see Table 2. Among the assumptions it is worth to mention the discussion on relaxing the large N_c behaviour of L_4^r and L_6^r, Sect. 6.5.1. We show the allowed region in the L_4^r-L_6^r-plane, where CHPT, as a well defined perturbative series, can exist without conflict with any of the known quantities up to $\mathcal{O}(p^6)$.

We also present the comparison with previous results and model estimates, pointing out the source of the difference. As it becomes immediately clear the main source of the theoretical uncertainties resides in the $\mathcal{O}(p^6)$ constants. We mention briefly how to treat the errors and show one way of treating the correlations using a 68% confidence level distribution of the L_i^r.

Once the low-energy constants are found we use them to give the phenomenological implications on the forthcoming $K_{\ell 4}$ experiments. We review the experimental assumptions of [17] finding some of them only borderline compatible with the theoretical expression. We also show the form-factors for different values of s_ℓ and present the partial-waves predicted from the full result. This provides insight in the relevant assumptions that the new experimental analysis should make.

The results were then used to obtain predictions for the π-π threshold parameters and the π-π phase-shifts. Good agreement with the existing experimental results was obtained as is visible from Table 4 and Figs. 14 and 15. We also warned the reader about the uncertainty in the relation between the theoretical knowledge of $K_{\ell 4}$ decays and π-π scattering, reflected in the unknown $\mathcal{O}(p^6)$ corrections to the relation between the two- and three-flavour low-energy constants. This is the reason we did not include π-π scattering data in our fit as was done in [5]. We do not expect large changes in the main results when this is done.

The variations of the vacuum expectation values, decay constants and masses in terms of the lowest order parameters were shown in Figs. 16 and 17 (at fixed ratio $\hat{m} : m_s$). They show, up to $\mathcal{O}(p^6)$, no evidence of strong infrared singularities.

Acknowledgements

We thank G. Colangelo, J. Gasser, M. Knecht, B. Moussallam and J. Stern for discussions and comments. Work supported in part by TMR, EC–Contract No. ERBFMRX–CT980169 (EURODAPHNE). P.T. was supported from the Swedish Natural Science Research Council (NFR).

A Some $\mathcal{O}(p^6)$ Contributions

In this appendix we give the explicit formulas for the $\mathcal{O}(p^6)$ part of the form-factors F and G of $K_{\ell 4}$ split in parts as in Eq. (4.3).

A.1 $L_i^r, L_i^r \times L_j^r$ and $L_i^r\times$ One-loop Contributions

The F_{LL} part of F is

$$
\begin{aligned}
F_{LL}= {}& m_\pi^4/(16\pi^2)\Big\{2/3L_1^r + 2/9L_2^r - 31/108L_3^r\Big\}\\
&+m_\pi^4\Big\{ - 256L_1^rL_5^r + 64L_2^rL_5^r - 48L_3^rL_5^r + 256(L_4^r)^2 + 416L_4^rL_5^r - 512L_4^rL_6^r - 512L_4^rL_8^r\\
&+56(L_5^r)^2 - 64L_5^rL_6^r - 64L_5^rL_8^r - 16L_5^rL_9^r\Big\}\\
&+m_\pi^2m_K^2/(16\pi^2)\Big\{8/9L_2^r + 8/27L_3^r\Big\}\\
&+m_\pi^2m_K^2\Big\{L_5^r\Big(256L_1^r + 64L_3^r - 64L_4^r - 32L_5^r - 128L_6^r + 8L_9^r\Big) + 512(L_4^r)^2 - 1024L_4^rL_6^r\Big\}\\
&+m_\pi^2m_\eta^2/(16\pi^2)\Big\{ - 2L_5^r\Big\}\\
&+m_\pi^2\Big\{L_5^r\Big(128s_\pi L_1^r + 32s_\pi L_3^r + 8s_\pi L_9^r - 32t_\pi L_2^r - 16t_\pi L_3^r + 8t_\pi L_9^r - 32u_\pi L_2^r + 8u_\pi L_9^r\Big)\\
&+\overline{A}(m_\pi^2)\Big(- 404/3L_1^r + 268/3L_2^r - 13/3L_3^r + 334/3L_4^r + 31/2L_5^r - 55/6L_9^r\Big)\\
&+\overline{A}(m_K^2)\Big(- 48L_1^r + 124/3L_2^r - 53/3L_3^r + 32L_4^r + 25L_5^r - 11L_9^r\Big)\\
&+\overline{A}(m_\eta^2)\Big(16L_1^r + 20/3L_2^r - 73/18L_3^r - 10L_4^r + 73/6L_5^r - 7/2L_9^r\Big)\Big\}\\
&+m_K^4/(16\pi^2)\Big\{ - 2/3L_1^r - 19/9L_2^r - 55/108L_3^r\Big\}\\
&+m_K^4\Big\{ - 64L_2^rL_5^r - 16L_3^rL_5^r + 8(L_5^r)^2 + 8L_5^rL_9^r\Big\}\\
&+m_K^2m_\eta^2/(16\pi^2)\Big\{8L_5^r\Big\}\\
&+m_K^2\Big\{L_5^r\Big(- 128s_\pi L_1^r - 32s_\pi L_3^r - 8s_\pi L_9^r + 32t_\pi L_2^r + 16t_\pi L_3^r - 8t_\pi L_9^r + 32u_\pi L_2^r - 8u_\pi L_9^r\Big)\\
&+\overline{A}(m_\pi^2)\Big(54L_2^r + 27/2L_3^r + 4/3L_4^r - 14/3L_5^r - 55/12L_9^r\Big)\\
&+\overline{A}(m_K^2)\Big(- 4/3L_1^r + 130/3L_2^r + 1/2L_3^r + 24L_4^r + 8L_5^r - 11/2L_9^r\Big)
\end{aligned}
$$

$$+\overline{A}(m_\eta^2)\Big(-32/3L_1^r+10/3L_2^r-49/18L_3^r+4L_4^r-8/3L_5^r-7/4L_9^r\Big)\Big\}$$

$$+m_\eta^4/(16\pi^2)\Big\{L_2^r+1/2L_3^r-6L_5^r\Big\}$$

$$+m_\eta^2\overline{A}(m_\eta^2)\Big\{8L_1^r+2L_2^r+L_3^r+3L_5^r\Big\}$$

$$+\overline{B}(m_\pi^2,m_\pi^2,s_\pi)m_\pi^4\Big\{80L_1^r+32L_3^r-80L_4^r-46L_5^r+48L_6^r+24L_8^r+6L_9^r\Big\}$$

$$+\overline{B}(m_\pi^2,m_\pi^2,s_\pi)m_\pi^2m_K^2\Big\{-32L_4^r+3L_9^r\Big\}$$

$$+\overline{B}(m_\pi^2,m_\pi^2,s_\pi)m_\pi^2/3\Big\{s_\pi\Big(-200L_1^r-68L_3^r+116L_4^r+46L_5^r-21L_9^r\Big)-9t_\pi L_9^r-9u_\pi L_9^r\Big\}$$

$$+\overline{B}(m_\pi^2,m_\pi^2,s_\pi)\Big\{m_K^2\Big(32/3s_\pi L_4^r-2s_\pi L_9^r\Big)+2s_\pi^2L_9^r+2s_\pi t_\pi L_9^r+2s_\pi u_\pi L_9^r\Big\}$$

$$+\overline{B}(m_\pi^2,m_K^2,t_\pi)m_\pi^4\Big\{8/3L_2^r-8/3L_3^r+14/3L_4^r+3L_5^r-L_9^r\Big\}$$

$$+\overline{B}(m_\pi^2,m_K^2,t_\pi)m_\pi^2m_K^2\Big\{-8/3L_2^r-16/3L_3^r+8/3L_4^r+5L_5^r-20/3L_6^r-3/2L_9^r\Big\}$$

$$+\overline{B}(m_\pi^2,m_K^2,t_\pi)m_\pi^2\Big\{s_\pi/2L_9^r+t_\pi\Big(8/3L_2^r+16/3L_3^r+14/3L_4^r-3L_5^r+3/2L_9^r\Big)+u_\pi/2L_9^r\Big\}$$

$$+\overline{B}(m_\pi^2,m_K^2,t_\pi)m_K^4\Big\{8/3L_4^r+4/3L_5^r-40/3L_6^r-20/3L_8^r-1/2L_9^r\Big\}$$

$$+\overline{B}(m_\pi^2,m_K^2,t_\pi)m_K^2\Big\{1/2s_\pi L_9^r+4t_\pi L_4^r+2t_\pi L_5^r+t_\pi L_9^r+1/2u_\pi L_9^r\Big\}$$

$$+\overline{B}(m_\pi^2,m_K^2,t_\pi)\Big\{-1/2s_\pi t_\pi L_9^r-1/2t_\pi^2L_9^r-1/2t_\pi u_\pi L_9^r\Big\}$$

$$+\overline{B}(m_\pi^2,m_K^2,u_\pi)m_\pi^4\Big\{56/3L_2^r+64/3L_4^r+20/3L_5^r-8/3L_9^r\Big\}$$

$$+\overline{B}(m_\pi^2,m_K^2,u_\pi)m_\pi^2m_K^2\Big\{40/3L_2^r+32L_6^r+16L_8^r-8/3L_9^r\Big\}$$

$$+\overline{B}(m_\pi^2,m_K^2,u_\pi)4/3m_\pi^2\Big\{s_\pi L_9^r+t_\pi L_9^r-10u_\pi L_2^r-8u_\pi L_4^r-4u_\pi L_5^r+2u_\pi L_9^r\Big\}$$

$$+\overline{B}(m_\pi^2,m_K^2,u_\pi)m_K^4\Big\{-16/3L_4^r-8/3L_5^r-2/3L_9^r\Big\}$$

$$+\overline{B}(m_\pi^2,m_K^2,u_\pi)m_K^2\Big\{2/3s_\pi L_9^r+2/3t_\pi L_9^r+16/3u_\pi L_4^r+8/3u_\pi L_5^r+4/3u_\pi L_9^r\Big\}$$

$$+\overline{B}(m_\pi^2,m_K^2,u_\pi)\Big\{-2/3s_\pi u_\pi L_9^r-2/3t_\pi u_\pi L_9^r-2/3u_\pi^2L_9^r\Big\}$$

$$+\overline{B}(m_K^2,m_K^2,s_\pi)m_\pi^2m_K^2\Big\{96L_1^r+24L_3^r-96L_4^r-24L_5^r+96L_6^r+48L_8^r\Big\}$$

$$+\overline{B}(m_K^2,m_K^2,s_\pi)m_\pi^2s_\pi\Big\{-256/3L_1^r+80/3L_2^r-16L_3^r+42L_4^r+10L_5^r-4L_9^r\Big\}$$

$$+\overline{B}(m_K^2,m_K^2,s_\pi)m_K^2s_\pi\Big\{-80L_1^r+16L_2^r-20L_3^r+28L_4^r-2L_9^r\Big\}$$

$$+\overline{B}(m_K^2,m_K^2,s_\pi)\Big\{48s_\pi^2L_1^r+48s_\pi^2L_2^r+24s_\pi^2L_3^r+2s_\pi^2L_9^r-16/3s_\pi t_\pi L_1^r-40/3s_\pi t_\pi L_2^r$$

$$-4s_\pi t_\pi L_3^r+2s_\pi t_\pi L_9^r-16/3s_\pi u_\pi L_1^r-40/3s_\pi u_\pi L_2^r-4s_\pi u_\pi L_3^r+2s_\pi u_\pi L_9^r\Big\}$$

$$+\overline{B}(m_\eta^2,m_K^2,t_\pi)m_\pi^4\Big\{-4L_3^r-28/3L_4^r-16/9L_5^r+8/3L_6^r+32/3L_7^r+8L_8^r-8/3L_9^r\Big\}$$

$$+\overline{B}(m_\eta^2,m_K^2,t_\pi)m_\pi^2m_K^2/3\Big\{2/3L_3^r-46/3L_4^r-22/3L_5^r+20L_6^r+32L_7^r+16L_8^r-2L_9^r\Big\}$$

$$+\overline{B}(m_\eta^2,m_K^2,t_\pi)m_\pi^2/3\Big\{\Big(3L_3^r+4L_9^r\Big)\Big(s_\pi+u_\pi\Big)+43/3t_\pi L_3^r+12t_\pi L_4^r-2t_\pi L_5^r+10t_\pi L_9^r\Big\}$$

$$+\overline{B}(m_\eta^2,m_K^2,t_\pi)m_K^4/3\Big\{-14/3L_3^r+20L_4^r+38/3L_5^r+8L_6^r-64L_7^r-28L_8^r+L_9^r\Big\}$$

$$+\overline{B}(m_\eta^2,m_K^2,t_\pi)m_K^2/3\Big\{\Big(-3L_3^r-L_9^r\Big)\Big(s_\pi+u_\pi\Big)+47/3t_\pi L_3^r+24t_\pi L_4^r-4t_\pi L_5^r+2t_\pi L_9^r\Big\}$$

$$+\overline{B}(m_\eta^2, m_K^2, t_\pi)\Big\{-4L_4^r m_K^2 m_\eta^2 - 2L_4^r m_\pi^2 m_\eta^2 - 2L_5^r m_\eta^4\Big\}$$

$$+\overline{B}(m_\eta^2, m_K^2, t_\pi)\Big\{-1/3 s_\pi t_\pi L_3^r - s_\pi t_\pi L_9^r - 7/3 t_\pi^2 L_3^r - t_\pi^2 L_9^r - 1/3 t_\pi u_\pi L_3^r - t_\pi u_\pi L_9^r\Big\}$$

$$+\overline{B}(m_\eta^2, m_\eta^2, s_\pi) m_\pi^4\Big\{56/9 L_4^r + 10/3 L_5^r - 16 L_6^r + 64 L_7^r + 24 L_8^r - 2L_9^r\Big\}$$

$$+\overline{B}(m_\eta^2, m_\eta^2, s_\pi) m_\pi^2 m_K^2\Big\{-224/9 L_4^r - 16/3 L_5^r + 64 L_6^r - 64 L_7^r - L_9^r\Big\}$$

$$+\overline{B}(m_\eta^2, m_\eta^2, s_\pi) m_\pi^2 m_\eta^2\Big\{112/3 L_1^r + 32/9 L_3^r - 24 L_4^r - 4L_5^r\Big\}$$

$$+\overline{B}(m_\eta^2, m_\eta^2, s_\pi) m_\pi^2\Big\{-4 s_\pi L_4^r - 2 s_\pi L_5^r + s_\pi L_9^r + t_\pi L_9^r + u_\pi L_9^r\Big\}$$

$$+\overline{B}(m_\eta^2, m_\eta^2, s_\pi)\Big\{16 s_\pi L_4^r m_K^2 + m_\eta^2\Big(-24 s_\pi L_1^r - 4 s_\pi L_3^r\Big)\Big\}$$

$$+\overline{B}_1(m_\pi^2, m_\pi^2, s_\pi) m_\pi^4\Big\{-8L_3^r + 32 L_4^r + 40 L_5^r + 64 L_6^r + 32 L_8^r - 8L_9^r\Big\}$$

$$+\overline{B}_1(m_\pi^2, m_\pi^2, s_\pi) m_\pi^2 m_K^2\Big\{-32 L_2^r - 8L_3^r + 64 L_4^r - 4L_9^r\Big\}$$

$$+\overline{B}_1(m_\pi^2, m_\pi^2, s_\pi) m_\pi^2\Big\{-368/3 s_\pi L_1^r + 80/3 s_\pi L_2^r - 32 s_\pi L_3^r + 24 s_\pi L_4^r + 8/3 s_\pi L_9^r + 16 t_\pi L_2^r$$

$$+4 t_\pi L_3^r + 4 t_\pi L_9^r + 16 u_\pi L_2^r + 4 u_\pi L_3^r + 4 u_\pi L_9^r\Big\}$$

$$+\overline{B}_1(m_\pi^2, m_\pi^2, s_\pi) m_K^2\Big\{128/3 s_\pi L_2^r + 32/3 s_\pi L_3^r - 32/3 s_\pi L_4^r - 2/3 s_\pi L_9^r\Big\}$$

$$+\overline{B}_1(m_\pi^2, m_\pi^2, s_\pi)\Big\{200/3 s_\pi^2 L_1^r + 12 s_\pi^2 L_2^r + 68/3 s_\pi^2 L_3^r + 2/3 s_\pi^2 L_9^r - 64/3 s_\pi t_\pi L_2^r$$

$$-16/3 s_\pi t_\pi L_3^r + 2/3 s_\pi t_\pi L_9^r - 64/3 s_\pi u_\pi L_2^r - 16/3 s_\pi u_\pi L_3^r + 2/3 s_\pi u_\pi L_9^r\Big\}$$

$$+\overline{B}_1(m_\pi^2, m_K^2, t_\pi) m_\pi^4\Big\{-8L_1^r - 20 L_2^r - 18 L_3^r - 46/3 L_4^r + 16/3 L_5^r - 4/3 L_9^r\Big\}$$

$$+\overline{B}_1(m_\pi^2, m_K^2, t_\pi) m_\pi^2 m_K^2/3\Big\{16 L_1^r + 8L_2^r - 2L_3^r + 56 L_4^r + 36 L_5^r - 76 L_6^r - 48 L_8^r - 4L_9^r\Big\}$$

$$+\overline{B}_1(m_\pi^2, m_K^2, t_\pi) m_\pi^2/3\Big\{8 s_\pi L_1^r + 4 s_\pi L_2^r + 5 s_\pi L_3^r + 2 s_\pi L_9^r - 24 t_\pi L_1^r + 12 t_\pi L_2^r + 39 t_\pi L_3^r$$

$$+22 t_\pi L_4^r - 20 t_\pi L_5^r + 10 t_\pi L_9^r + 8 u_\pi L_1^r + 4 u_\pi L_2^r + 5 u_\pi L_3^r + 2 u_\pi L_9^r\Big\}$$

$$+\overline{B}_1(m_\pi^2, m_K^2, t_\pi) m_K^4/3\Big\{8L_1^r + 4L_2^r - 4L_3^r - 40 L_4^r - 20 L_5^r + 40 L_6^r + 20 L_8^r - L_9^r\Big\}$$

$$+\overline{B}_1(m_\pi^2, m_K^2, t_\pi) m_K^2/3\Big\{-8 s_\pi L_1^r - 4 s_\pi L_2^r + s_\pi L_3^r + s_\pi L_9^r - 8 t_\pi L_1^r + 4 t_\pi L_2^r$$

$$+17 t_\pi L_3^r - 4 t_\pi L_4^r - 2 t_\pi L_5^r + 5 t_\pi L_9^r - 8 u_\pi L_1^r - 4 u_\pi L_2^r + u_\pi L_3^r + u_\pi L_9^r\Big\}$$

$$+\overline{B}_1(m_\pi^2, m_K^2, t_\pi)\Big\{8 s_\pi t_\pi L_1^r + 4 s_\pi t_\pi L_2^r - s_\pi t_\pi L_3^r - 4 s_\pi t_\pi L_9^r - 8 t_\pi^2 L_2^r - 13 t_\pi^2 L_3^r$$

$$-4 t_\pi^2 L_9^r + 8 t_\pi u_\pi L_1^r + 4 t_\pi u_\pi L_2^r - t_\pi u_\pi L_3^r - 4 t_\pi u_\pi L_9^r\Big\}/3$$

$$+\overline{B}_1(m_\pi^2, m_K^2, u_\pi) m_\pi^4\Big\{-40 L_1^r - 20 L_2^r - 20 L_3^r - 56/3 L_4^r\Big\}$$

$$+\overline{B}_1(m_\pi^2, m_K^2, u_\pi) m_\pi^2 m_K^2\Big\{-32/3 L_1^r - 16/3 L_2^r - 16/3 L_3^r - 16/3 L_4^r\Big\}$$

$$+\overline{B}_1(m_\pi^2, m_K^2, u_\pi) m_\pi^2/3\Big\{32 s_\pi L_1^r + 16 s_\pi L_2^r + 16 s_\pi L_3^r + 32 t_\pi L_1^r + 16 t_\pi L_2^r + 16 t_\pi L_3^r$$

$$+48 u_\pi L_1^r - 48 u_\pi L_2^r + 24 u_\pi L_3^r + 8 u_\pi L_4^r - 4 u_\pi L_5^r + 4 u_\pi L_9^r\Big\}$$

$$+\overline{B}_1(m_\pi^2, m_K^2, u_\pi) m_K^4/3\Big\{-40 L_1^r - 20 L_2^r - 20 L_3^r + 24 L_4^r\Big\}$$

$$+\overline{B}_1(m_\pi^2, m_K^2, u_\pi) m_K^2\Big\{16/3 s_\pi L_1^r + 8/3 s_\pi L_2^r + 8/3 s_\pi L_3^r + 16/3 t_\pi L_1^r + 8/3 t_\pi L_2^r$$

$$+8/3t_\pi L_3^r + 16/3u_\pi L_1^r - 32/3u_\pi L_2^r + 8/3u_\pi L_3^r - 56/3u_\pi L_4^r - 16/3u_\pi L_5^r + 2/3u_\pi L_9^r\Big\}$$

$$+\overline{B}_1(m_\pi^2, m_K^2, u_\pi)1/3\Big\{ - 16s_\pi u_\pi L_1^r - 8s_\pi u_\pi L_2^r - 8s_\pi u_\pi L_3^r - 2s_\pi u_\pi L_9^r - 16t_\pi u_\pi L_1^r$$

$$-8t_\pi u_\pi L_2^r - 8t_\pi u_\pi L_3^r - 2t_\pi u_\pi L_9^r + 24u_\pi^2 L_1^r + 52u_\pi^2 L_2^r + 12u_\pi^2 L_3^r - 2u_\pi^2 L_9^r\Big\}$$

$$+\overline{B}_1(m_K^2, m_\pi^2, t_\pi)m_\pi^2 m_K^2\Big\{ - 10/3L_4^r + 20/3L_6^r\Big\}$$

$$+\overline{B}_1(m_K^2, m_\pi^2, t_\pi)m_K^4\Big\{ - 20/3L_4^r - 10/3L_5^r + 40/3L_6^r + 20/3L_8^r\Big\}$$

$$+\overline{B}_1(m_K^2, m_K^2, s_\pi)m_\pi^2\Big\{256/3s_\pi L_1^r - 80/3s_\pi L_2^r + 16s_\pi L_3^r - 36s_\pi L_4^r - 2s_\pi L_5^r + 2s_\pi L_9^r\Big\}$$

$$+\overline{B}_1(m_K^2, m_K^2, s_\pi)m_K^2\Big\{32/3s_\pi L_1^r - 64/3s_\pi L_2^r + 16s_\pi L_4^r + s_\pi L_9^r\Big\}$$

$$+\overline{B}_1(m_K^2, m_K^2, s_\pi)\Big\{ - 80/3s_\pi^2 L_1^r - 200/3s_\pi^2 L_2^r - 22s_\pi^2 L_3^r - s_\pi^2 L_9^r + 16/3s_\pi t_\pi L_1^r$$

$$+40/3s_\pi t_\pi L_2^r + 4s_\pi t_\pi L_3^r - s_\pi t_\pi L_9^r + 16/3s_\pi u_\pi L_1^r + 40/3s_\pi u_\pi L_2^r + 4s_\pi u_\pi L_3^r - s_\pi u_\pi L_9^r\Big\}$$

$$+\overline{B}_1(m_K^2, m_\eta^2, t_\pi)m_\pi^4\Big\{1/3L_4^r + 1/3L_5^r - 8/3L_6^r - 8/3L_8^r\Big\}$$

$$+\overline{B}_1(m_K^2, m_\eta^2, t_\pi)\Big\{m_\pi^2 m_K^2\Big(25/3L_4^r + 7L_5^r - 20/3L_6^r\Big) + m_\pi^2\Big(- 3t_\pi L_4^r - 3t_\pi L_5^r\Big)\Big\}$$

$$+\overline{B}_1(m_K^2, m_\eta^2, t_\pi)\Big\{m_K^4\Big(46/3L_4^r + 2/3L_5^r - 8/3L_6^r - 4/3L_8^r\Big) - 6t_\pi L_4^r m_K^2\Big\}$$

$$+\overline{B}_1(m_\eta^2, m_K^2, t_\pi)m_\pi^4\Big\{25/3L_3^r + 55/3L_4^r + 16/9L_5^r - 8/3L_6^r - 32/3L_7^r - 8L_8^r + 17/3L_9^r\Big\}$$

$$+\overline{B}_1(m_\eta^2, m_K^2, t_\pi)m_\pi^2 m_K^2/3\Big\{ - 56/3L_3^r + 73L_4^r + 22/3L_5^r - 20L_6^r - 32L_7^r - 16L_8^r - 5/2L_9^r\Big\}$$

$$+\overline{B}_1(m_\eta^2, m_K^2, t_\pi)m_\pi^2\Big\{ - 19/9s_\pi L_3^r - 17/6s_\pi L_9^r - 79/9t_\pi L_3^r - 3t_\pi L_4^r + 2t_\pi L_5^r - 35/6t_\pi L_9^r$$

$$-19/9u_\pi L_3^r - 17/6u_\pi L_9^r\Big\}$$

$$+\overline{B}_1(m_\eta^2, m_K^2, t_\pi)m_K^4/3\Big\{ - 7/3L_3^r - 74L_4^r - 38/3L_5^r - 8L_6^r + 64L_7^r + 28L_8^r - 11/2L_9^r\Big\}$$

$$+\overline{B}_1(m_\eta^2, m_K^2, t_\pi)\Big\{2L_4^r m_\pi^2 m_\eta^2 + 4L_4^r m_K^2 m_\eta^2 + 2L_5^r m_\eta^4\Big\}$$

$$+\overline{B}_1(m_\eta^2, m_K^2, t_\pi)m_K^2\Big\{25/9s_\pi L_3^r + 11/6s_\pi L_9^r - 41/9t_\pi L_3^r - 6t_\pi L_4^r + 4t_\pi L_5^r + 1/3t_\pi L_9^r$$

$$+25/9u_\pi L_3^r + 11/6u_\pi L_9^r\Big\}$$

$$+\overline{B}_1(m_\eta^2, m_K^2, t_\pi)\Big\{\Big(1/3L_3^r + 3/2L_9^r\Big)\Big(s_\pi + u_\pi\Big)t_\pi + 4t_\pi^2 L_3^r + 3/2t_\pi^2 L_9^r\Big\}$$

$$+\overline{B}_1(m_\eta^2, m_\eta^2, s_\pi)\Big\{\Big(m_\pi^4 + m_\pi^2 m_K^2\Big)\Big(32/3L_2^r + 8/9L_3^r\Big)\Big\}$$

$$+\overline{B}_1(m_\eta^2, m_\eta^2, s_\pi)m_\pi^2\Big\{ - 112/3s_\pi L_1^r - 32/9s_\pi L_3^r + 24s_\pi L_4^r + 4s_\pi L_5^r - 16/3t_\pi L_2^r$$

$$-4/9t_\pi L_3^r - 16/3u_\pi L_2^r - 4/9u_\pi L_3^r\Big\}$$

$$+\overline{B}_1(m_\eta^2, m_\eta^2, s_\pi)\Big\{24s_\pi^2 L_1^r + 12s_\pi^2 L_2^r + 8s_\pi^2 L_3^r\Big\}$$

$$+\overline{B}_{21}(m_\pi^2, m_\pi^2, s_\pi)\Big\{\Big(m_\pi^4 + m_\pi^2 m_K^2\Big)\Big(32L_2^r + 8L_3^r\Big)\Big\}$$

$$+\overline{B}_{21}(m_\pi^2, m_\pi^2, s_\pi)\Big\{m_\pi^2\Big(- 32s_\pi L_2^r - 32/3s_\pi L_4^r - 40/3s_\pi L_5^r + 8/3s_\pi L_9^r - 16t_\pi L_2^r$$

$$-4t_\pi L_3^r - 16u_\pi L_2^r - 4u_\pi L_3^r\Big) + m_K^2\Big(- 64/3s_\pi L_4^r + 4/3s_\pi L_9^r\Big)\Big\}$$

$$+\overline{B}_{21}(m_\pi^2, m_\pi^2, s_\pi)4/3\Big\{44s_\pi^2 L_1^r + 9s_\pi^2 L_2^r + 16s_\pi^2 L_3^r - s_\pi^2 L_9^r - s_\pi t_\pi L_9^r - s_\pi u_\pi L_9^r\Big\}$$

$$+\overline{B}_{21}(m_\pi^2, m_K^2, t_\pi) m_\pi^4 \Big\{ 40L_1^r + 20L_2^r + 10L_3^r + 16L_4^r + 9L_5^r - 3L_9^r \Big\}$$

$$+\overline{B}_{21}(m_\pi^2, m_K^2, t_\pi) m_\pi^2 m_K^2 \Big\{ -112/3L_1^r - 56/3L_2^r - 10/3L_3^r - 8L_4^r - 9L_5^r + 3/2L_9^r \Big\}$$

$$+\overline{B}_{21}(m_\pi^2, m_K^2, t_\pi) m_\pi^2/3 \Big\{ -32s_\pi L_1^r - 16s_\pi L_2^r - 8s_\pi L_3^r + s_\pi/2L_9^r + 48t_\pi L_2^r + 36t_\pi L_3^r$$

$$-52t_\pi L_4^r - 23t_\pi L_5^r + 19/2t_\pi L_9^r - 32u_\pi L_1^r - 16u_\pi L_2^r - 8u_\pi L_3^r + u_\pi/2L_9^r \Big\}$$

$$+\overline{B}_{21}(m_\pi^2, m_K^2, t_\pi) m_K^4 \Big\{ -8/3L_1^r - 4/3L_2^r + 4/3L_3^r - 8L_4^r + 3/2L_9^r \Big\}$$

$$+\overline{B}_{21}(m_\pi^2, m_K^2, t_\pi) m_K^2 \Big\{ 32/3s_\pi L_1^r + 16/3s_\pi L_2^r + 2/3s_\pi L_3^r - 3/2s_\pi L_9^r - 16/3t_\pi L_4^r$$

$$-20/3t_\pi L_5^r - 2/3t_\pi L_9^r + 32/3u_\pi L_1^r + 16/3u_\pi L_2^r + 2/3u_\pi L_3^r - 3/2u_\pi L_9^r \Big\}$$

$$+\overline{B}_{21}(m_\pi^2, m_K^2, t_\pi) \Big\{ -5/6s_\pi t_\pi L_9^r - 8t_\pi^2 L_1^r - 44/3t_\pi^2 L_2^r - 34/3t_\pi^2 L_3^r - 5/6t_\pi^2 L_9^r - 5/6t_\pi u_\pi L_9^r \Big\}$$

$$+\overline{B}_{21}(m_\pi^2, m_K^2, u_\pi) \Big\{ \Big(20m_\pi^4 + 16/3m_\pi^2 m_K^2 \Big) \Big(2L_1^r + L_2^r + L_3^r \Big) \Big\}$$

$$+\overline{B}_{21}(m_\pi^2, m_K^2, u_\pi) \Big\{ \Big(16/3m_\pi^2 + 8/3m_K^2 \Big) \Big(s_\pi + t_\pi \Big) \Big(-2L_1^r - L_2^r - L_3^r \Big) \Big\}$$

$$+\overline{B}_{21}(m_\pi^2, m_K^2, u_\pi) \Big\{ m_K^4 \Big(40/3L_1^r + 20/3L_2^r + 20/3L_3^r \Big) - 8u_\pi^2 L_1^r + 4/3u_\pi^2 L_2^r - 4u_\pi^2 L_3^r \Big\}$$

$$+\overline{B}_{21}(m_K^2, m_K^2, s_\pi) \Big\{ 64/3s_\pi^2 L_1^r - 56/3s_\pi^2 L_2^r + 2s_\pi^2 L_3^r \Big\}$$

$$+\overline{B}_{21}(m_K^2, m_\eta^2, t_\pi) \Big\{ m_\pi^4 \Big(9L_4^r + 9L_5^r \Big) + m_\pi^2 m_K^2 \Big(9L_4^r - 9L_5^r \Big) + m_\pi^2 \Big(-3t_\pi L_4^r - 3t_\pi L_5^r \Big) \Big\}$$

$$+\overline{B}_{21}(m_K^2, m_\eta^2, t_\pi) \Big\{ m_K^4 \Big(-18L_4^r \Big) + m_K^2 \Big(-6t_\pi L_4^r \Big) \Big\}$$

$$+\overline{B}_{21}(m_\eta^2, m_K^2, t_\pi) \Big\{ m_\pi^4 \Big(-13/3L_3^r - 9L_4^r - 3L_9^r \Big) + m_\pi^2 m_K^2 \Big(56/9L_3^r - 9L_4^r + 3/2L_9^r \Big) \Big\}$$

$$+\overline{B}_{21}(m_\eta^2, m_K^2, t_\pi) \Big\{ m_\pi^2 \Big(\Big(10/9s_\pi + 4t_\pi + 10/9u_\pi \Big) L_3^r - t_\pi L_4^r - 4/3t_\pi L_5^r$$

$$+\Big(3s_\pi + 5t_\pi + 3u_\pi \Big) L_9^r/2 \Big) + m_K^4 \Big(7/9L_3^r + 18L_4^r + 3/2L_9^r \Big) + m_K^2 \Big(-16/9s_\pi L_3^r$$

$$-3/2s_\pi L_9^r - 2t_\pi L_4^r - 8/3t_\pi L_5^r - t_\pi L_9^r - 16/9u_\pi L_3^r - 3/2u_\pi L_9^r \Big) \Big\}$$

$$+\overline{B}_{21}(m_\eta^2, m_K^2, t_\pi) \Big\{ -1/2s_\pi t_\pi L_9^r - 5/3t_\pi^2 L_3^r - 1/2t_\pi^2 L_9^r - 1/2t_\pi u_\pi L_9^r \Big\}$$

$$-\overline{B}_{21}(m_\eta^2, m_\eta^2, s_\pi) \Big\{ \Big(m_\pi^4 + m_\pi^2 m_K^2 \Big) \Big(32/3L_2^r + 8/9L_3^r \Big) \Big\}$$

$$+\overline{B}_{21}(m_\eta^2, m_\eta^2, s_\pi) m_\pi^2 \Big\{ 16/3t_\pi L_2^r + 4/9t_\pi L_3^r + 16/3u_\pi L_2^r + 4/9u_\pi L_3^r \Big\}$$

$$+\overline{B}_{21}(m_\eta^2, m_\eta^2, s_\pi) \Big\{ -12s_\pi^2 L_2^r - 4s_\pi^2 L_3^r \Big\}$$

$$+\overline{B}_{22}(m_\pi^2, m_\pi^2, s_\pi) m_\pi^2 \Big\{ 272/3L_2^r + 56/3L_3^r - 32/3L_4^r - 40/3L_5^r + 8/3L_9^r \Big\}$$

$$+\overline{B}_{22}(m_\pi^2, m_\pi^2, s_\pi) m_K^2 \Big\{ 128/3L_2^r + 32/3L_3^r - 64/3L_4^r + 4/3L_9^r \Big\}$$

$$+\overline{B}_{22}(m_\pi^2, m_\pi^2, s_\pi) \Big\{ 176s_\pi L_1^r - 128s_\pi L_2^r + 24s_\pi L_3^r - 4s_\pi L_9^r - 64t_\pi L_2^r - 4t_\pi L_3^r - 4t_\pi L_9^r$$

$$-64u_\pi L_2^r - 28u_\pi L_3^r - 4u_\pi L_9^r \Big\}/3$$

$$+\overline{B}_{22}(m_\pi^2, m_K^2, t_\pi) m_\pi^2/3 \Big\{ -32L_1^r - 112L_2^r + 88L_3^r - 196L_4^r - 104L_5^r + 32L_9^r \Big\}$$

$$+\overline{B}_{22}(m_\pi^2, m_K^2, t_\pi) m_K^2 \Big\{ 4L_3^r - 88/3L_4^r - 20/3L_5^r + 16/3L_9^r \Big\}$$

$$+\overline{B}_{22}(m_\pi^2, m_K^2, t_\pi) \Big\{ -16/3s_\pi L_1^r + 40/3s_\pi L_2^r - 16/3s_\pi L_3^r - 16/3s_\pi L_9^r + 64/3t_\pi L_1^r$$

$$-24t_\pi L_2^r - 4t_\pi L_3^r - 16/3t_\pi L_9^r + 32/3u_\pi L_1^r + 40/3u_\pi L_2^r - 4/3u_\pi L_3^r - 16/3u_\pi L_9^r\Big\}$$

$$+\overline{B}_{22}(m_\pi^2, m_K^2, u_\pi)\Big\{m_\pi^2/3\Big(160L_1^r + 80L_2^r + 80L_3^r + 16L_4^r\Big) + 16m_K^2\Big(2L_1^r + L_2^r + L_3^r\Big)\Big\}$$

$$-\overline{B}_{22}(m_\pi^2, m_K^2, u_\pi)8/3\Big\{\Big(2L_1^r + L_2^r + L_3^r\Big)\Big(s_\pi + t_\pi\Big) + 10u_\pi L_1^r + 3u_\pi L_2^r + 5u_\pi L_3^r\Big\}$$

$$+\overline{B}_{22}(m_K^2, m_K^2, s_\pi)\Big\{m_\pi^2\Big(32/3L_1^r + 368/3L_2^r + 32L_3^r\Big) + m_K^2\Big(32/3L_1^r + 80/3L_2^r + 8L_3^r\Big)\Big\}$$

$$+\overline{B}_{22}(m_K^2, m_K^2, s_\pi)\Big\{32/3s_\pi L_1^r - 208/3s_\pi L_2^r - 12s_\pi L_3^r - 16/3t_\pi L_1^r - 64/3t_\pi L_2^r - 6t_\pi L_3^r$$

$$-16/3u_\pi L_1^r - 16/3u_\pi L_2^r - 2u_\pi L_3^r\Big\}$$

$$+\overline{B}_{22}(m_K^2, m_\eta^2, t_\pi)\Big\{m_\pi^2\Big(-30L_4^r - 30L_5^r\Big) - 60m_K^2 L_4^r\Big\}$$

$$+\overline{B}_{22}(m_\eta^2, m_K^2, t_\pi)m_\pi^2\Big\{268/9L_3^r + 26L_4^r - 4/3L_5^r + 10L_9^r\Big\}$$

$$+\overline{B}_{22}(m_\eta^2, m_K^2, t_\pi)m_K^2\Big\{8/9L_3^r + 52L_4^r - 8/3L_5^r + 5L_9^r\Big\}$$

$$+\overline{B}_{22}(m_\eta^2, m_K^2, t_\pi)\Big\{-22/3s_\pi L_3^r - 5s_\pi L_9^r + 20/3t_\pi L_3^r - 5t_\pi L_9^r - 16/3u_\pi L_3^r - 5u_\pi L_9^r\Big\}$$

$$+\overline{B}_{22}(m_\eta^2, m_\eta^2, s_\pi)\Big\{m_\pi^2\Big(112/3L_2^r + 136/9L_3^r\Big) - 24s_\pi L_2^r - 8s_\pi L_3^r\Big\}$$

$$+\overline{B}_{31}(m_\pi^2, m_\pi^2, s_\pi)\Big(m_\pi^2 + m_K^2\Big)\Big\{-128/3s_\pi L_2^r - 32/3s_\pi L_3^r\Big\}$$

$$+\overline{B}_{31}(m_\pi^2, m_\pi^2, s_\pi)8/3\Big\{-6s_\pi^2 L_1^r - 3s_\pi^2 L_2^r - 3s_\pi^2 L_3^r + \Big(8L_2^r + 2L_3^r\Big)\Big(u_\pi + t_\pi\Big)s_\pi\Big\}$$

$$+\overline{B}_{31}(m_\pi^2, m_K^2, t_\pi)\Big\{m_\pi^4\Big(-32L_1^r - 16L_2^r - 4L_3^r\Big) + m_\pi^2 m_K^2\Big(32L_1^r + 16L_2^r + 4L_3^r\Big)\Big\}$$

$$+\overline{B}_{31}(m_\pi^2, m_K^2, t_\pi)m_\pi^2\Big\{\Big(8L_1^r + 4L_2^r + L_3^r\Big)\Big(s_\pi + u_\pi\Big) + 8t_\pi L_1^r + 4t_\pi L_2^r - t_\pi L_3^r\Big\}$$

$$+\overline{B}_{31}(m_\pi^2, m_K^2, t_\pi)m_K^2\Big\{-4\Big(s_\pi - t_\pi/3 + u_\pi\Big)\Big(2L_1^r + L_2^r\Big) - \Big(s_\pi + t_\pi/3 + u_\pi\Big)L_3^r\Big\}$$

$$+\overline{B}_{31}(m_\pi^2, m_K^2, t_\pi)\Big\{\Big(-8L_1^r - 4L_2^r + L_3^r\Big)\Big(s_\pi + u_\pi\Big)t_\pi/3 + \Big(8L_1^r + 4L_2^r + L_3^r\Big)t_\pi^2\Big\}$$

$$+\overline{B}_{31}(m_\pi^2, m_K^2, u_\pi)\Big(m_\pi^2 + m_K^2/3\Big)\Big\{-16u_\pi L_1^r - 8u_\pi L_2^r - 8u_\pi L_3^r\Big\}$$

$$+\overline{B}_{31}(m_\pi^2, m_K^2, u_\pi)8/3\Big\{2s_\pi u_\pi L_1^r + s_\pi u_\pi L_2^r + s_\pi u_\pi L_3^r + 2t_\pi u_\pi L_1^r + t_\pi u_\pi L_2^r + t_\pi u_\pi L_3^r\Big\}$$

$$+\overline{B}_{31}(m_K^2, m_K^2, s_\pi)\Big(m_\pi^2 + m_K^2\Big)\Big\{-32/3s_\pi L_1^r - 80/3s_\pi L_2^r - 8s_\pi L_3^r\Big\}$$

$$+\overline{B}_{31}(m_K^2, m_K^2, s_\pi)4/3\Big\{\Big(4L_1^r + 10L_2^r + 3L_3^r\Big)\Big(t_\pi + u_\pi\Big)s_\pi\Big\}$$

$$+\overline{B}_{31}(m_K^2, m_\eta^2, t_\pi)\Big\{m_\pi^2\Big(-s_\pi - t_\pi - u_\pi\Big)L_3^r + m_K^2\Big(s_\pi - 1/3t_\pi + u_\pi\Big)L_3^r\Big\}$$

$$+\overline{B}_{31}(m_K^2, m_\eta^2, t_\pi)\Big\{4L_3^r\Big(m_\pi^4 - m_\pi^2 m_K^2\Big) + \Big(1/3s_\pi t_\pi - t_\pi^2 + 1/3t_\pi u_\pi\Big)L_3^r\Big\}$$

$$+\overline{B}_{32}(m_\pi^2, m_\pi^2, s_\pi)\Big\{m_\pi^2\Big(64L_1^r - 160/3L_2^r + 32/3L_3^r\Big) - m_K^2\Big(256/3L_2^r + 64/3L_3^r\Big)\Big\}$$

$$-\overline{B}_{32}(m_\pi^2, m_\pi^2, s_\pi)32/3\Big\{6s_\pi L_1^r + 7s_\pi L_2^r + 4s_\pi L_3^r - 4t_\pi L_2^r - t_\pi L_3^r - 4u_\pi L_2^r - u_\pi L_3^r\Big\}$$

$$+\overline{B}_{32}(m_\pi^2, m_K^2, t_\pi)\Big\{m_\pi^2\Big(96L_1^r + 48L_2^r + 8L_3^r\Big) - m_K^2\Big(32/3L_1^r + 16/3L_2^r + 8/3L_3^r\Big)\Big\}$$

$$+\overline{B}_{32}(m_\pi^2, m_K^2, t_\pi)\Big\{-64/3s_\pi L_1^r - 32/3s_\pi L_2^r - 4/3s_\pi L_3^r + 112/3t_\pi L_1^r + 56/3t_\pi L_2^r$$

$$+10/3t_\pi L_3^r - 112/3u_\pi L_1^r - 56/3u_\pi L_2^r - 10/3u_\pi L_3^r\Big\}$$

$$-\overline{B}_{32}(m_\pi^2, m_K^2, u_\pi)\Big\{16/3\Big(3m_\pi^2 + m_K^2 + s_\pi + t_\pi - u_\pi\Big)\Big(2L_1^r + L_2^r + L_3^r\Big)\Big\}$$

$$+\overline{B}_{32}(m_K^2,m_K^2,s_\pi)\Big(m_\pi^2+m_K^2\Big)\Big\{-64/3L_1^r-160/3L_2^r-16L_3^r\Big\}$$

$$+\overline{B}_{32}(m_K^2,m_K^2,s_\pi)\Big\{-32s_\pi L_1^r-80s_\pi L_2^r-24s_\pi L_3^r+80t_\pi L_1^r+104t_\pi L_2^r+48t_\pi L_3^r$$

$$-16u_\pi L_1^r+56u_\pi L_2^r\Big\}/3$$

$$+\overline{B}_{32}(m_K^2,m_\eta^2,t_\pi)L_3^r\Big\{-12m_\pi^2+4/3m_K^2+8/3s_\pi-14/3t_\pi+14/3u_\pi\Big\}$$

$$+\overline{A}(m_\pi^2)\Big\{-4/3s_\pi L_1^r-16s_\pi L_2^r-19/3s_\pi L_3^r+55/12s_\pi L_9^r-27t_\pi L_2^r-27/2t_\pi L_3^r$$

$$+55/12t_\pi L_9^r-27u_\pi L_2^r+55/12u_\pi L_9^r\Big\}$$

$$+\overline{A}(m_K^2)\Big\{-56/3s_\pi L_1^r-32/3s_\pi L_2^r-10s_\pi L_3^r+11/2s_\pi L_9^r-14/3t_\pi L_2^r+17/3t_\pi L_3^r$$

$$+11/2t_\pi L_9^r-110/3u_\pi L_2^r+11/2u_\pi L_9^r\Big\}$$

$$+\overline{A}(m_\eta^2)\Big\{-12s_\pi L_1^r-s_\pi L_3^r-3t_\pi L_2^r+11/6t_\pi L_3^r-3u_\pi L_2^r+7/4\Big(s_\pi+t_\pi+u_\pi\Big)L_9^r\Big\} \qquad \text{(A.1)}$$

For G form-factor the expression reads

$$G_{LL}=m_\pi^4/(16\pi^2)\Big\{-2L_1^r-10/9L_2^r-49/108L_3^r\Big\}$$

$$+m_\pi^4\Big\{-16L_3^rL_5^r+32L_4^rL_5^r+56(L_5^r)^2-64L_5^rL_6^r-64L_5^rL_8^r-16L_5^rL_9^r\Big\}$$

$$+m_\pi^2m_K^2/(16\pi^2)\Big\{8/9L_2^r+8/27L_3^r\Big\}$$

$$+m_\pi^2m_K^2\Big\{64L_4^rL_5^r-32(L_5^r)^2-128L_5^rL_6^r+8L_5^rL_9^r\Big\}$$

$$+m_\pi^2m_\eta^2/(16\pi^2)\Big\{-2/3L_5^r\Big\}$$

$$+m_\pi^2\Big\{8s_\pi L_5^rL_9^r+32t_\pi L_2^rL_5^r+16t_\pi L_3^rL_5^r+8t_\pi L_5^rL_9^r-32u_\pi L_2^rL_5^r+8u_\pi L_5^rL_9^r$$

$$+\overline{A}(m_\pi^2)\Big(-4L_1^r-10L_2^r-19L_3^r+46/3L_4^r+161/6L_5^r-83/6L_9^r\Big)$$

$$+\overline{A}(m_K^2)\Big(32L_2^r+17/3L_3^r-8/3L_4^r+25/3L_5^r-19/3L_9^r\Big)$$

$$+\overline{A}(m_\eta^2)\Big(8/3L_1^r+2/3L_2^r+53/18L_3^r-2L_4^r-11/6L_5^r+1/2L_9^r\Big)\Big\}$$

$$+m_K^4/(16\pi^2)\Big\{2L_1^r-7/9L_2^r-1/108L_3^r\Big\}$$

$$+m_K^4\Big\{16L_3^rL_5^r+8(L_5^r)^2+8L_5^rL_9^r\Big\}$$

$$+m_K^2m_\eta^2/(16\pi^2)\Big\{8/3L_5^r\Big\}$$

$$+m_K^2\Big\{-8s_\pi L_5^rL_9^r-32t_\pi L_2^rL_5^r-16t_\pi L_3^rL_5^r-8t_\pi L_5^rL_9^r+32u_\pi L_2^rL_5^r-8u_\pi L_5^rL_9^r$$

$$+\overline{A}(m_\pi^2)\Big(-27/2L_3^r-4/3L_4^r-2/3L_5^r-83/12L_9^r\Big)$$

$$+\overline{A}(m_K^2)\Big(4L_1^r+26L_2^r+5/6L_3^r+32/3L_4^r-8/3L_5^r-19/6L_9^r\Big)$$

$$+\overline{A}(m_\eta^2)\Big(-32/3L_1^r-8/3L_2^r-47/18L_3^r-4L_4^r-8/3L_5^r+1/4L_9^r\Big)\Big\}$$

$$+m_\eta^4/(16\pi^2)\Big\{L_2^r+1/6L_3^r-2L_5^r\Big\}$$

$$+m_\eta^2\Big\{8\overline{A}(m_\eta^2)L_1^r+2\overline{A}(m_\eta^2)L_2^r+3\overline{A}(m_\eta^2)L_3^r+\overline{A}(m_\eta^2)L_5^r\Big\}$$

$$+\overline{B}(m_\pi^2,m_K^2,t_\pi)m_\pi^4\Big\{-8/3L_2^r+8/3L_3^r-14/3L_4^r-3L_5^r+L_9^r\Big\}$$

$$+\overline{B}(m_\pi^2,m_K^2,t_\pi)m_\pi^2m_K^2\Big\{8/3L_2^r+16/3L_3^r-8/3L_4^r-5L_5^r+20/3L_6^r+3/2L_9^r\Big\}$$

$$-\overline{B}(m_\pi^2, m_K^2, t_\pi)m_\pi^2/2\Big\{s_\pi L_9^r + 2t_\pi\Big(8/3L_2^r + 16/3L_3^r + 14/3L_4^r - 3L_5^r + 3/2L_9^r\Big) + u_\pi L_9^r\Big\}$$

$$+\overline{B}(m_\pi^2, m_K^2, t_\pi)m_K^4\Big\{ - 8/3L_4^r - 4/3L_5^r + 40/3L_6^r + 20/3L_8^r + 1/2L_9^r\Big\}$$

$$+\overline{B}(m_\pi^2, m_K^2, t_\pi)m_K^2\Big\{ - 1/2s_\pi L_9^r - 4t_\pi L_4^r - 2t_\pi L_5^r - t_\pi L_9^r - 1/2u_\pi L_9^r\Big\}$$

$$+\overline{B}(m_\pi^2, m_K^2, t_\pi)\Big\{1/2s_\pi t_\pi L_9^r + 1/2t_\pi^2 L_9^r + 1/2t_\pi u_\pi L_9^r\Big\}$$

$$+\overline{B}(m_\pi^2, m_K^2, u_\pi)m_\pi^4\Big\{56/3L_2^r + 64/3L_4^r + 20/3L_5^r - 8/3L_9^r\Big\}$$

$$+\overline{B}(m_\pi^2, m_K^2, u_\pi)m_\pi^2 m_K^2\Big\{40/3L_2^r + 32L_6^r + 16L_8^r - 8/3L_9^r\Big\}$$

$$+\overline{B}(m_\pi^2, m_K^2, u_\pi)4/3m_\pi^2\Big\{s_\pi L_9^r + t_\pi L_9^r - 10u_\pi L_2^r - 8u_\pi L_4^r - 4u_\pi L_5^r + 2u_\pi L_9^r\Big\}$$

$$+\overline{B}(m_\pi^2, m_K^2, u_\pi)m_K^4\Big\{ - 16/3L_4^r - 8/3L_5^r - 2/3L_9^r\Big\}$$

$$+\overline{B}(m_\pi^2, m_K^2, u_\pi)m_K^2\Big\{2/3s_\pi L_9^r + 2/3t_\pi L_9^r + 16/3u_\pi L_4^r + 8/3u_\pi L_5^r + 4/3u_\pi L_9^r\Big\}$$

$$+\overline{B}(m_\pi^2, m_K^2, u_\pi)\Big\{ - 2/3s_\pi u_\pi L_9^r - 2/3t_\pi u_\pi L_9^r - 2/3u_\pi^2 L_9^r\Big\}$$

$$+\overline{B}(m_\eta^2, m_K^2, t_\pi)m_\pi^4\Big\{4L_3^r + 28/3L_4^r + 16/9L_5^r - 8/3L_6^r - 32/3L_7^r - 8L_8^r + 8/3L_9^r\Big\}$$

$$+\overline{B}(m_\eta^2, m_K^2, t_\pi)m_\pi^2 m_K^2/3\Big\{ - 2/3L_3^r + 46L_4^r + 22/3L_5^r - 20L_6^r - 32L_7^r - 16L_8^r + 2L_9^r\Big\}$$

$$+\overline{B}(m_\eta^2, m_K^2, t_\pi)m_\pi^2 m_\eta^2\Big\{2L_4^r - 2L_5^r\Big\}$$

$$-\overline{B}(m_\eta^2, m_K^2, t_\pi)m_\pi^2/3\Big\{\Big(s_\pi + u_\pi\Big)\Big(3L_3^r - 4L_9^r\Big) + t_\pi\Big(- 43/3L_3^r - 12L_4^r + 2L_5^r - 10L_9^r\Big)\Big\}$$

$$+\overline{B}(m_\eta^2, m_K^2, t_\pi)m_K^4\Big\{14/9L_3^r - 20/3L_4^r - 38/9L_5^r - 8/3L_6^r + 64/3L_7^r + 28/3L_8^r - 1/3L_9^r\Big\}$$

$$+\overline{B}(m_\eta^2, m_K^2, t_\pi)\Big\{m_K^2 m_\eta^2\Big(4L_4^r + 8L_5^r\Big) - 4L_5^r m_\eta^4\Big\}$$

$$+\overline{B}(m_\eta^2, m_K^2, t_\pi)m_K^2/3\Big\{\Big(3L_3^r + L_9^r\Big)\Big(s_\pi + u_\pi\Big) - t_\pi\Big(47/3L_3^r + 24L_4^r - 4L_5^r + 2L_9^r\Big)\Big\}$$

$$+\overline{B}(m_\eta^2, m_K^2, t_\pi)\Big\{1/3s_\pi t_\pi L_3^r + s_\pi t_\pi L_9^r + 7/3t_\pi^2 L_3^r + t_\pi^2 L_9^r + 1/3t_\pi u_\pi L_3^r + t_\pi u_\pi L_9^r\Big\}$$

$$+\overline{B}_1(m_\pi^2, m_K^2, t_\pi)m_\pi^4\Big\{8L_1^r + 20L_2^r + 18L_3^r + 46/3L_4^r - 16/3L_5^r + 4/3L_9^r\Big\}$$

$$+\overline{B}_1(m_\pi^2, m_K^2, t_\pi)m_\pi^2 m_K^2/3\Big\{ - 16L_1^r - 8L_2^r + 2L_3^r - 56L_4^r - 36L_5^r + 76L_6^r + 48L_8^r + 4L_9^r\Big\}$$

$$+\overline{B}_1(m_\pi^2, m_K^2, t_\pi)m_\pi^2/3\Big\{ - 8s_\pi L_1^r - 4s_\pi L_2^r - 5s_\pi L_3^r - 2s_\pi L_9^r + 24t_\pi L_1^r - 12t_\pi L_2^r$$

$$-39t_\pi L_3^r - 22t_\pi L_4^r + 20t_\pi L_5^r - 10t_\pi L_9^r - 8u_\pi L_1^r - 4u_\pi L_2^r - 5u_\pi L_3^r - 2u_\pi L_9^r\Big\}$$

$$+\overline{B}_1(m_\pi^2, m_K^2, t_\pi)m_K^4/3\Big\{ - 8L_1^r - 4L_2^r + 4L_3^r + 40L_4^r + 20L_5^r - 40L_6^r - 20L_8^r + L_9^r\Big\}$$

$$+\overline{B}_1(m_\pi^2, m_K^2, t_\pi)m_K^2/3\Big\{8s_\pi L_1^r + 4s_\pi L_2^r - s_\pi L_3^r - s_\pi L_9^r + 8t_\pi L_1^r - 4t_\pi L_2^r - 17t_\pi L_3^r$$

$$+4t_\pi L_4^r + 2t_\pi L_5^r - 5t_\pi L_9^r + 8u_\pi L_1^r + 4u_\pi L_2^r - u_\pi L_3^r - u_\pi L_9^r\Big\}$$

$$+\overline{B}_1(m_\pi^2, m_K^2, t_\pi)\Big\{\Big(s_\pi + u_\pi\Big)t_\pi\Big(- 8L_1^r - 4L_2^r + L_3^r + 4L_9^r\Big) + t_\pi^2\Big(8L_2^r + 13L_3^r + 4L_9^r\Big)\Big\}$$

$$+\overline{B}_1(m_\pi^2, m_K^2, u_\pi)m_\pi^4\Big\{ - 40L_1^r - 20L_2^r - 20L_3^r - 56/3L_4^r\Big\}$$

$$+\overline{B}_1(m_\pi^2, m_K^2, u_\pi)m_\pi^2 m_K^2\Big\{ - 32/3L_1^r - 16/3L_2^r - 16/3L_3^r - 16/3L_4^r\Big\}$$

$$+\overline{B}_1(m_\pi^2, m_K^2, u_\pi)4/3m_\pi^2\Big\{\Big(8L_1^r + 4L_2^r + 4L_3^r\Big)\Big(s_\pi + t_\pi\Big)$$

$$+u_\pi\Big(12L_1^r-12L_2^r+6L_3^r+2L_4^r-L_5^r+L_9^r\Big)\Big\}$$

$$+\overline{B}_1(m_\pi^2,m_K^2,u_\pi)m_K^4\Big\{-40/3L_1^r-20/3L_2^r-20/3L_3^r+8L_4^r\Big\}$$

$$+\overline{B}_1(m_\pi^2,m_K^2,u_\pi)8/3m_K^2\Big\{2s_\pi L_1^r+s_\pi L_2^r+s_\pi L_3^r+2t_\pi L_1^r+t_\pi L_2^r+t_\pi L_3^r$$

$$+2u_\pi L_1^r-4u_\pi L_2^r+u_\pi L_3^r-7u_\pi L_4^r-2u_\pi L_5^r+1/4u_\pi L_9^r\Big\}$$

$$+\overline{B}_1(m_\pi^2,m_K^2,u_\pi)1/3\Big\{-16s_\pi u_\pi L_1^r-8s_\pi u_\pi L_2^r-8s_\pi u_\pi L_3^r-2s_\pi u_\pi L_9^r$$

$$-16t_\pi u_\pi L_1^r-8t_\pi u_\pi L_2^r-8t_\pi u_\pi L_3^r-2t_\pi u_\pi L_9^r+24u_\pi^2L_1^r+52u_\pi^2L_2^r+12u_\pi^2L_3^r-2u_\pi^2L_9^r\Big\}$$

$$+\overline{B}_1(m_K^2,m_\pi^2,t_\pi)10/3\Big\{m_\pi^2m_K^2\Big(L_4^r-2L_6^r\Big)+m_K^4\Big(2L_4^r+L_5^r-4L_6^r-2L_8^r\Big)\Big\}$$

$$+\overline{B}_1(m_K^2,m_\eta^2,t_\pi)m_\pi^4\Big\{-1/3L_4^r-1/3L_5^r+8/3L_6^r+8/3L_8^r\Big\}$$

$$+\overline{B}_1(m_K^2,m_\eta^2,t_\pi)\Big\{m_\pi^2m_K^2\Big(-25/3L_4^r-7L_5^r+20/3L_6^r\Big)+6m_K^26t_\pi L_4^r\Big\}$$

$$+\overline{B}_1(m_K^2,m_\eta^2,t_\pi)\Big\{3m_\pi^2t_\pi\Big(L_4^r+L_5^r\Big)+m_K^4/3\Big(-46L_4^r-2L_5^r+8L_6^r+4L_8^r\Big)\Big\}$$

$$+\overline{B}_1(m_\eta^2,m_K^2,t_\pi)m_\pi^4/3\Big\{-25L_3^r-55L_4^r-16/3L_5^r+8L_6^r+32L_7^r+24L_8^r-17L_9^r\Big\}$$

$$+\overline{B}_1(m_\eta^2,m_K^2,t_\pi)m_\pi^2m_K^2/3\Big\{56/3L_3^r-73L_4^r-22/3L_5^r+20L_6^r+32L_7^r+16L_8^r+5/2L_9^r\Big\}$$

$$-\overline{B}_1(m_\eta^2,m_K^2,t_\pi)\Big\{m_\pi^2m_\eta^2\Big(2L_4^r-4/3L_5^r\Big)+m_K^2m_\eta^2\Big(4L_4^r+16/3L_5^r\Big)+2m_\eta^4L_5^r\Big\}$$

$$+\overline{B}_1(m_\eta^2,m_K^2,t_\pi)m_\pi^2\Big\{19/9s_\pi L_3^r+17/6s_\pi L_9^r+79/9t_\pi L_3^r+3t_\pi L_4^r-2t_\pi L_5^r$$

$$+35/6t_\pi L_9^r+19/9u_\pi L_3^r+17/6u_\pi L_9^r\Big\}$$

$$+\overline{B}_1(m_\eta^2,m_K^2,t_\pi)m_K^4/3\Big\{7/3L_3^r+74L_4^r+38/3L_5^r+8L_6^r-64L_7^r-28L_8^r+11/2L_9^r\Big\}$$

$$+\overline{B}_1(m_\eta^2,m_K^2,t_\pi)m_K^2\Big\{-25/9s_\pi L_3^r-11/6s_\pi L_9^r+41/9t_\pi L_3^r+6t_\pi L_4^r-4t_\pi L_5^r$$

$$-1/3t_\pi L_9^r-25/9u_\pi L_3^r-11/6u_\pi L_9^r\Big\}$$

$$-\overline{B}_1(m_\eta^2,m_K^2,t_\pi)\Big\{\Big(1/3L_3^r+3/2L_9^r\Big)\Big(s_\pi+u_\pi\Big)t_\pi+4t_\pi^2L_3^r+3/2t_\pi^2L_9^r\Big\}$$

$$+\overline{B}_{21}(m_\pi^2,m_K^2,t_\pi)m_\pi^4\Big\{-40L_1^r-20L_2^r-10L_3^r-16L_4^r-9L_5^r+3L_9^r\Big\}$$

$$+\overline{B}_{21}(m_\pi^2,m_K^2,t_\pi)m_\pi^2m_K^2\Big\{112/3L_1^r+56/3L_2^r+10/3L_3^r+8L_4^r+9L_5^r-3/2L_9^r\Big\}$$

$$+\overline{B}_{21}(m_\pi^2,m_K^2,t_\pi)m_\pi^2\Big\{32/3s_\pi L_1^r+16/3s_\pi L_2^r+8/3s_\pi L_3^r-3/2s_\pi L_9^r-16t_\pi L_2^r-12t_\pi L_3^r$$

$$+52/3t_\pi L_4^r+23/3t_\pi L_5^r-19/6t_\pi L_9^r+32/3u_\pi L_1^r+16/3u_\pi L_2^r+8/3u_\pi L_3^r-3/2u_\pi L_9^r\Big\}$$

$$+\overline{B}_{21}(m_\pi^2,m_K^2,t_\pi)m_K^4\Big\{8/3L_1^r+4/3L_2^r-4/3L_3^r+8L_4^r-3/2L_9^r\Big\}$$

$$+\overline{B}_{21}(m_\pi^2,m_K^2,t_\pi)m_K^2\Big\{-32/3s_\pi L_1^r-16/3s_\pi L_2^r-2/3s_\pi L_3^r+3/2s_\pi L_9^r+16/3t_\pi L_4^r$$

$$+20/3t_\pi L_5^r+2/3t_\pi L_9^r-32/3u_\pi L_1^r-16/3u_\pi L_2^r-2/3u_\pi L_3^r+3/2u_\pi L_9^r\Big\}$$

$$+\overline{B}_{21}(m_\pi^2,m_K^2,t_\pi)\Big\{5/2s_\pi t_\pi L_9^r+t_\pi^2\Big(24L_1^r+44L_2^r+34L_3^r+5/2L_9^r\Big)+5/2t_\pi u_\pi L_9^r\Big\}/3$$

$$+\overline{B}_{21}(m_\pi^2,m_K^2,u_\pi)\Big\{\Big(20m_\pi^4+16/3m_\pi^2m_K^2\Big)\Big(2L_1^r+L_2^r+L_3^r\Big)\Big\}$$

$$+\overline{B}_{21}(m_\pi^2,m_K^2,u_\pi)16/3m_\pi^2\Big\{-2s_\pi L_1^r-s_\pi L_2^r-s_\pi L_3^r-2t_\pi L_1^r-t_\pi L_2^r-t_\pi L_3^r+u_\pi L_4^r\Big\}$$

$$+\overline{B}_{21}(m_\pi^2, m_K^2, u_\pi) m_K^4 \Big\{ 40/3 L_1^r + 20/3 L_2^r + 20/3 L_3^r \Big\}$$

$$-\overline{B}_{21}(m_\pi^2, m_K^2, u_\pi) 8/3 m_K^2 \Big\{ 2 s_\pi L_1^r + s_\pi L_2^r + s_\pi L_3^r + 2 t_\pi L_1^r + t_\pi L_2^r + t_\pi L_3^r \Big\}$$

$$+\overline{B}_{21}(m_\pi^2, m_K^2, u_\pi) \Big\{ -8 u_\pi^2 L_1^r + 4/3 u_\pi^2 L_2^r - 4 u_\pi^2 L_3^r \Big\}$$

$$+\overline{B}_{21}(m_K^2, m_\eta^2, t_\pi) \Big\{ -9 m_\pi^4 \Big(L_4^r + L_5^r \Big) + 9 m_\pi^2 m_K^2 \Big(-L_4^r + L_5^r \Big) + 3 m_\pi^2 t_\pi \Big(L_4^r + L_5^r \Big) \Big\}$$

$$+\overline{B}_{21}(m_K^2, m_\eta^2, t_\pi) \Big\{ 18 m_K^4 18 L_4^r + 6 m_K^2 t_\pi L_4^r + m_\pi^4 \Big(13/3 L_3^r + 9 L_4^r + 3 L_9^r \Big) \Big\}$$

$$+\overline{B}_{21}(m_\eta^2, m_K^2, t_\pi) m_\pi^2 m_K^2 \Big\{ -56/9 L_3^r + 9 L_4^r - 3/2 L_9^r \Big\}$$

$$-\overline{B}_{21}(m_\eta^2, m_K^2, t_\pi) m_\pi^2 \Big\{ \Big(10/9 L_3^r + 3/2 L_9^r \Big) \Big(s_\pi + u_\pi \Big) - t_\pi \Big(-4 L_3^r + L_4^r + 4/3_5^r - 5/2 L_9^r \Big) \Big\}$$

$$+\overline{B}_{21}(m_\eta^2, m_K^2, t_\pi) m_K^4 \Big\{ -7/9 L_3^r - 18 L_4^r - 3/2 L_9^r \Big\}$$

$$+\overline{B}_{21}(m_\eta^2, m_K^2, t_\pi) m_K^2 \Big\{ \Big(16/9 L_3^r + 3/2 L_9^r \Big) \Big(s_\pi + u_\pi \Big) + 2 t_\pi L_4^r + 8/3 t_\pi L_5^r + t_\pi L_9^r \Big\}$$

$$+\overline{B}_{21}(m_\eta^2, m_K^2, t_\pi) \Big\{ 1/2 s_\pi t_\pi L_9^r + 5/3 t_\pi^2 L_3^r + 1/2 t_\pi^2 L_9^r + 1/2 t_\pi u_\pi L_9^r \Big\}$$

$$+\overline{B}_{22}(m_\pi^2, m_\pi^2, s_\pi) \Big\{ m_\pi^2 \Big(8 L_3^r - 32 L_4^r - 24 L_5^r + 8 L_9^r \Big) + m_K^2 \Big(8 L_3^r + 4 L_9^r \Big) \Big\}$$

$$+\overline{B}_{22}(m_\pi^2, m_\pi^2, s_\pi) 4 \Big\{ 4 s_\pi L_1^r - 2 s_\pi L_2^r + 2 s_\pi L_3^r - s_\pi L_9^r - t_\pi L_3^r - t_\pi L_9^r - u_\pi L_3^r - u_\pi L_9^r \Big\}$$

$$+\overline{B}_{22}(m_\pi^2, m_K^2, t_\pi) m_\pi^2 \Big\{ -64/3 L_1^r - 80/3 L_2^r - 64/3 L_3^r + 4/3 L_4^r - 4/3 L_5^r + 4/3 L_9^r \Big\}$$

$$+\overline{B}_{22}(m_\pi^2, m_K^2, t_\pi) m_K^2 \Big\{ 32 L_1^r + 4 L_3^r - 8/3 L_4^r + 20/3 L_5^r + 2/3 L_9^r \Big\}$$

$$+\overline{B}_{22}(m_\pi^2, m_K^2, t_\pi) \Big\{ 16/3 s_\pi L_1^r + 8/3 s_\pi L_2^r + 4/3 s_\pi L_3^r - 2/3 s_\pi L_9^r + 32/3 t_\pi L_1^r + 8 t_\pi L_2^r$$

$$+16 t_\pi L_3^r - 2/3 t_\pi L_9^r - 32/3 u_\pi L_1^r + 8/3 u_\pi L_2^r - 8/3 u_\pi L_3^r - 2/3 u_\pi L_9^r \Big\}$$

$$+\overline{B}_{22}(m_\pi^2, m_K^2, u_\pi) m_\pi^2 \Big\{ 160/3 L_1^r + 80/3 L_2^r + 80/3 L_3^r + 16/3 L_4^r \Big\}$$

$$+\overline{B}_{22}(m_\pi^2, m_K^2, u_\pi) m_K^2 \Big\{ 32 L_1^r + 16 L_2^r + 16 L_3^r \Big\}$$

$$+\overline{B}_{22}(m_\pi^2, m_K^2, u_\pi) \Big\{ -16/3 s_\pi L_1^r - 8/3 s_\pi L_2^r - 8/3 s_\pi L_3^r - 16/3 t_\pi L_1^r - 8/3 t_\pi L_2^r$$

$$-8/3 t_\pi L_3^r - 80/3 u_\pi L_1^r - 8 u_\pi L_2^r - 40/3 u_\pi L_3^r \Big\}$$

$$+\overline{B}_{22}(m_K^2, m_K^2, s_\pi) m_\pi^2 \Big\{ 32 L_1^r + 12 L_3^r - 12 L_5^r + 4 L_9^r \Big\}$$

$$+\overline{B}_{22}(m_K^2, m_K^2, s_\pi) m_K^2 \Big\{ 32 L_1^r + 12 L_3^r - 16 L_4^r + 2 L_9^r \Big\}$$

$$+\overline{B}_{22}(m_K^2, m_K^2, s_\pi) 2 \Big\{ 2 s_\pi L_3^r - s_\pi L_9^r - 8 t_\pi L_1^r - 3 t_\pi L_3^r - t_\pi L_9^r - 8 u_\pi L_1^r - 3 u_\pi L_3^r - u_\pi L_9^r \Big\}$$

$$+\overline{B}_{22}(m_K^2, m_\eta^2, t_\pi) \Big\{ m_\pi^2 \Big(-6 L_4^r - 6 L_5^r \Big) - 12 m_K^2 L_4^r \Big\}$$

$$+\overline{B}_{22}(m_\eta^2, m_K^2, t_\pi) m_\pi^2 \Big\{ -16/9 L_3^r + 10 L_4^r + 4/3 L_5^r + 2 L_9^r \Big\}$$

$$+\overline{B}_{22}(m_\eta^2, m_K^2, t_\pi) m_K^2 \Big\{ 28/9 L_3^r + 20 L_4^r + 8/3 L_5^r + L_9^r \Big\}$$

$$+\overline{B}_{22}(m_\eta^2, m_K^2, t_\pi) \Big\{ -2/3 s_\pi L_3^r - s_\pi L_9^r + 16/3 t_\pi L_3^r - t_\pi L_9^r - 8/3 u_\pi L_3^r - u_\pi L_9^r \Big\}$$

$$+\overline{B}_{31}(m_\pi^2, m_K^2, t_\pi) \Big\{ \Big(m_\pi^4 - m_\pi^2 m_K^2 \Big) \Big(32 L_1^r + 16 L_2^r + 4 L_3^r \Big) \Big\}$$

$$-\overline{B}_{31}(m_\pi^2, m_K^2, t_\pi) m_\pi^2 \Big\{ 4 \Big(2 L_1^r + L_2^r \Big) \Big(s_\pi + t_\pi + u_\pi \Big) + s_\pi L_3^r - t_\pi L_3^r + u_\pi L_3^r \Big\}$$

$$\begin{aligned}
&+\overline{B}_{31}(m_\pi^2, m_K^2, t_\pi) m_K^2 \Big\{ \Big(s_\pi + u_\pi\Big) \Big(8L_1^r + 4L_2^r + L_3^r\Big) - 8/3 t_\pi L_1^r - 4/3 t_\pi L_2^r + 1/3 t_\pi L_3^r \Big\} \\
&+\overline{B}_{31}(m_\pi^2, m_K^2, t_\pi) \Big\{ \Big(s_\pi + u_\pi\Big) t_\pi/3 \Big(8L_1^r + 4L_2^r - L_3^r\Big) - 8t_\pi^2 L_1^r - 4t_\pi^2 L_2^r - t_\pi^2 L_3^r \Big\} \\
&-\overline{B}_{31}(m_\pi^2, m_K^2, u_\pi) 8u_\pi \Big\{ \Big(m_\pi^2 + m_K^2/3\Big) \Big(2L_1^r + L_2^r + L_3^r\Big) \Big\} \\
&+\overline{B}_{31}(m_\pi^2, m_K^2, u_\pi) 8/3 \Big\{ 2s_\pi u_\pi L_1^r + s_\pi u_\pi L_2^r + s_\pi u_\pi L_3^r + 2t_\pi u_\pi L_1^r + t_\pi u_\pi L_2^r + t_\pi u_\pi L_3^r \Big\} \\
&+\overline{B}_{31}(m_K^2, m_\eta^2, t_\pi) L_3^r \Big\{ 4\Big(- m_\pi^4 + m_\pi^2 m_K^2\Big) - 1/3 s_\pi t_\pi + t_\pi^2 - 1/3 t_\pi u_\pi \Big\} \\
&+\overline{B}_{31}(m_K^2, m_\eta^2, t_\pi) L_3^r \Big\{ m_\pi^2 \Big(s_\pi + t_\pi + u_\pi\Big) + m_K^2 \Big(- s_\pi + 1/3 t_\pi - u_\pi\Big) \Big\} \\
&+\overline{B}_{32}(m_\pi^2, m_K^2, t_\pi) \Big\{ m_\pi^2 \Big(64L_1^r + 32L_2^r + 12L_3^r\Big) - m_K^2/3 \Big(64L_1^r + 32L_2^r + 4L_3^r\Big) \Big\} \\
&+\overline{B}_{32}(m_\pi^2, m_K^2, t_\pi) \Big\{ - 32s_\pi L_1^r - 16s_\pi L_2^r - 8s_\pi L_3^r - 112t_\pi L_1^r - 56t_\pi L_2^r \\
&-10t_\pi L_3^r + 16u_\pi L_1^r + 8u_\pi L_2^r - 2u_\pi L_3^r \Big\}/3 \\
&-\overline{B}_{32}(m_\pi^2, m_K^2, u_\pi) \Big\{ 16/3 \Big(3m_\pi^2 + 3m_K^2 - s_\pi - t_\pi + u_\pi\Big) \Big(2L_1^r + L_2^r + L_3^r\Big) \Big\} \\
&+\overline{B}_{32}(m_K^2, m_K^2, s_\pi) \Big(m_\pi^2 + m_K^2\Big) \Big\{ - 32L_1^r - 16L_2^r - 16L_3^r \Big\} \\
&+\overline{B}_{32}(m_K^2, m_K^2, s_\pi) \Big\{ 16t_\pi L_1^r + 8t_\pi L_2^r + 8t_\pi L_3^r + 16u_\pi L_1^r + 8u_\pi L_2^r + 8u_\pi L_3^r \Big\} \\
&+\overline{B}_{32}(m_K^2, m_\eta^2, t_\pi) \Big\{ 8\Big(- m_\pi^2 + m_K^2/3\Big) L_3^r + 4/3 s_\pi L_3^r + 14/3 t_\pi L_3^r - 2/3 u_\pi L_3^r \Big\} \\
&+\overline{A}(m_\pi^2) \Big(83/12 s_\pi L_9^r + 27t_\pi L_2^r + 27/2 t_\pi L_3^r + 83/12 t_\pi L_9^r - 27u_\pi L_2^r + 83/12 u_\pi L_9^r\Big) \\
&+\overline{A}(m_K^2) \Big(19/6 s_\pi L_9^r + 14/3 t_\pi L_2^r - 17/3 t_\pi L_3^r + 19/6 t_\pi L_9^r - 110/3 u_\pi L_2^r + 19/6 u_\pi L_9^r\Big) \\
&+\overline{A}(m_\eta^2) \Big(- 1/4 s_\pi L_9^r + 27t_\pi + 3t_\pi L_2^r - 11/6 t_\pi L_3^r - 1/4 t_\pi L_9^r - 3u_\pi L_2^r - 1/4 u_\pi L_9^r\Big)
\end{aligned} \tag{A.2}$$

A.2 $\mathcal{L}_6$ Contribution

Here we collect the relevant contribution coming from the tree diagram involving a $\mathcal{O}(p^6)$ Lagrangian vertex [16]. Each C_i^r is finite and as was explained in Sect. 5, at present, for their numerical estimate one has to resort to models.

For the F form-factor we obtain

$$\begin{aligned}
F_{ct} = {} & m_\pi^4 \Big\{ - 32C_4^r - 32C_5^r - 24C_6^r - 64C_7^r + 8C_8^r + 8C_{10}^r + 16C_{11}^r - 80C_{12}^r - 176C_{13}^r + 32C_{14}^r \\
&+8C_{15}^r + 128C_{16}^r - 48C_{17}^r - 32C_{23}^r + 16C_{25}^r + 32C_{26}^r + 128C_{28}^r + 8C_{64}^r + 8C_{65}^r + 8C_{66}^r - 16C_{67}^r \\
&+32C_{68}^r + 16C_{69}^r + 16C_{83}^r + 32C_{84}^r + 8C_{90}^r \Big\} \\
&+m_\pi^2 m_K^2 \Big\{ - 16C_4^r + 8C_5^r - 40C_6^r - 64C_7^r - 24C_8^r + 16C_{10}^r + 48C_{11}^r + 24C_{12}^r - 96C_{13}^r - 16C_{14}^r \\
&+80C_{15}^r + 64C_{17}^r - 16C_{22}^r - 16C_{23}^r - 8C_{25}^r - 16C_{26}^r - 32C_{29}^r - 64C_{30}^r - 32C_{36}^r + 16C_{63}^r + 20C_{64}^r \\
&+4C_{65}^r - 4C_{66}^r - 24C_{67}^r + 16C_{68}^r + 8C_{69}^r + 8C_{83}^r + 16C_{84}^r + 12C_{90}^r \Big\} \\
&+m_\pi^2 s_\pi \Big\{ 20C_1^r + 64C_2^r + 8C_3^r + 8C_4^r + 16C_5^r + 16C_6^r + 32C_7^r + 16C_{13}^r + 8C_{22}^r + 8C_{25}^r - 4C_{64}^r \\
&-4C_{65}^r - 12C_{66}^r + 8C_{67}^r - 32C_{68}^r - 16C_{69}^r - 8C_{83}^r - 16C_{84}^r - 4C_{90}^r \Big\} \\
&+m_\pi^2 t_\pi \Big\{ - 20C_1^r - 64C_2^r + 8C_3^r - 4C_4^r - 8C_6^r - 8C_8^r + 8C_{12}^r + 32C_{13}^r + 12C_{22}^r + 16C_{23}^r - 20C_{25}^r \\
&+4C_{63}^r - 4C_{64}^r - 4C_{65}^r + 6C_{66}^r + 16C_{67}^r - 16C_{68}^r - 10C_{69}^r - 12C_{83}^r - 16C_{84}^r + 8C_{88}^r - 10C_{90}^r \Big\}
\end{aligned}$$

$$
\begin{aligned}
&+m_\pi^2 u_\pi\Big\{-12C_1^r-64C_2^r-8C_3^r+36C_4^r-8C_{10}^r-16C_{11}^r+8C_{12}^r+80C_{13}^r-12C_{22}^r+16C_{23}^r\\
&+4C_{25}^r-4C_{63}^r-4C_{64}^r-4C_{65}^r-6C_{66}^r+16C_{67}^r-16C_{68}^r-6C_{69}^r-4C_{83}^r-16C_{84}^r-6C_{90}^r\Big\}\\
&+m_K^4\Big\{8C_5^r+16C_6^r+8C_{10}^r+32C_{11}^r-8C_{12}^r+8C_{22}^r+16C_{23}^r-8C_{34}^r+8C_{63}^r+8C_{64}^r\\
&-4C_{66}^r-8C_{67}^r+4C_{90}^r\Big\}\\
&+m_K^2 s_\pi\Big\{4C_1^r+8C_3^r+16C_4^r+32C_6^r+32C_7^r+16C_8^r+8C_{12}^r+32C_{13}^r-16C_{23}^r+8C_{25}^r-8C_{63}^r\\
&-8C_{64}^r+8C_{67}^r-8C_{68}^r-4C_{69}^r-4C_{90}^r\Big\}\\
&+m_K^2 t_\pi\Big\{-4C_1^r+8C_3^r+4C_4^r-8C_5^r-16C_6^r-24C_{12}^r-64C_{13}^r-4C_{22}^r-8C_{23}^r-12C_{63}^r\\
&-8C_{64}^r+6C_{66}^r+12C_{67}^r+2C_{69}^r+4C_{83}^r+4C_{88}^r-10C_{90}^r\Big\}\\
&+m_K^2 u_\pi\Big\{4C_1^r-8C_3^r-4C_4^r-8C_{10}^r-32C_{11}^r+16C_{12}^r+32C_{13}^r-4C_{22}^r-8C_{23}^r-4C_{63}^r-8C_{64}^r\\
&+6C_{66}^r+12C_{67}^r-2C_{69}^r-4C_{83}^r-2C_{90}^r\Big\}\\
&+s_\pi^2\Big\{-8C_1^r-32C_2^r+8C_4^r+4C_{66}^r+8C_{68}^r+4C_{69}^r\Big\}\\
&+s_\pi t_\pi\Big\{4C_1^r+32C_2^r-4C_4^r-2C_{66}^r-4C_{67}^r+8C_{68}^r+6C_{69}^r-2C_{88}^r+2C_{90}^r\Big\}\\
&+s_\pi u_\pi\Big\{8C_1^r+32C_2^r-8C_3^r-20C_4^r+6C_{66}^r-4C_{67}^r+8C_{68}^r+2C_{69}^r-2C_{88}^r+2C_{90}^r\Big\}\\
&+t_\pi^2\Big\{4C_1^r-4C_4^r-2C_{66}^r-2C_{67}^r-2C_{69}^r-6C_{88}^r+6C_{90}^r\Big\}\\
&+t_\pi u_\pi\Big\{-4C_1^r-8C_3^r+4C_4^r-6C_{66}^r-12C_{67}^r+2C_{69}^r-2C_{88}^r+2C_{90}^r\Big\}\\
&+u_\pi^2\Big\{8C_3^r-2C_{67}^r\Big\},
\end{aligned}
\tag{A.3}
$$

while for the G form-factor the contribution is

$$
\begin{aligned}
G_{ct} &= m_\pi^4\Big\{-24C_4^r-8C_6^r-8C_8^r+8C_{10}^r+16C_{11}^r-16C_{13}^r+8C_{15}^r+16C_{17}^r+8C_{22}^r-8C_{25}^r\\
&+8C_{63}^r+8C_{64}^r+8C_{65}^r-4C_{66}^r+12C_{69}^r+8C_{83}^r+12C_{90}^r\Big\}\\
&+m_\pi^2 m_K^2\Big\{-16C_4^r-8C_5^r-24C_6^r-8C_8^r+16C_{10}^r+48C_{11}^r-24C_{12}^r-64C_{13}^r+16C_{14}^r\\
&+16C_{15}^r-16C_{22}^r+16C_{25}^r+16C_{26}^r-32C_{29}^r+16C_{63}^r+20C_{64}^r+4C_{65}^r\\
&+4C_{66}^r+8C_{69}^r+8C_{83}^r+12C_{90}^r\Big\}\\
&+m_\pi^2 s_\pi\Big\{-4C_1^r+8C_3^r+8C_4^r-16C_{12}^r-16C_{13}^r-8C_{63}^r-4C_{64}^r-4C_{65}^r+4C_{66}^r\\
&-8C_{69}^r+4C_{88}^r-12C_{90}^r\Big\}\\
&+m_\pi^2 t_\pi\Big\{4C_1^r+8C_3^r+12C_4^r+8C_6^r+8C_8^r-8C_{12}^r+4C_{22}^r+16C_{23}^r+4C_{25}^r-4C_{63}^r-4C_{64}^r\\
&-4C_{65}^r-2C_{66}^r-4C_{67}^r-10C_{69}^r-4C_{83}^r+4C_{88}^r-10C_{90}^r\Big\}\\
&+m_\pi^2 u_\pi\Big\{-4C_1^r-8C_3^r+20C_4^r-8C_{10}^r-16C_{11}^r+8C_{12}^r+16C_{13}^r-12C_{22}^r-16C_{23}^r\\
&+4C_{25}^r-4C_{63}^r-4C_{64}^r-4C_{65}^r+2C_{66}^r+4C_{67}^r-6C_{69}^r-4C_{83}^r-6C_{90}^r\Big\}\\
&+m_K^4\Big\{-8C_4^r-8C_5^r-16C_6^r+8C_{10}^r+32C_{11}^r-40C_{12}^r-64C_{13}^r-8C_{34}^r+8C_{64}^r+4C_{69}^r+8C_{83}^r\Big\}\\
&+m_K^2 s_\pi\Big\{-4C_1^r+8C_3^r+8C_{12}^r-32C_{13}^r+8C_{22}^r-8C_{25}^r-8C_{64}^r-4C_{69}^r-8C_{83}^r+4C_{88}^r-4C_{90}^r\Big\}
\end{aligned}
$$

$$
\begin{aligned}
&+m_K^2 t_\pi\Big\{4C_1^r+8C_3^r+4C_4^r+8C_5^r+16C_6^r+8C_{12}^r+4C_{22}^r+8C_{23}^r-4C_{63}^r-8C_{64}^r-2C_{66}^r\\
&-6C_{69}^r-4C_{83}^r-2C_{90}^r\Big\}\\
&+m_K^2 u_\pi\Big\{-4C_1^r-8C_3^r+12C_4^r-8C_{10}^r-32C_{11}^r+16C_{12}^r+32C_{13}^r-4C_{22}^r-8C_{23}^r\\
&-8C_{23}^r-4C_{63}^r-8C_{64}^r-2C_{66}^r-2C_{69}^r-4C_{83}^r-2C_{90}^r\Big\}+s_\pi^2\Big\{-4C_{88}^r+4C_{90}^r\Big\}\\
&+s_\pi t_\pi\Big\{4C_1^r-4C_4^r-2C_{66}^r+6C_{69}^r-2C_{88}^r+2C_{90}^r\Big\}\\
&+s_\pi u_\pi\Big\{-8C_3^r-4C_4^r-2C_{66}^r+2C_{69}^r-2C_{88}^r+2C_{90}^r\Big\}\\
&+t_\pi^2\Big\{-4C_1^r+4C_4^r+2C_{66}^r+2C_{67}^r+2C_{69}^r-2C_{88}^r+2C_{90}^r\Big\}\\
&+t_\pi u_\pi\Big\{4C_1^r-8C_3^r-12C_4^r+2C_{66}^r+2C_{69}^r-2C_{88}^r+2C_{90}^r\Big\}+u_\pi^2\Big\{8C_3^r-2C_{67}^r\Big\}. \qquad \text{(A.4)}
\end{aligned}
$$

A.2.1 Resonance Contribution

The aim of this section is to give an estimate, based on Resonance Saturation as discussed in Sect. 5, of the previous combinations of $\mathcal{O}(p^6)$ constants. The main drawback of this method is that it does not specify the scale at which it should be apply. A rough estimate of this uncertainty is obtained varying the scale μ, let's say between 0.5 and 1 GeV, and comparing the results with the scale at the ρ mass.
Using the equations of motion for integrating out the massive fields we get for the F form-factor

$$
\begin{aligned}
F_{RS} &= \frac{1}{F_0^2 M_S^4}\Big\{c_m^2\Big(-8m_\pi^4+12m_\pi^2 m_K^2-4m_K^4\Big)+c_m c_d\Big(4m_\pi^4-4m_\pi^2 m_K^2+8m_\pi^2 s_\pi-4m_\pi^2 t_\pi\Big)\\
&+c_d^2\Big(-8m_\pi^2 s_\pi+2m_\pi^2 t_\pi+2m_K^2 t_\pi+4s_\pi^2-2t_\pi^2\Big)\Big\}\\
&+\frac{1}{F_0^2\sqrt{2}M_V^4}\Big\{f_V f_\chi\Big(-4m_\pi^4+m_\pi^2(-6m_K^2+2s_\pi+t_\pi+3u_\pi)-2m_K^4+m_K^2(2s_\pi+3t_\pi+u_\pi)\Big)\\
&+g_V f_\chi\Big(12m_\pi^4+10m_\pi^2 m_K^2-4m_\pi^2 s_\pi+10m_\pi^2 t_\pi-6m_\pi^2 u_\pi+2m_K^4-4m_K^2 s_\pi-2m_K^2 u_\pi\Big)\\
&+g_V\alpha_V\Big(2m_\pi^4-m_\pi^2(m_K^2+s_\pi-t_\pi+u_\pi)-m_K^4+m_K^2(s_\pi+2t_\pi+u_\pi)+s_\pi u_\pi-2t_\pi(s_\pi+u_\pi)\Big)\\
&+\sqrt{2}g_V f_V\Big(-2m_\pi^2 t_\pi-m_K^2 t_\pi+(s_\pi t_\pi+s_\pi u_\pi+3t_\pi^2+t_\pi u_\pi)/2\Big)\\
&+\sqrt{2}g_V^2\Big(5m_\pi^2 t_\pi+m_K^2 t_\pi-s_\pi t_\pi-s_\pi u_\pi-t_\pi u_\pi\Big)+\sqrt{2}f_\chi^2\Big(32m_\pi^4+16m_\pi^2 m_K^2\Big)\\
&+\sqrt{2}f_\chi\alpha_V\Big(16m_\pi^4+8m_\pi^2 m_K^2-8m_\pi^2 s_\pi-12m_\pi^2 t_\pi-4m_\pi^2 u_\pi+4m_K^2 t_\pi-4m_K^2 u_\pi\Big)\\
&+\sqrt{2}f_\chi^2\Big(32m_\pi^4+16m_\pi^2 m_K^2\Big)\Big\}\\
&+\frac{\sqrt{2}s_\ell}{F_0^2 M_A^2}\Big\{f_A\gamma_A^{(1)}\Big(-m_\pi^2-m_K^2+u_\pi\Big)+f_A\gamma_A^{(2)}\Big(3m_\pi^2-m_K^2-2s_\pi+t_\pi\Big)\Big\}, \qquad \text{(A.5)}
\end{aligned}
$$

and for the G form-factor

$$
\begin{aligned}
G_{RS} &= \frac{1}{F_0^2 M_S^4}\Big\{4c_m^2\Big(m_\pi^2 m_K^2-m_K^4\Big)-4c_m c_d m_\pi^2\Big(m_\pi^2-m_K^2-t_\pi\Big)-2t_\pi c_d^2\Big(m_\pi^2+m_K^2-t_\pi\Big)\Big\}\\
&+\frac{1}{F_0^2\sqrt{2}M_V^4}\Big\{f_V f_\chi\Big(-6m_\pi^4-6m_\pi^2 m_K^2+4m_\pi^2 s_\pi+(3m_\pi^2+m_K^2)(u_\pi+t_\pi)\Big)\\
&+g_V f_\chi\Big(8m_\pi^4+14m_\pi^2 m_K^2-2m_\pi^2 t_\pi-6m_\pi^2 u_\pi+2m_K^4+4m_K^2 s_\pi-2m_K^2 u_\pi\Big)
\end{aligned}
$$

$$
\begin{aligned}
&+g_V\alpha_V\Big(-2m_\pi^4+m_\pi^2(m_K^2+3s_\pi+t_\pi+u_\pi)+m_K^4-m_K^2(s_\pi+u_\pi)-2s_\pi t_\pi-s_\pi u_\pi\Big)\\
&+\sqrt{2}g_V f_V\Big(-m_\pi^2(s_\pi+t_\pi)-m_K^2 s_\pi+s_\pi^2+(s_\pi t_\pi+s_\pi u_\pi+t_\pi^2+t_\pi u_\pi)/2\Big)\\
&+\sqrt{2}g_V^2\Big((2s_\pi+t_\pi)(m_\pi^2+m_K^2)-s_\pi t_\pi-s_\pi u_\pi-t_\pi u_\pi\Big)\\
&+\sqrt{2}f_\chi\alpha_V\Big(8m_\pi^4+8m_\pi^2m_K^2-4m_\pi^2(t_\pi+u_\pi)+8m_K^4-4m_K^2(2s_\pi+t_\pi+u_\pi)\Big)\\
&+48\sqrt{2}f_\chi^2m_\pi^2m_K^2\Big\}\\
&+\frac{\sqrt{2}s_\ell}{F_0^2M_A^2}\Big\{f_A\gamma_A^{(1)}\Big(-m_\pi^2-m_K^2+u_\pi\Big)+f_A\gamma_A^{(2)}\Big(m_\pi^2+m_K^2-t_\pi\Big)\Big\}\,. \qquad \text{(A.6)}
\end{aligned}
$$

As can be seen from Eqs. (A.5), (A.6) the axial-vector contribution vanishes at $s_\ell = 0$ and thus has no influence on the values quoted in Eq. (6.12).

B Scattering Lengths

Using the definitions of Eq. (6.21) is rather straightforward to evaluate the threshold parameters a_l^I and b_l^I not displayed in [7].

$$
\begin{aligned}
b_2^0 &= \frac{m_\pi^{-2}}{80\pi^3F_\pi^4}\left\{-\frac{481}{2520}+x\left[-\frac{1849}{17010}-\frac{1583\pi^2}{22680}-\frac{1}{84}\,\overline{b}_1-\frac{124}{315}\,\overline{b}_2-\frac{179}{378}\,\overline{b}_3-\frac{773}{210}\,\overline{b}_4-\overline{b}_5+\frac{17}{3}\,\overline{b}_6\right]\right\},\\
b_2^2 &= \frac{1}{240\pi^3F_\pi^4m_\pi^2}\left\{-\frac{277}{840}+x\left[\frac{193\pi^2}{7560}-\frac{24218}{2835}-\frac{1}{7}\,\overline{b}_1-\frac{337}{420}\,\overline{b}_2+\frac{157}{126}\,\overline{b}_3+\frac{87}{14}\,\overline{b}_4-3\,\overline{b}_5+5\,\overline{b}_6\right]\right\},\\
a_3^1 &= \frac{1}{560\pi^3F_\pi^4m_\pi^2}\left\{\frac{11}{168}+x\left[\frac{4111}{1134}+\frac{37\pi^2}{840}+\frac{1}{14}\,\overline{b}_1+\frac{17}{84}\,\overline{b}_2-\frac{151}{126}\,\overline{b}_3-\frac{653}{126}\,\overline{b}_4+\overline{b}_5+\overline{b}_6\right]\right\},\\
b_3^1 &= \frac{1}{35280\pi^3F_\pi^4m_\pi^4}\left\{-\frac{47}{15}+x\left[\frac{549221}{5400}-\frac{41\pi^2}{18}-5\,\overline{b}_1-\frac{169}{15}\,\overline{b}_2-\frac{958}{5}\,\overline{b}_3-418\,\overline{b}_4\right]\right\}. \qquad \text{(B.1)}
\end{aligned}
$$

where

$$
x=\frac{m_\pi^2}{16\pi^2F_\pi^2}, \quad \overline{b}_{1,2,3,4}=16\pi^2b_{1,2,3,4}\,, \quad \overline{b}_{5,6}=(16\pi^2)^2b_{5,6}\,. \qquad \text{(B.2)}
$$

For the rest of the notation and the expression for the b_i coefficients, we refer to App. D in [7].

C Vacuum Expectation Values at $\mathcal{O}(p^6)$

Here we collect the relevant formulas for the vacuum condensate in the limit $m_u = m_d$. As can be seen they can be cast in terms of the simplest one-loop integral $\overline{A}$ defined in App. D.

For the non-strange current we find

$$
\begin{aligned}
\langle 0|\overline{q}q|0\rangle^{(4)} &= \frac{1}{F_\pi^2}\Big\{3/2\overline{A}(m_\pi^2)+\overline{A}(m_K^2)+\overline{A}(m_\eta^2)/6+4m_\pi^2\Big(4L_6^r+2L_8^r+H_2^r\Big)+32m_K^2L_6^r\Big\},\\
\langle 0|\overline{q}q|0\rangle^{(6)} &= \frac{1}{F_\pi^4}\Big\{\frac{1}{(16\pi)^2}\Big(m_\pi^4(47/3888\pi^2+47/648)-m_\pi^2m_K^2(113/1944\pi^2+113/324)\\
&\quad+m_\pi^2m_\eta^2(19/432\pi^2+19/72)+m_K^4(19/486\pi^2+19/81)-m_K^2m_\eta^2(13/216\pi^2+13/36)\\
&\quad+m_\eta^4(5/216\pi^2+5/36)\Big)\\
&\quad+21/8\Big(\overline{A}(m_\pi^2)\Big)^2+7/2\overline{A}(m_\pi^2)\overline{A}(m_K^2)+7/12\overline{A}(m_\pi^2)\overline{A}(m_\eta^2)\\
&\quad+\overline{A}(m_\pi^2)\Big(m_\pi^2(-24L_4^r-12L_5^r+112L_6^r+68L_8^r+10H_2^r)+112m_K^2L_6^r\Big)+\Big((\overline{A}(m_K^2)\Big)^2
\end{aligned}
$$

$$
\begin{aligned}
&-\overline{A}(m_K^2)\overline{A}(m_\eta^2)/6+\overline{A}(m_\eta^2)^2/72\\
&+\overline{A}(m_K^2)\Big(m_\pi^2(8L_5^r+32L_6^r+8L_8^r+4H_2^r)+m_K^2(-32L_4^r-16L_5^r+128L_6^r+32L_8^r)\Big)\\
&+\overline{A}(m_\eta^2)\Big(m_\pi^2/3(20/3L_5^r-16L_6^r+64L_7^r+12L_8^r-2H_2^r)\\
&-m_K^2/3(32/3L_5^r-112L_6^r+64L_7^r)-8m_\eta^2L_4^r\Big)\\
&+64m_\pi^4\Big((L_4^r+L_5^r)(4L_6^r+2L_8^r+H_2^r)-4(L_6^r)^2-6L_6^rL_8^r-L_6^rH_2^r-2(L_8^r)^2-L_8^rH_2^r\Big)\\
&+128m_\pi^2m_K^2\Big((L_4^r-L_6^r)(8L_6^r+2L_8^r+H_2^r)+2L_5^rL_6^r\Big)\\
&+m_K^4\Big(1024L_4^rL_6^r+256L_5^rL_6^r-1024(L_6^r)^2-512L_6^rL_8^r\Big)\Big\}\\
&+\frac{4}{F_\pi^2}\Big\{m_\pi^4\Big(12C_{19}^r+20C_{20}^r+12C_{21}^r-C_{94}^r\Big)+m_\pi^2m_K^2\Big(48C_{21}^r+2C_{94}^r\Big)+m_K^4\Big(16C_{20}^r+48C_{21}^r\Big)\Big\}\,,
\end{aligned}
\tag{C.1}
$$

where $\langle 0|\overline{q}q|0\rangle$ stands for $\langle 0|\overline{u}u|0\rangle$ either $\langle 0|\overline{d}d|0\rangle$. The results for the strange quark reads

$$
\begin{aligned}
\langle 0|\overline{s}s|0\rangle^{(4)}=&\ \frac{2}{F_\pi^2}\Big\{\overline{A}(m_K^2)+\overline{A}(m_\eta^2)/3+m_\pi^2(8L_6^r-4L_8^r-2H_2^r)+4m_K^2(4L_6^r+2L_8^r+H_2^r)\Big\}\\
\langle 0|\overline{s}s|0\rangle^{(6)}=&\ \frac{1}{F_\pi^4}\Big\{\frac{1}{(16\pi)^2}(\pi^2/6+1)\Big(-7/162m_\pi^4+13/81m_\pi^2m_K^2+1/36m_\pi^2m_\eta^2+4/81m_K^4\\
&-2/3m_K^2m_\eta^2+17/36m_\eta^4\Big)\\
&+4\overline{A}(m_\pi^2)\overline{A}(m_K^2)+4/3\overline{A}(m_\pi^2)\overline{A}(m_\eta^2)+2\Big(\overline{A}(m_K^2)\Big)^2+2/9\Big(\overline{A}(m_\eta^2)\Big)^2\\
&+\overline{A}(m_\pi^2)\Big(m_\pi^2(-24L_4^r+88L_6^r-20L_8^r-10H_2^r)+16m_K^2(4L_6^r+2L_8^r+H_2^r)\Big)\\
&+\overline{A}(m_K^2)\Big(4m_\pi^2(4L_5^r+12L_6^r-2L_8^r-H_2^r)+8m_K^2(-4L_4^r-4L_5^r+20L_6^r+10L_8^r+H_2^r)\Big)\\
&+\overline{A}(m_\eta^2)\Big(m_\pi^2/3(80/3L_5^r+8L_6^r-128L_7^r-60L_8^r+2H_2^r)\\
&+m_K^2/3(-128/3L_5^r+160L_6^r+128L_7^r+144L_8^r+8H_2^r)-8m_\eta^2L_4^r\Big)\\
&+m_\pi^4\Big((L_4^r+L_5^r-L_6^r)(256L_6^r-128L_8^r-64H_2^r)+128(L_8^r)^2+64L_8^rH_2^r\Big)\\
&+64m_\pi^2m_K^2\Big(16L_4^rL_6^r+4L_5^rL_6^r+2L_5^rL_8^r+L_5^rH_2^r-16(L_6^r)^2\Big)\\
&+64m_K^4\Big(4(L_4^r+L_5^r)(4L_6^r+2L_8^r+H_2^r)-4L_6^r(4L_6^r+4L_8^r+H_2^r)-4(L_8^r)^2-2L_8^rH_2^r\Big)\Big\}\\
&+\frac{1}{F_\pi^2}\Big\{4m_\pi^4\Big(12C_{19}^r+4C_{20}^r+12C_{21}^r+C_{94}^r\Big)-64m_\pi^2m_K^2\Big(3C_{19}^r+C_{20}^r-3C_{21}^r\Big)\\
&+192m_K^4\Big(C_{19}^r+C_{20}^r+C_{21}^r\Big)\Big\}\,.
\end{aligned}
\tag{C.2}
$$

D Loop Integrals

In this Appendix we collect for completeness some familiar formulas for the one-loop integrals. The two-loop integrals that appear we discussed in [9] and for the others we used the expressions of [27]. We have not discussed these integrals in more detail here since we do not present any formulas involving them.

Through the calculation one has to use one-loop integrals of one, two and three point functions. The latter disappears after mass renormalization and the use of some recursion relation. All in all we only have to deal with the following set of functions – in the remainder we use $d = 4 - 2\epsilon$.

$$\begin{aligned}
A(m_1^2) &= \frac{1}{i}\int \frac{d^dq}{(2\pi)^d}\frac{1}{q^2 - m_1^2}\,, \\
B(m_1^2, m_2^2, p^2) &= \frac{1}{i}\int \frac{d^dq}{(2\pi)^d}\frac{1}{(q^2 - m_1^2)((q-p)^2 - m_2^2)}\,, \\
B_\mu(m_1^2, m_2^2, p^2) &= \frac{1}{i}\int \frac{d^dq}{(2\pi)^d}\frac{q_\mu}{(q^2 - m_1^2)((q-p)^2 - m_2^2)} \\
&= p_\mu B_1(m_1^2, m_2^2, p^2)\,, \\
B_{\mu\nu}(m_1^2, m_2^2, p^2) &= \frac{1}{i}\int \frac{d^dq}{(2\pi)^d}\frac{q_\mu q_\nu}{(q^2 - m_1^2)((q-p)^2 - m_2^2)} \\
&= p_\mu p_\nu B_{21}(m_1^2, m_2^2, p^2) + g_{\mu\nu}B_{22}(m_1^2, m_2^2, p^2)\,, \\
B_{\mu\nu\alpha}(m_1^2, m_2^2, p^2) &= \frac{1}{i}\int \frac{d^dq}{(2\pi)^d}\frac{q_\mu q_\nu q_\alpha}{(q^2 - m_1^2)((q-p)^2 - m_2^2)} \\
&\quad = p_\mu p_\nu p_\alpha B_{31}(m_1^2, m_2^2, p^2) + (p_\mu g_{\nu\alpha} + p_\nu g_{\mu\alpha} + p_\alpha g_{\mu\nu})B_{32}(m_1^2, m_2^2, p^2)\,.
\end{aligned} \tag{D.1}$$

An expansion in ϵ leads to the following series

$$\begin{aligned}
A(m_1^2) &= \frac{m_1^2}{16\pi^2}\lambda_0 + \overline{A}(m_1^2) + \epsilon\overline{A}^\epsilon(m_1^2) + \ldots\,, \\
B_{ij}(m_1^2, m_2^2, p^2) &= \frac{1}{16\pi^2}\text{pole}_{ij} + \overline{B}_{ij}(m_1^2, m_2^2, p^2) + \epsilon\overline{B}_{ij}^\epsilon(m_1^2, m_2^2, p^2) + \ldots\,,
\end{aligned} \tag{D.2}$$

with $\overline{A}$, $\overline{B}_{ij}$ defining finite quantities and where "pole_{ij}" denotes the singular part of each of the B_{ij} functions,

$$\begin{aligned}
&\text{pole} = \lambda_0\,, \quad \text{pole}_1 = \frac{\lambda_0}{2}\,, \quad \text{pole}_{21} = \frac{\lambda_0}{3}\,, \quad \text{pole}_{22} = \frac{\lambda_0}{4}(m_1^2 + m_2^2 - \frac{p^2}{3})\,, \\
&\text{pole}_{31} = \frac{\lambda_0}{4}\,, \quad \text{pole}_{32} = \frac{\lambda_0}{24}(2m_1 + 4m_2^2 - p^2)\,,
\end{aligned} \tag{D.3}$$

with

$$\lambda_0 = \frac{1}{\epsilon} + \ln(4\pi) + 1 - \gamma\,. \tag{D.4}$$

After some simpler algebraic manipulation, the functions defined in Eq. (D.1) can be related to the basic integrals $A(m_1^2)$ and $B_1(m_1^2, m_2^2, p^2)$ through the identities

$$\begin{aligned}
B_{31}(m_1^2, m_2^2, p^2) &= \frac{1}{2p^2}\Big(A(m_2^2) - (m_2^2 - m_1^2 - p^2)B_{21}(m_1^2, m_2^2, p^2) - 4B_{32}(m_1^2, m_2^2, p^2)\Big)\,, \\
B_{32}(m_1^2, m_2^2, p^2) &= \frac{1}{2p^2}\Big(-\frac{m_1^2}{d}A(m_1^2) + \frac{m_2^2}{d}A(m_2^2) - (m_2^2 - m_1^2 - p^2)B_{22}(m_1^2, m_2^2, p^2)\Big)\,, \\
B_{21}(m_1^2, m_2^2, p^2) &= \frac{1}{p^2}\Big(A(m_2^2) + m_1^2B(m_1^2, m_2^2, p^2) - dB_{22}(m_1^2, m_2^2, p^2)\Big)\,, \\
B_{22}(m_1^2, m_2^2, p^2) &= \frac{1}{2(d-1)}\Big(A(m_2^2) + 2m_1^2B(m_1^2, m_2^2, p^2) \\
&\quad -(p^2 + m_1^2 - m_2^2)B_1(m_1^2, m_2^2, p^2)\Big)\,, \\
B_1(m_1^2, m_2^2, p^2) &= \frac{1}{2p^2}\Big(A(m_2^2) - A(m_1^2) + (m_1^2 - m_2^2 + p^2)B(m_1^2, m_2^2, p^2)\Big)\,, \\
B(m_1^2, m_1^2, 0) &= \frac{(d-2)}{2m_1^2}A(m_1^2)\,.
\end{aligned} \tag{D.5}$$

Notice that the inclusion of the previous identities is only done at the final (numerical) level in order to avoid cancellations between different terms occurring in the form-factors. Then the one-loop contribution is reduced to

$$\begin{aligned}
\overline{A}(m_1^2) &= -\frac{m_1^2}{16\pi^2}\ln(m_1^2)\,, \\
\overline{B}(m_1^2,m_2^2,p^2) &= -\frac{1}{16\pi^2}\frac{m_1^2\ln(m_1^2)-m_2^2\ln(m_2^2)}{m_1^2-m_2^2} \\
&\quad +\frac{1}{(32\pi^2)}\left(2+\left(-\frac{\Delta}{p^2}+\frac{\Sigma}{\Delta}\right)\ln\frac{m_1^2}{m_2^2}-\frac{\nu}{p^2}\ln\frac{(p^2+\nu)^2-\Delta^2}{(p^2-\nu)^2-\Delta^2}\right)\,, \qquad \text{(D.6)}
\end{aligned}$$

with $\Delta = m_1^2 - m_2^2$, $\Sigma = m_1^2 + m_2^2$ and $\nu^2 = [p^2-(m_1+m_2)^2][p^2-(m_1-m_2)^2]$. Similarly combining Eqs. (D.2) and (D.5) one can obtain the expressions of the ϵ terms in the expansion as functions of $\overline{A}^\epsilon$ and $\overline{B}^\epsilon$. A straightforward calculation leads to

$$\begin{aligned}
16\pi^2\overline{A}^\epsilon(m_1^2) &= m_1^2\Big[\frac{C^2}{2}+\frac{1}{2}+\frac{\pi^2}{12}+\frac{1}{2}\ln^2(m_1^2)-C\ln(m_1^2)\Big] \\
16\pi^2\overline{B}^\epsilon(m_1^2,m_2^2,p^2) &= \frac{C^2}{2}-\frac{1}{2}+\frac{\pi^2}{12}+(C-1)\overline{B}(m_1^2,m_2^2,p^2)+\frac{1}{2}\int_0^1 dx\,\ln^2(m^2)\,,
\end{aligned} \qquad \text{(D.7)}$$

with $C = \ln(4\pi)+1-\gamma$ and $m^2 = (1-x)m_1^2 + xm_2^2 - x(1-x)p^2$.

References

[1] For a series of lectures and more references see A. Pich, lectures given at Les Houches Summer School in Theoretical Physics, Session 68: Probing the Standard Model of Particle Interactions, Les Houches, France, 28 Jul - 5 Sep 1997, hep-ph/9806303.

[2] J. Gasser and H. Leutwyler, Nucl. Phys. **B250** (1985) 465.

[3] L. Chounet, J. Gaillard and M.K. Gaillard, Phys. Rept. **4** (1972) 199.

[4] J. Bijnens, Nucl. Phys. **B337** (1990) 635; C. Riggenbach *et al.*, Phys. Rev. **D43** (1991) 127.

[5] J. Bijnens, G. Colangelo and J. Gasser, Nucl. Phys. **B427** (1994) 427 hep-ph/9403390.

[6] J. Bijnens *et al.*, Phys. Lett. **B374** (1996) 210 hep-ph/9511397.

[7] J. Bijnens *et al.*, Nucl. Phys. **B508** (1997) 263 hep-ph/9707291.

[8] M. Knecht *et al.*, Nucl. Phys. **B457** (1995) 513 hep-ph/9507319.

[9] G. Amorós, J. Bijnens and P. Talavera, Nucl. Phys. in press, hep-ph/9907264.

[10] S. Bellucci, J. Gasser and M. E. Sainio, Nucl. Phys. **B423** (1994) 80 hep-ph/9401206; U. Burgi, Nucl. Phys. **B479** (1996) 392 hep-ph/9602429; J. Bijnens and P. Talavera, Nucl. Phys. **B489**, (1997) 387 hep-ph/9610269; P. Post and K. Schilcher, Phys. Rev. Lett. **79** (1997) 4088; E. Golowich and J. Kambor, Nucl. Phys. **B447** (1995) 373 hep-ph/9501318; E. Golowich and J. Kambor, Phys. Rev. **D58** (1998) 036004 hep-ph/9710214; K.Maltman, Phys. Rev. **D53** (1996) 2573.

[11] J. Bijnens, G. Colangelo and P. Talavera, JHEP **9805** (1998) 014 hep-ph/9805389.

[12] G. Amorós, J. Bijnens and P. Talavera, hep-ph/9912398.

[13] N. Cabibbo and A. Maksymowicz, Phys. Rev. **137** (1965) B438.

[14] Ll. Ametller *et al.*, Phys. Lett. **B303** (1993) 140 hep-ph/9302219.

[15] A. Pais and S.B. Treiman, Phys. Rev. **168** (1968) 1858; F.A. Berends, A. Donnachie and G.C. Oades, Phys. Lett. **B26** (1967) 109; Phys. Rev. **171** (1968) 1457.

[16] J. Bijnens, G. Colangelo and G. Ecker, JHEP **02** (1999) 020 hep-ph/9902437.

[17] L. Rosselet *et al.*, Phys. Rev. **D15** (1977) 574.

[18] G. Makoff *et al.*, Phys. Rev. Lett. **70** (1993) 1591; Erratum **75** (1995) 2069.

[19] Particle Data Group, C. Caso *et al.*, Eur. Phys. J. **C3** (1998) 1.

[20] S. Weinberg, Phys. Rev. Lett. **17** (1966) 336; Erratum **18** (1967) 1178.

[21] J. Bijnens, G. Colangelo and G. Ecker, Phys. Lett. **B441** (1998) 437 hep-ph/9808421.

[22] B. Ananthanarayan and P. Buttiker, Phys. Rev. **D54** (1996) 1125 hep-ph/9601285.

[23] L. Girlanda *et al.*, Phys. Lett. **B409** (1997) 461 hep-ph/9703448.

[24] J. Bijnens, G. Colangelo and G. Ecker, Ann. Phys. (NY) **280** (2000) 100 hep-ph/9907333.

[25] A.I. Davydychev and J.B. Tausk, Nucl. Phys. **B397** (1993) 123.

[26] J. Gasser and M. E. Sainio, Eur. Phys. J. **C6** (1999) 297 hep-ph/9803251.

[27] A. Ghinculov and J.J. van der Bij, Nucl. Phys. **B436** (1995) 30 hep-ph/9405418; A. Ghinculov and Y. Yao, Nucl. Phys. **B516** (1998) 385 hep-ph/9702266.

[28] G. Ecker *et al.*, Nucl. Phys. **B321** (1989) 311; G. Ecker *et al.*, Phys. Lett. **B223** (1989) 425.

[29] E. Golowich and J. Kambor, Phys. Lett. **B421** (1998) 319 hep-ph/9711256; Phys. Rev. Lett. **79** (1997) 4092 hep-ph/9707341; Phys. Rev. **D53** (1996) 2651 hep-ph/9509304; and E. Golowich and J. Kambor in [10].

[30] J. Prades, Z. Phys. **C63** (1994) 491 hep-ph/9302246; Erratum Eur. Phys. J. **C11** (1999) 571.

[31] P. Herrera-Siklody, hep-ph/9902446; P. Herrera-Siklody et al., Phys. Lett. **B419** (1998) 326 hep-ph/9710268.

[32] J.F. Donoghue, B.R. Holstein and D. Wyler, Phys. Rev. **D47** (1993) 2089; J. Bijnens, Phys. Lett. **B306** (1993) 343 hep-ph/9302217; J. Bijnens and J. Prades, Nucl. Phys. **B490** (1997) 239 hep-ph/9610360; B. Moussallam, Nucl. Phys. **B504** (1997) 381 hep-ph/9701400.

[33] N. H. Fuchs, M. Knecht and J. Stern, hep-ph/0001188.

[34] D. Espriu, E. de Rafael and J. Taron, Nucl. Phys. **B345** (1990) 22.

[35] S. Peris, M. Perrottet and E. de Rafael, JHEP **9805** (1998) 011 hep-ph/9805442.

[36] S. Descotes, L. Girlanda and J. Stern, JHEP **0001** (2000) 041 hep-ph/9910537.

[37] J. Bijnens, C. Bruno and E. de Rafael, Nucl. Phys. **B390** (1993) 501 hep-ph/9206236.

[38] M. F. Golterman and S. Peris, Phys. Rev. **D61** (2000) 034018 hep-ph/9908252.

[39] G. Amorós and J. Bijnens, J. Phys. **G25** (1999) 1607 hep-ph/9902463.

[40] O. Dumbrajs *et al.*, Nucl. Phys. **B216** (1983) 277.

[41] W. Hoogland *et al.*, Nucl. Phys. **B126** (1977) 109.

[42] V. A. Novikov *et al.*,y Nucl. Phys. **B191** (1981) 301.

[43] M. A. Shifman, A. I. Vainshtein and V. I. Zakharov, Nucl. Phys. **B147** (1979) 385.

[44] G. 't Hooft, Nucl. Phys. **B72** (1974) 461; G. Veneziano, Nucl. Phys. **B117** (1976) 519; E. Witten, Nucl. Phys. **B160** (1979) 57.

[45] S. Peris and E. de Rafael, Phys. Lett. **B348** (1995) 539 hep-ph/9412343.

[46] B. Moussallam, hep-ph/9909292.